Fractal Geometry in Physical Systems

Daniel Wójcik

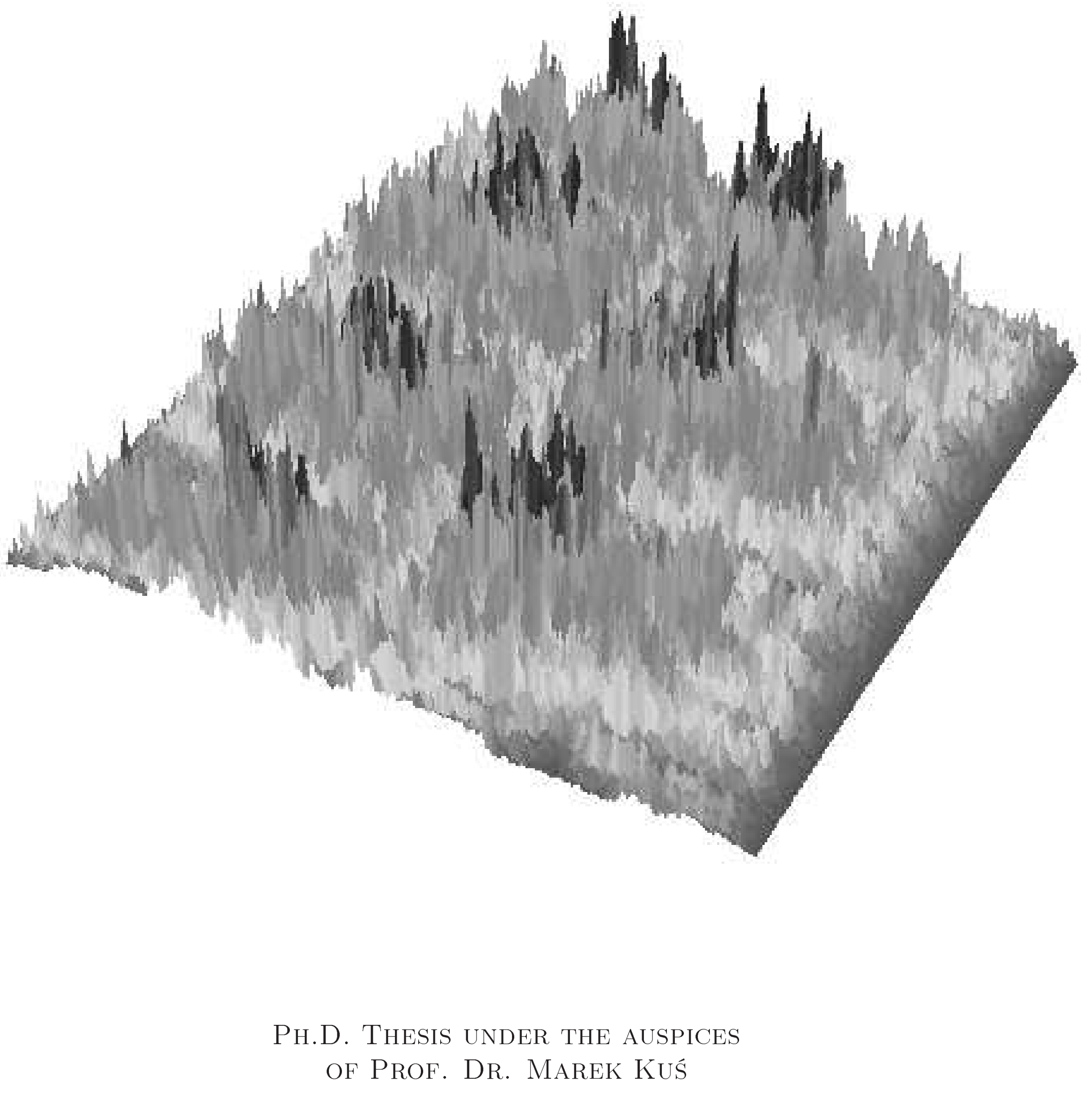

Ph.D. Thesis under the auspices
of Prof. Dr. Marek Kuś

Center for Theoretical Physics
of the Polish Academy of Sciences

Warsaw $*$ 2000

Dedicated to
MAGDA
for the joy she brought
into our lives,
and to
ANIA
who favored me with the time
in which to write this work.

Geometria fraktalna w układach fizycznych

Daniel Wójcik

Praca doktorska napisana pod opieką
prof. dr hab. Marka Kusia

Centrum Fizyki Teoretycznej
Polskiej Akademii Nauk

Warszawa ∗ 2000

Cover figure: space-time plot of the quantum fractal in the well (chapter 4). Time flows along NE-SW axes, the well is located along the NW-SE axes.

Contents

Acknowledgements

This work would never have taken its present form without the positive influence of many people. Our teachers, friends, colleagues, family, all the people we meet on the track of our life, they all shape our perception of the world which is inevitably reflected in our work. Lack of space in a paper is usually the excuse not to thank everybody properly. The thesis, however, seems to be a good place to give credit to all those to whom its due.

My warmest thanks go to the whole staff of the Center of Theoretical Physics of the Polish Academy of Sciences where this work have been carried for the last four years, in particular to

- *Prof. Iwo Białynicki-Birula*, my first director, for his invitation to work at the Center, his faith in me, many discussions and fruitful collaboration;
- *Prof. Kazimierz Rzążewski*, for his support in my actions, especially for the help with my January trip to Dynamics Days 2000 in Santa Fe and several American universities which was a major stimulus to my work;
- *Prof. Marek Kuś*, my advisor, for bearing up with me in the toughest days of my ineffectiveness, his support, discussions, wit and Winnie-the-Pooh;
- *Prof. Karol Życzkowski*, some day, perhaps, I'll find a way to thank you properly for everything;
- *Prof. Łukasz Turski* and *Prof. Jerzy Kijowski*, for helpful discussions;
- all my colleagues, *Czarek, Piotr, Sonnet, Krzysiek, Magda, Zbyszek, Radka, Paweł, Michał*, for the atmosphere created in our institute and bearing up with some of my seminar ideas;
- Naszym wspaniałym Paniom *Teresie Barańskiej, Zofii Kempistej, doc. Ewie Sobczak* i *dr Danucie Śledziewskiej-Błockiej* za znakomite wsparcie logistyczne przez te wszystkie lata.

This work has also been strongly influenced by

- *Prof. Andrzej Nowak*, whose inspiration gave the first spark to my work;
- *Prof. Andrzej Wróbel* and *Prof. Witold Klonowski*, who provided me with data from their experiments, which are still the challenge I hope to face some day;

- *Yura Hlushchuk, Nazar Savytsky, Dr. Szymon Bauch, Prof. Leszek Sirko*, whose experiments continue to stimulate me and I'm sure our collaboration will soon bring fruit.

My January 2000 trip to United States was instrumental in speeding up the work covered in this thesis. Hospitality of the people who invited a stranger is gratefully acknowledged, in temporal order I thank

- *Prof. Nitant Kenkre*, and other people in University of New Mexico, Albuqeurque, especially *Dave Dunlap* and *Betty Fry*;

- *Prof. Harry Swinney*, and his Austin crew, especially *Dan Goldman*, who made my stay so grand, *Brendan Plapp, Charles Baroud* and *John Burgess* for discussions, and all the others for their time;

- *Dr. Paul So*, for his invitation and *Prof. Steven Schiff* for his hospitality in the Krasnov Institute of Advanced Study in Fairfax; discussions with *P.S., S.S, Ernesto Barretto, Bruce Gluckmann, Sławek Nasuto, Lou Pecora* are acknowledged;

- *Prof. J. Robert Dorfman*, my host at the University of Maryland, for his time and insight; talks to *Panja* and *Kiryl* were of help in clearing up some ideas.

Numerous people have influenced the way I understand the world and science.

- My perception of physics and geometry was seriously influenced by my work with *Prof. Jacek Tafel* and close contacts with *Prof. Antoni Sym* during my university years.

- My view on the topics covered in this work was also shaped thanks to the support of *Prof. Renata Dmowska* over the years.

- I thank all my friends who back me up, in particular *Mariusz Białecki* and *Piotr Szymczak*, whose friendship and support in both scientific and private life I have always treasured.

- Dziękuję mojej rodzinie, a zwłaszcza rodzicom, *Marii i Krzysztofowi Wójcikom* i siostrze *Agacie Wójcik*, za ich nieustające wsparcie we wszystkich moich poczynaniach, oraz moim teściom, *Emilii i Bolesławowi Stachowom*, za opiekę nad żoną i córką w czasie kiedy ta praca powstawała, oraz za zdjęcia fraktali.

I thank my wife, *Dr. Anna Stachow-Wójcik*, for her lasting support, for discussions, and for *Magda*. I dedicate this work to them.

This work has been partially supported by the Polish Committee of Scientific Research under grants nr 2 P03B 036 16, 2 P03B 044 13.

Fractals in science

The left bank of the Vistula, when measured with increased precision would furnish lengths ten, hundred and even thousand times as great as the length read off the school map. A statement nearly adequate to reality would be to call most arcs encountered in nature not rectifiable. This statement is contrary to the belief that not rectifiable arcs are an inventions of mathematicians and that natural arcs are rectifiable: it is the opposite that is true.

Hugo Steinhaus, *"Length, shape and area"*,
Colloquium Mathematicum **3** *(1954) 1–13;*
also in "Selected papers" p. 653.

Introduction

The aim of Physics is to understand the world, and its means are experiments. The physicists do not consider a phenomenon understood until they can observe it (or its signatures) and predict it. In order to do it we construct various theories, such as classical and quantum mechanics, or electrodynamics, which are surprisingly successful in the description of many phenomena within their limits of applicability.

Unfortunately — or luckily — the Nature's complexity is overwhelming which forces us to construct simple *models* of many phenomena in the hope of grasping their fundamental aspects.

All the phenomena take place somewhere, sometime and happen to something. Thus we are forced to construct and study models of spacetime and inhabiting it objects. An important class of their physical properties are the geometric properties.

For many years we have used the Euclidean or Riemannian geometry to describe the geometric properties of nature. Thus the natural models of physical objects have been solids, spheres, smooth manifolds and so on. Analysis of these objects naturally leads to smooth, analytic functions.

The success of these models is indisputable. One of its consequences is our tendency to oversimplify life and consider too crude models, like spherical cows, etc.

When we abandon our prejudices we cannot fail to see that there are objects in nature which are not described well in the language of traditional geometry. Sponges, cauliflowers, clouds, attractors and repellers of dynamical systems, typical Brownian paths, distribution of matter in the Universe and many other. But there is a language which perfectly describes many of the above mentioned objects. It is the *fractal geometry*.

While the Euclid-Riemann geometry concentrates on the locally smooth structure of the object, the fractal geometry examines its *self-similarity*, or *scaling*. Some objects can be described in terms of both geometries. For example, a square — a typical object of Euclidean geometry — consists of four parts similar to the original object in scale 1:2 (figure 1a). There are objects, however, with less trivial scaling, for which the fractal geometry is the natural language. An example is the *Sierpiński carpet* which consists of eight identical parts similar to the original figure in scale 1:3 (figure 1b).

Following Mandelbrot we call *fractals* the complex, porous, mangled objects characterized by a non-trivial scaling, and exhibiting similar structures at every resolution. Several mathematicians and physicists fancied these crinkled objects long before him but it was Benoit Mandelbrot who first fully realized the importance of fractals. Thanks to the beautiful pictures and deep observations in his seminal books [144, 145, 146] fractals gained attention of a substantial group of scientists.

Probably the simplest fractal is the *Cantor set*. To construct it you take the closed interval $I_0 = [0,1]$. Then you divide it into three equal parts and take out the *open* middle one $]1/3, 2/3[$ leaving two *closed* intervals $I_1 = [0,1/3] \cup [2/3,1]$. The construction is recursive, thus at the n-th step from each of the 2^{n-1} closed sets comprising I_{n-1} you take out the open middle-third obtaining I_{n+1} which consists of 2^n closed intervals each of length $(1/3)^n$. The sets I_n are often called *prefractals* and the *Cantor set* is the limiting set $I_\infty = \bigcap_{n=0}^{\infty} I_n$.

Another simple fractal is the *Sierpiński carpet*. Its construction starts with a square $S_0 = [0,1] \times [0,1]$. In the first step you divide S_0 into nine equal squares and take out the open middle one $]1/3, 2/3[\times]1/3, 2/3[$ leaving the closed set S_1 consisting of eight squares each of side three times smaller than the original. In the n-th step you divide each of the 8^{n-1} squares composing S_{n-1} into nine equal squares and remove the middle one obtaining this way S_n composed of 8^n squares. Again, *Sierpiński carpet* is the limiting set $S_\infty = \bigcap_{n=0}^{\infty} S_n$. Figure 2 shows the first three prefractals of Sierpiński carpet, figure 1b shows its fifth prefractal.

Recursive construction of the Cantor set and the Sierpiński carpet induces interesting scaling properties of the length or the area of their prefractals. Each Cantor prefractal I_n consists of 2^n intervals of length $\varepsilon_n = 1/3^n$, therefore its length $l_n = (2/3)^n$ is a power function of the resolution ε_n:

$$l_n = \mathrm{vol}^1(I_n) = \left(\frac{2}{3}\right)^n = \left(\frac{1}{3}\right)^{n\frac{\ln(2/3)}{\ln(1/3)}} = \varepsilon_n^{1-d_f},$$

where $d_f = \frac{\ln 2}{\ln 3} \approx 0.63092975357$ is called the *fractal dimension*. Also the number of intervals of length ε_n, which is $N(\varepsilon_n) = 2^n$, scales with the resolution: $N(\varepsilon_n) = 2^n = \varepsilon_n^{\frac{\ln 2}{\ln(1/3)}} = \varepsilon_n^{-d_f}$.

Similarly, the area a_n of S_n scales with the resolution as

$$a_n = \mathrm{vol}^2(S_n) = \left(\frac{8}{9}\right)^n = \left(\frac{1}{3}\right)^{n\frac{\ln(8/9)}{\ln(1/3)}} = \varepsilon_n^{2-d_f},$$

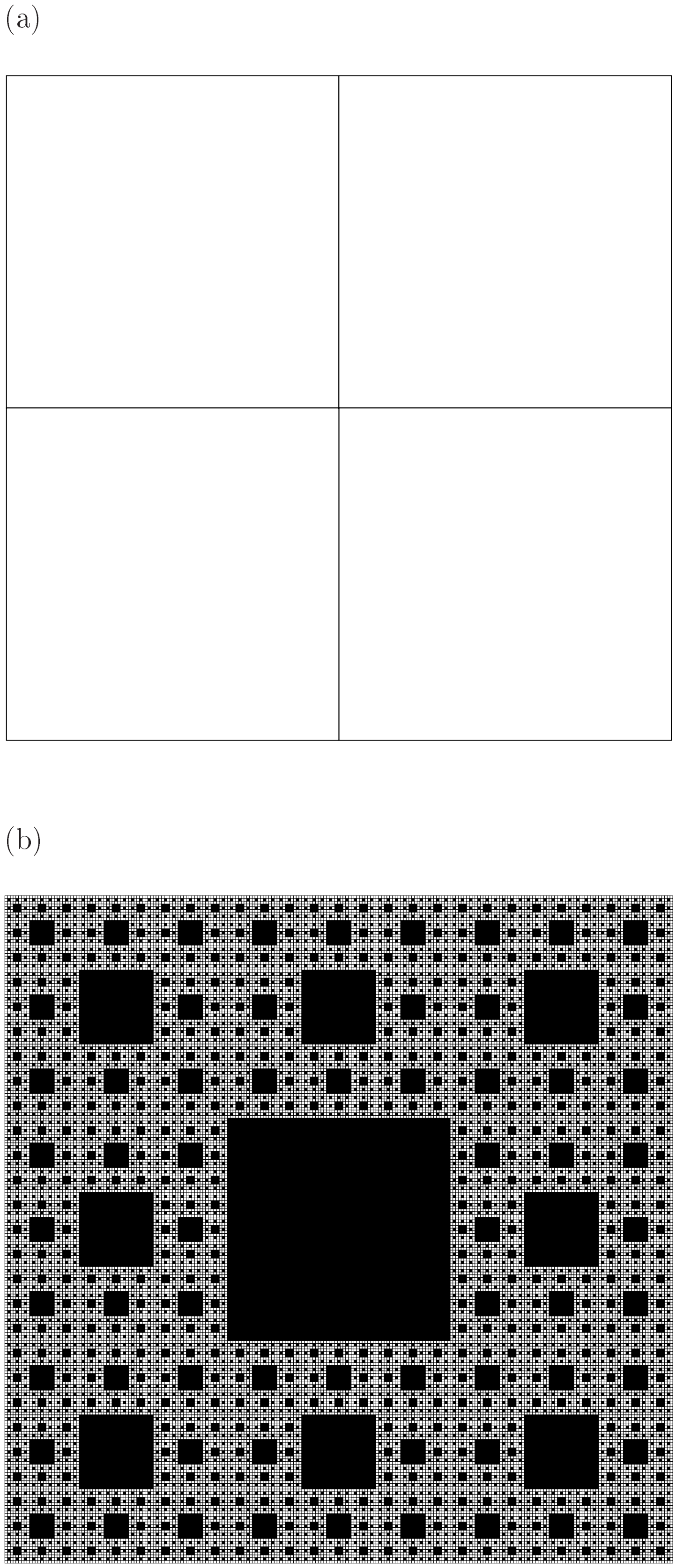

Figure 1: Two self-similar objects: a square (a) and a Sierpiński carpet (b).

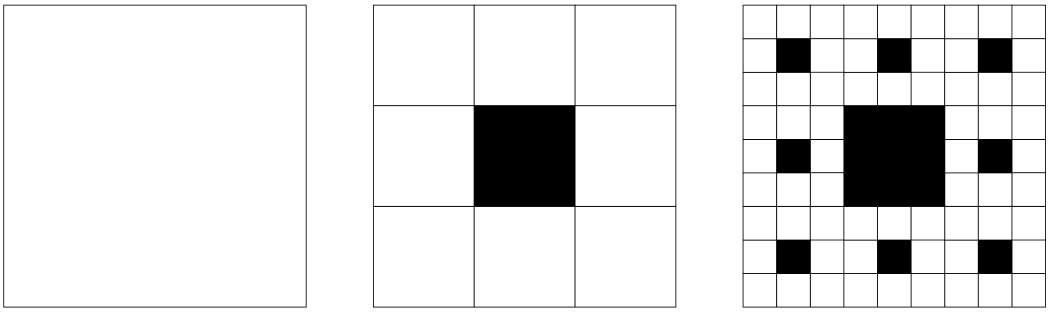

Figure 2: The first three prefractals of Sierpiński carpet.

where $d_f = \frac{\ln 8}{\ln 3} \approx 1.8927892607$ is the fractal dimension of the Sierpiński carpet. Again, the number of squares $N(\varepsilon_n)$ of side ε_n scales as $\varepsilon_n^{-d_f}$.

Another meaning of prefractals, apart from their being intermediate construction steps of fractals, is that they are approximations of the fractals as seen at a given resolution ε. Thus one can consider the lengths l_n and areas a_n as approximate values of length or area of a fractal at a given resolution. Thus if the length or area at resolution ε is a power function of ε

$$\mathrm{vol}^d(A(\varepsilon)) \sim \varepsilon^{d-d_f},$$

where $A(\varepsilon)$ is fractal A seen (measured) at resolution ε, then the *fractal dimension* of the fractal A is d_f. Also the scaling of the number of d-dimensional boxes needed to cover the fractal A is governed by the same exponent:

$$N(\varepsilon_n) \sim \varepsilon_n^{-d_f}.$$

We will come back to the notion of fractal dimension in the next chapter where it is made precise.

Both the Cantor set and the Sierpiński carpet are *self-similar sets*, that is they consist of parts *exactly* similar to the whole. For instance, the Cantor set consists of two parts similar to the whole set in scale 1:3, the Sierpiński carpet consists of eight parts similar to the whole set also in scale 1:3. Similarity in scale q means that we contract all the distances $1/q$ times.

This class of fractals is too narrow. Nature often breaks the symmetry which can lead to different scaling in various directions, like in the case of growth processes when the gravity differentiates the vertical direction from the horizontal. Also when we consider graphs of functions, like trajectories of stochastic processes, different variables have different physical meaning, thus it is to be expected they can scale differently.

Indeed, the simplest physical model of a *self-affine* fractal is a trajectory of a Brownian particle or a graph of a trajectory of an ant wandering randomly on a lattice. Consider an ant placed at $x = 0$ in a one-dimensional lattice. At every step the ant goes to the next site to the right or to the left of the one it occupies. The probability to go right or left is the same. The question is how far on the average the ant moves from the origin with time. Of course, average position must be 0, because the problem is symmetric. However $\langle x^2 \rangle$ is positive and grows linearly with time t. Thus a typical length scales as

$$l(t) := \sqrt{\langle x^2 \rangle} \sim \sqrt{t}.$$

One usually expects that for long enough times a typical trajectory will better and better approximate the average behavior. Thus asymptotically one expects to observe the above scaling for $x(t)$. This means, that when you cut a piece of the graph of the trajectory (a subset of $\mathbb{R}^2 \supset \{(t, x(t)) : t \in [t_0, t_1]\}$), contract it four times in t and two times in x, it will resemble any other fragment of the whole trajectory plotted within time interval $(t_1 - t_0)/4$. Such sets, consisting of parts similar to the whole after scaling with different scales in different variables, are called *self-affine fractals*. Fractal wave functions which we construct in chapter 4 are other examples of such fractals.

In physics we usually encounter *random* fractals which are self-similar or self-affine only statistically. Often the scaling can be inferred only for the ensemble averages of some functions. The notions of fractal dimensions are flexible enough to tackle these cases.

It should also be clear for the reader that no scaling in physics can hold for infinity of scales. This is contrary to mathematics where the inductive procedure can be repeated *ad infinitum*. Thus in Nature we will not find "true" fractals, just as we will not find "true" squares, triangles, spheres and straight lines. In spite of this obvious limitation, fractals found many applications in almost every branch of physics and other sciences [146, 4, 157, 225, 135, 174]. From the physicist's point of view, one tends to call an object *fractal*, if the scaling behavior can be observed for at least several orders of magnitude [146]. Such models turn out to be very effective in many cases.

An appropriate discussion of all the phenomena and theories where fractals were found indispensable or useful could easily take hundreds of pages. A recent monograph by Paul Meakin [157] which concentrates on fractals in growth processes far from equilibrium quotes 1356 references and is almost 700 pages long. In what follows we will present a panorama of known applications of fractals, but we will not even attempt completeness. We will try to quote review papers in the hope they will provide entries for the reader who wants to pursue a particular application further.

We will also not discuss the historical development of ideas. The books of Mandelbrot [144, 145, 146] and the collection of original papers by Edgar [68] can be good starting points for readers with historical inclinations.

Applications

Before Mandelbrot the scaling concepts were applied to a relatively small class of problems such as critical phenomena [216], structure of polymers [56]. Mandelbrot was the first who stressed the intuitive geometric content of the scaling ideas since the beginning [121].

After the publication of his books multiple applications followed, fractals turned out to be useful and almost universal models. A lot of research from the early tide of enthusiasm will drown in the wake of time, there are some fields, however, where fractals are sure to stay.

One of such fields is dynamical systems theory. The connections between deterministic chaos, dynamical systems and fractals are manifold. Thus attractors [64, 167, 193, 195, 196, 66] and repellers [123, 220] of chaotic dynamical systems have often been found to be fractal. Strange (i.e. fractal) attractors were also found in non-chaotic dynamical systems [101]. In many problems with several attractors boundaries of their basins are interwoven at every scale and fractal [105, 102]. Spatiotemporal chaos leads to appearance of coherent structures which can be fractal [50, 157, 12]. The recent general theory of Pesin [178] allows one to treat dimensions, Lyapunov exponents and entropies on equal footing.

In problems of chaotic scattering one often encounters fractal sets. For instance, deflection angle versus impact parameter has been shown to be singular on a fractal set of parameters [63, 88, 30, 29].

The second important field where fractals are indispensable is the physics of non-equilibrium growth processes. The recent monograph of Paul Meakin [157] can be consulted for a detailed review of the field. Also the older books of Vicsek [243] and Feder [83] can be consulted, or the papers by Erzan et al. [73], Meakin [155, 156], Stanley and Meakin [217]. The rapid development of the field of fractal growth started with the introduction of diffusion-limited aggregation model by Witten and Sander [253, 254]. Structures observed in simulations arise naturally in many processes of physical or chemical interest ranging from viscous fingering [161, 47, 143], dendritic solidification [17, 38, 162], thin-film morphology [70], colloid aggregation [250], to electrochemical deposition [36, 148].

The field where the use of fractals cannot be overemphasized is the physics and chemistry of anomalous diffusion. In Fickian diffusion the average square position scales linearly with time. It is typical of Gaussian uncorrelated stochastic processes. Often observed deviations with different scaling exponents have been explained with two basic models: fractional Brownian motion, where the increments are normally distributed but no longer independent, or stable processes (Levy flights, Levy walks), where the increments are independent, but do not have a finite variance. Several good reviews appeared in the recent years. One can recommend [132, 34, 111, 158, 159, 251].

Let us briefly recall some other applications of fractal geometry.

It has been claimed that the distribution of visible matter in the universe can be fractal [49, 33, 221]. These observations are still a subject of a heated debate [54, 179] and stimulate the development of mathematical tools that can help in precise formulation of statements, like the porosities of measures [65]. One may note that the theoretical and modeling methods developed in the context of non-equilibrium growth and aggregation processes were used to study the evolution of galaxies [142, 209, 205] and galaxy distributions [244, 21].

The fluctuations of energy bursts generated by high-energy collisions both in accelerators and in cosmic showers have been shown to have multifractal character [25, 26, 57].

The flicker noise ($1/f$ noise) [249] has been suggested to have fractal origin, in this respect the so-called SOC model (self-organized criticality) gained some popularity, but also other models were considered, like Stuart Kauffman's EOC (edge of chaos) or Carlson and Doyle HOT (highly optimized tolerance) [10, 9, 18, 40, 249].

Fractals were shown to develop from an everywhere constant probability density in infinite potential well models in quantum mechanics [22]. Of similar mathematical character are the Talbot images of coherently illuminated diffraction gratings [23].

Configurations of Ising spins at critical points [252], the region of high vorticity in fully developed turbulence [186], percolating clusters and their backbones [55] were shown to be fractal. Distribution of atomic spectral lines of energized atoms were shown to have multifractal character [199].

Fractals were used for efficient encoding images (IFS, iterated function systems advocated by Michael Barnsley) [14, 13]. Clouds, trees, rivers, mountains were described and modeled with the help of fractals.

We would like to once again apologize a disappointed reader if her favorite papers have not been quoted. An adequate review of the literature would easily extend the size of this work thus our presentation of necessity is very short and subjective. We only hope the books and papers quoted will give the casual reader some idea of the breadth of applications of fractal geometry and lead to the most of the relevant sources.

Plan and scope of the text

Our aim in this work is to show that despite over twenty years of active research fractal geometry is still a fruitful theory and can help to understand many phenomena. Astonishing fractal objects still await to be found and practical methods to be used in all fields of science can be conceived within this framework. We shall concentrate on two applications in whose development we took part.

In chapter 3 we present a method to distinguish interacting from non-interacting subsystems of the given system. Given two time series of essentially arbitrary variables coming from the subsystems one estimates the dimensions of attractors reconstructed from the data. Required information is obtained by comparison of the calculated dimensions. Theory and numerical examples are provided in support of the validity and practicality of the proposed method.

In chapter 4 we construct fractal solutions of the Schrödinger equation for a large class of potentials. They have arbitrary prescribed fractal dimension. To our knowledge this is the second such construction proposed (the first was published in the paper by Michael V. Berry [22]) but it gives the first correct proof of fractality of such states.

To let the reader appreciate our results in the next two chapters we outline the basic analytical and numerical methods we used in our work.

The main notions of fractal geometry are all kinds of fractal dimensions. We recall the most often used definitions in chapter 1. The definitions and their properties will be compared. We will concentrate on the fundamental properties of the Rényi dimensions and on the analysis of fractal graphs of functions.

In chapter 2 we will discuss the present status of the theory and practice of estimating dimensions of attractors from time series data. We will usually assume no knowledge of the dynamics governing the system. Some methods applicable in other cases will also be mentioned.

Summary of the main results is provided in the last chapter.

We have provided the proofs in three cases:

- if the result presented has been obtained by us (most of the results in chapters 3 and 4),
- if we feel the result is important for subsequent discussion and cannot be readily found (calculation of the box-counting dimension of the graph of the Weierstrass function);
- in some cases we suspect the results may have been obtained earlier but we were unable to track down the references and thus were forced to prove them ourselves (several results in chapter 1).

This text has been prepared in LaTeX with the help of GNU emacs and AucTeX. The C compiler used in this research was gcc. Most pictures were prepared with the help of gnuplot, the rest with Mathematica (trademark Wolfram Research; the only commercial program we used here). Nonlinear data analysis was performed with the help of the TISEAN package. All the programs ran under Red Hat Linux.

Chapter 1

Elements of fractal geometry

> *"Fractal" is a new science and we need to wait a half-century before the really good ideas can be filtered out.*
>
> Claude Tricot, *"Curves and fractal dimension"*

In this chapter we introduce several fractal dimensions which are the fundamental notions of the fractal geometry. It is convenient to first discuss the geometric fractal dimensions, which are used to characterize sets. Probably the simplest of them are the box-counting dimensions. While the easiest to calculate, they have some inconvenient properties. The remedies are the Hausdorff and the packing dimensions, which are dual to each other, in a sense. We will use neither the Hausdorff nor the packing dimensions in subsequent chapters, however they are the most important theoretical constructions in fractal geometry. We feel that any introduction to the theory of fractal dimension would be incomplete without them.

It often happens that a given geometric object can be naturally decomposed into a number of sets of different dimensions. This observation leads to multifractal spectra of dimensions which are generalizations of the above definitions. They are used to characterize measures (probability measures, mass distributions, etc.). We start with the Rényi dimensions, which are natural generalizations of the box-counting dimensions. Then we briefly discuss the so-called f_α spectrum. We will use the Rényi dimensions in chapter 3 where we propose a method to distinguish interacting from non-interacting systems on the basis of the fractal dimensions of some attractors estimated from experimental data. The f_α spectrum will not be used, but its importance in applications and theory deserves a place in this introduction.

The last — more specialized — section develops some facts useful in calculating the box-counting dimensions of graphs of functions. We will use these results in chapter 4 to show fractality of certain solutions of the Schrödinger equation which we construct.

The sections 1.1.2, 1.1.3, 1.2.2, and 1.3.7 contain material we do not use in the following chapters. They can be omitted at the first reading. We decided not to move them to appendices in order to keep the logic of the discussion.

1.1 Geometric fractal dimensions and their properties

Suppose you want to characterize an object in the real space, like an apple, a piece of string or a sponge. There are several features you might consider, for instance the color of the object, its smell, its shape, its elastic properties, etc. An important class of characteristics are geometric properties. Thus you may consider the volume of the object, its area, its length and so on.

Each of the three objects mentioned above has well defined volume which corresponds to the three dimensional Lebesgue measure of the sets representing the objects in an abstract $\mathbb{R}^3$ space. However, for a piece of string it seems much more convenient to use the length of the piece instead of the volume. This is a consequence of the fact that the string can be considered as a product of an interval and a disk whose diameter is much smaller in comparison with the length of the interval. This is why you cannot buy five liters of a string in a shop but you can get as many meters as you like. Thus to characterize geometry of a string you would use the one dimensional Lebesgue measure.

It is clear that neither volume, nor length, nor area are proper measures to characterize a sponge. Its complex interwoven structure begs for an adequate measure which must be here somehow constructed. One solution was proposed in 1919 by Felix Hausdorff [110], a German mathematician born in Wrocław (1868–1942). We will devote some time to this measure in section 1.1.2.

It is interesting to observe that the above characterization consists of two steps. First we must decide which measure is most adequate to characterize the given object (is it length? area? volume?). Therefore we must find out the *dimension* D of the object. Then we ask what is the D-dimensional volume of the (representation of the) object in question (is it a large or a small object according to the specified measure).

In this chapter we will concentrate on the first question: how can one define the dimension in cases less obvious than an apple or a string.

Classical dimension theory [117, 71, 72] developed as a part of topology. It considered several definitions of dimension. One of them is the *inductive dimension*. You assign dimension 0 to a set of separate points. Then the inductive dimension of a set is $n+1$ if and only if the inductive dimension of its boundary is n. Thus the dimension of an interval is 1, because its boundary consists of two points. The dimension of a square is 2, because its boundary consists of four intervals, and so on. Of course, to make this definition precise one has to make the notions of boundary precise, decide what is the dimension of a sum of sets of different dimensions (say, a maximum), etc. We will not go into these details [117, 71, 72].

In what follows we introduce several definitions which can be used to characterize any set and give correct answers for simple sets like squares, triangles, points, intervals, balls, etc. According to these definitions there exist objects of non-integer dimension. These are ramified, porous, very complex objects which are called *fractals* [146]. They are often characterized by statistical or true self-similarity which, loosely speaking, means that at every scale they show up similar features. Fractals are the main objects of interest of the fractal geometry, and its main tools are the *fractal dimensions*.

1.1.1 Box-counting dimensions

Consider a measurement of the volume of an apple. One of the possibilities is to slice the apple into cubes of $\delta_0 = 1$cm long sides with a salad slicer. Of course, some of the resultant pieces will not be cubes but will have smaller volume. Nevertheless, we can approximate the volume of the apple by the number of slices $N(\delta_0)$ times the volume of a maximal slice δ_0^3. Thus

$$V(\delta_0) = N(\delta_0) \cdot \delta_0^3. \tag{1.1}$$

We can now cut every slice into cubes of side $\delta_1 = 1/2$cm. Again, some of the resultant pieces will not be perfect cubes but we expect the number

$$V(\delta_1) = N(\delta_1) \cdot \delta_1^3 \tag{1.2}$$

to be a better approximation of the true volume of the apple than $V(\delta_0)$. Repeating our procedure of cutting each piece into cubes of size $\delta_n = 1/2^n$cm and counting resultant pieces we observe fast convergence of the approximate volumes

$$V(\delta_n) = N(\delta_n) \cdot \delta_n^3 \tag{1.3}$$

to the number which we call the volume of the apple

$$V = \lim_{n\to\infty} V(\delta_n) = \lim_{n\to\infty} N(\delta_n) \cdot \delta_n^3. \tag{1.4}$$

This implies that the number of pieces must scale like the reversal of the cube length:

$$N(\delta) \propto \delta^{-3} = \delta^{-D}, \tag{1.5}$$

where the constant of proportionality is the volume V, and $D = 3$. Also

$$V(\delta) \propto \delta^{-3}\delta^3 = \delta^{3-D}. \tag{1.6}$$

Thus

$$\begin{aligned} D &\approx 3 - \lim_{\text{large}\,n} \frac{\ln V(\delta_n)}{\ln \delta_n} \qquad (1.7)\\ &\approx \lim_{\text{large}\,n} \frac{\ln N(\delta_n)}{\ln 1/\delta_n}. \end{aligned}$$

Let us perform a similar procedure for the piece of string. We straighten the string and cut it with scissors into pieces of linear size δ_n. This corresponds to slicing the straightened string with the salad slicer but is easier to perform. It is clear that the number of slices for a long range of n is approximately proportional to $1/\delta_n$, where the constant of proportionality is L — the length of the string we want to estimate. Thus the approximate volume

$$V(\delta_n) = N(\delta_n) \cdot \delta_n^3 \propto \delta_n^{-1}\delta_n^3 = \delta_n^{3-1} \tag{1.8}$$

would tend to 0 with decreasing δ

$$V = \lim_{\text{large}\, n} N(\delta_n) \cdot \delta_n^3 = 0. \tag{1.9}$$

Certainly, for *really* small δ_n we would obtain some positive value of volume, because of the finite diameter of the section of the string. This is a typical situation for all the real objects[1]. Nevertheless, it is usually the value of L that we are interested in.

One can therefore observe for a long range of n the following scaling behaviors of $V(\delta)$ and $N(\delta)$:

$$V(\delta) \propto \delta^{3-1} = \delta^{3-D}, \qquad N(\delta) \propto \delta^{-1} = \delta^{-D}, \tag{1.10}$$

where $D = 1$. Again, D can be obtained as one of the limits (1.7).

It turns out that for many objects similar procedures of dividing an object into pieces of linear size δ lead to the following scaling behavior

$$V(\delta) \propto \delta^{3-D}, \qquad N(\delta) \propto \delta^{-D}, \tag{1.11}$$

or

$$\begin{aligned} D &\approx 3 - \frac{\ln V(\delta_n)}{\ln \delta_n} && (1.12) \\ &\approx \frac{\ln N(\delta_n)}{\ln 1/\delta_n}. && (1.13) \end{aligned}$$

where D is called the *Minkowski dimension* if the scaling of volume is considered, and the *box-counting dimension* if one considers scaling of $N(\delta)$.

Measuring the volume of the sponge we would observe that its approximate volume $V(\delta_n)$ would decrease with decreasing δ_n, because when we refine the scale in every cube of side δ_n there are many wholes of size larger than δ_{n+1} which are not counted in the next approximation of the volume. On the other hand, the structure of a sponge is that of a ramified piece of paper, thus the number of cubes needed to cover the whole sponge $N(\delta_n)$ must grow faster than in case of a plane figure, which is two dimensional. Therefore, one can observe the following scaling behavior of $V(\delta)$ and $N(\delta)$

$$V(\delta) \propto \delta^{3-D}, \qquad N(\delta) \propto \delta^{-D}, \tag{1.14}$$

[1]In fact, going deeper we would see the structure of the string, all the smaller threads that compose it, then the molecular structure and so on. Typically, every physical object has many scales with different scaling thus it can only be considered as a physical fractal and we can only speak of effective dimension which is just a scaling exponent of $N(\delta)$ or $V(\delta)$ within some range [146, 125].

where $3 > D > 2$. Thus D in this case is non-integer and we have an object more voluminous than a piece of paper and flatter than an apple. Thus a sponge is a fractal of box-counting dimension between 2 and 3.

To make the above discussion precise enough to make some definitive statements consider a bounded set $A \subset \mathbb{R}^n$. Divide the space into a grid of n-dimensional boxes of side δ, i.e. boxes of the form

$$[m_1\delta, (m_1 + 1)\delta] \times \ldots \times [m_n\delta, (m_n + 1)\delta]. \tag{1.15}$$

Let $N(\delta)$ be the number of these boxes covering the set A. It is always finite because A is bounded.

Definition 1.1 *The* box-counting dimension *of the set A is the limit*

$$\dim_B(A) := \lim_{\delta\to 0} \frac{\ln N(\delta)}{\ln 1/\delta}. \tag{1.16}$$

Of course, this limit may not exist for a given set. In this case one considers the *upper* and the *lower box-counting dimensions* defined respectively as

$$\overline{\dim}_B(A) := \limsup_{\delta\to 0} \frac{\ln N(\delta)}{\ln 1/\delta}, \tag{1.17}$$

$$\underline{\dim}_B(A) := \liminf_{\delta\to 0} \frac{\ln N(\delta)}{\ln 1/\delta}. \tag{1.18}$$

They always exist and satisfy

$$\overline{\dim}_B(A) \geq \underline{\dim}_B(A). \tag{1.19}$$

The box-counting dimension exists if the upper and lower box-counting dimensions are equal.

Several equivalent definitions of the box-counting dimension are available. Depending on situation some of them are more convenient than the other. Below we list some of the more popular.

Definition 1.2 *The* box-counting dimension *of a set $A \subset \mathbb{R}^n$ is*

$$\dim_B(A) := \lim_{\delta\to 0} \frac{\ln N(\delta)}{\ln 1/\delta}, \tag{1.20}$$

where $N(\delta)$ is one of the following:

1. *the number of δ-grid cubes that intersect A;*

2. *the smallest number of closed balls of diameter δ that cover A;*

3. *the smallest number of cubes of side δ that cover A;*

4. *the smallest number of sets of diameter at most δ that cover A;*

5. *the largest number of disjoint balls of diameter δ with centers in A.*

The proof of equivalence is not difficult ([76], p. 38–40).

Alternatively, we may use the Minkowski-Bouligand approach. Let $K_\delta(x)$ be a closed ball centered at x of radius δ. Thus $K_\delta(x) := \{y \in \mathbb{R}^n : |x - y| \le \delta\}$.

Definition 1.3 Minkowski sausage *or* δ-parallel body *of* $A \subset \mathbb{R}^n$ *is*

$$\begin{aligned} A_\delta &:= \bigcup_{x \in A} K_\delta(x) && (1.21) \\ &= \{y \in \mathbb{R}^n : \exists x \in A,\ |x - y| \le \delta\}. && (1.22) \end{aligned}$$

Thus the Minkowski sausage of A is the set of all the points located within δ of A.

Definition 1.4 *The* box-counting dimension *of a set $A \subset \mathbb{R}^n$ is*

$$\dim_B(A) := \lim_{\delta \to 0} \left(n - \frac{\ln V(\delta)}{\ln 1/\delta} \right), \tag{1.23}$$

where $V(\delta) = \mathrm{vol}^n(A_\delta)$ is the volume of the Minkowski sausage of A.

In fact, $V(\delta)$ can be the volume of any reasonable cover of A by sets of size δ, thus instead of closed balls in (1.21) we could use closed boxes of side δ, ellipsoids with constant ratios of axes, etc. Under certain conditions we might also use horizontal or vertical (or tilted) intervals of length δ or 2δ. This is the most convenient definition to analyze graphs of fractal curves and will be discussed subsequently (section 1.3).

It is useful to have multiple definitions for at least two reasons. Firstly, every definition is best suited to some class of problems. Secondly, even though equivalent in continuum limit, the above definitions are different when discretized. This leads to several inequivalent algorithms of estimating the box-counting dimension which is important for applications [61, 62, 239].

Example 1.1.1: While the box-counting dimension seems very natural and can be (in principle) estimated from data it has some drawbacks. Consider, for example, the set A of all the rational numbers in $[0, 1]$. It is a countable set, thus one would like it to have dimension zero. It is easy to check, however, that it's dimension is 1, because every box in every δ-grid on $[0, 1]$ contains some point of A, thus must be counted in $N(\delta)$. This means that a small ($\equiv$ countable) set can change the dimension arbitrarily. For instance if C is the triadic Cantor set of dimension $\ln 2/\ln 3$ then the set B consisting of A and C translated so they do not intersect will have box-counting dimension equal to 1. But the Cantor set is uncountable and the set of all rationals A is countable, thus a smaller set has larger dimension!

Example 1.1.2: One might think that the problem lies in the fact that A is not closed, because its closure is interval $[0, 1]$ which one would want to have dimension 1, which it has. Thus one could restrict his or her attention to closed sets. Alas, the set $F = \{0, 1, 1/2, 1/3, 1/4, \ldots\}$ is countable and compact, and yet its box-counting dimension is 1/2.

$\triangle$

Nevertheless, box-counting dimension is the simplest fractal dimension, it is widely applicable, and in many situations it turns out to be extremely useful. It is often equal to the Hausdorff dimension which does not exhibit anomalies discussed above, but is very difficult to estimate from data. We present its definition in the next section.

Other properties of the box-counting dimension will be discussed in section 1.1.4 since most of them are shared by the Hausdorff and packing dimensions.

1.1.2 Hausdorff dimension

To obtain definitions of other fractal dimensions let us reconsider definitions 1.2. We will generalize definition 2 (and 4) to obtain the Hausdorff dimension, and definition 5 to obtain the packing dimension.

Let $N(\delta)$ be the smallest number of closed balls of diameter δ necessary to cover set A. If the box-counting dimension of A is D then for sufficiently small δ we have

$$N(\delta) \approx N\delta^{-D}. \tag{1.24}$$

Therefore the box-counting dimension may also be defined as

$$\begin{aligned} \dim_B(A) &= \inf\{\alpha : N(\delta)\delta^\alpha = 0\} && (1.25)\\ &= \sup\{\alpha : N(\delta)\delta^\alpha = \infty\}. && (1.26) \end{aligned}$$

But this can also be written as

$$\dim_B(A) = \inf\{\alpha : \sum_i \delta^\alpha = 0\} = \inf\{\alpha : \sum_i |U_i|^\alpha = 0\}, \tag{1.27}$$

where the sum is taken over all the balls U_i in the cover, and $|U_i|$ stands for the diameter of U_i, which is δ. If we now allow more general covers, namely covers of arbitrary sets of diameter less or equal to δ, and keep the last expression for dimension, we then get the *Hausdorff dimension*. Let us formalize this discussion.

Consider a countable (or finite) family of sets U_i covering A. Thus $A \subset \bigcup_i U_i$. Suppose the *diameter* of each of U_i is not bigger than δ:

$$|U_i| := \sup\{|x-y| : x, y \in U_i\} \le \delta. \tag{1.28}$$

Such a family of sets is called a *δ-cover* of A.

Let α be non-negative. For $\delta > 0$ we define

$$H_\delta^\alpha(A) := \inf\left\{\sum_i |U_i|^\alpha : \{U_i\} \text{ is a } \delta-\text{cover of } A\right\}. \tag{1.29}$$

Thus it is very similar to the quantity that is minimized in the definition of the box-counting dimension (1.27), which is

$$\inf\{\sum_i |U_i|^\alpha : \{U_i\} \text{ is a cover of } A \text{ consisting of closed balls of diameter } \delta\}. \tag{1.30}$$

Definition 1.5 *The* α-dimensional Hausdorff measure *of A is*

$$H^\alpha(A) := \lim_{\delta\to 0} H^\alpha_\delta(A). \tag{1.31}$$

This limit exists for every set A even though it is usually 0 or ∞. It can also be shown to be a measure [110, 75, 192, 149]. For integer α it is equivalent to the Lebesgue measure and

$$H^n(A) = c_n \mathrm{vol}^n(A), \tag{1.32}$$

where c_n is the volume of an n-dimensional ball of diameter 1.

Let $\beta > \alpha$, $1 > \delta > 0$. Take a δ-cover $\{U_i\}$ of A. Obviously,

$$\sum_i |U_i|^\beta = \sum_i |U_i|^\alpha |U_i|^{\beta-\alpha} \le \delta^{\beta-\alpha} \sum_i |U_i|^\alpha, \tag{1.33}$$

thus taking infima of both sides we obtain

$$H^\beta_\delta(A) \le \delta^{\beta-\alpha} H^\alpha_\delta(A). \tag{1.34}$$

Taking the limit $\delta \to 0$ we immediately see $H^\alpha(A) < \infty$ implies $H^\beta(A) = 0$. Thus there must be a critical value of α at which $H^\alpha(A)$ jumps from ∞ to 0 (figure 1.1). We call this value the *Hausdorff dimension of A*.

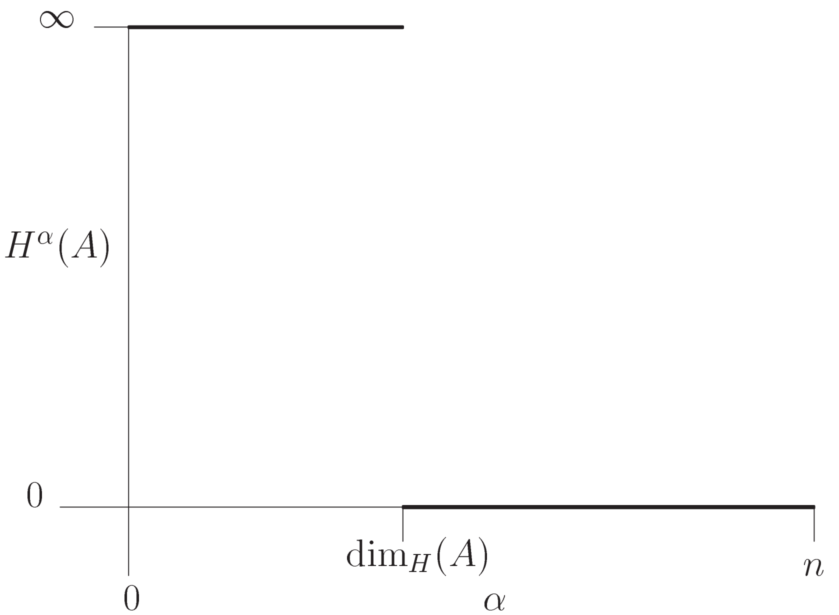

Figure 1.1: Graph of $H^\alpha(A)$ against α. The Hausdorff dimension is the value of α at which there is a jump from ∞ to 0.

Definition 1.6 *The* Hausdorff dimension *of set A is*

$$\dim_H(A) = \inf\{\alpha \,:\, H^\alpha(A) = 0\} = \sup\{\alpha \,:\, H^\alpha(A) = \infty\}. \tag{1.35}$$

It follows that

$$H^\alpha(A) = \begin{cases} \infty & \text{for}\, \alpha < \dim_H(A), \\ 0 & \text{for}\, \alpha > \dim_H(A). \end{cases} \tag{1.36}$$

For $\alpha = \dim_H(A)$ the Hausdorff measure $H^\alpha(A)$ can be 0, ∞, or finite.

Hausdorff dimension is very important in the mathematical theory of fractal dimensions due to its convenient properties. Unfortunately, in real problems it is difficult to calculate and practically impossible to obtain from data. It is, however, conjectured that often, especially for sets arising as attractors of some dynamical systems, it is equal to the box-counting dimension [80, 76, 116]. This equality is often implicitly assumed in the literature. Nevertheless, it is good to always specify which dimension one is speaking about, because they do have different properties and can behave very differently in analysis.

Some properties of the Hausdorff dimension will be reviewed and compared with the properties of other dimensions in section 1.1.4.

1.1.3 Packing dimension

Another elegant definition can be obtained from the last version of the definition 1.2.

Let $N(\delta)$ be the largest number of closed balls of diameter δ that can be packed with their centers in the set A. If the box-counting dimension of A is D then for sufficiently small δ we have

$$N(\delta) \approx N\delta^{-D}. \tag{1.37}$$

Therefore the box-counting dimension may again be defined as

$$\dim_B(A) = \inf\{\alpha \,:\, \sum_i |U_i|^\alpha = 0\}, \tag{1.38}$$

where the sum is taken over all the balls in the cover. But this time we *maximize* the number of balls in the family. If we now allow more general covers, namely covers of arbitrary sets of diameter at most δ, we can arrive at the *packing dimension.*

Let $\alpha \geq 0$, $\delta > 0$. Define

$$P_\delta^\alpha(A) \;:=\; \sup\{\sum_i |U_i|^\alpha \,:\, \{U_i\}\, \text{is a collection of disjoint balls} \tag{1.39}$$

$$\text{of diameter at most}\, \delta \,\text{with centers in}\, A\}. \tag{1.40}$$

When δ decreases, fewer families are available, therefore the supremum (1.39) decreases. Thus the following limit exists

$$P_0^\alpha(A) := \lim_{\delta\to 0} P_\delta^\alpha(A). \tag{1.41}$$

This set function, however, turns out to be not a measure [76]. But the construction can be improved.

Definition 1.7 *The* α-dimensional packing measure *of A is*

$$P^\alpha(A) := \inf\left\{\sum_i P_0^\alpha(A_i) \,:\, A \subset \bigcup_{i=1}^\infty A_i\right\}. \tag{1.42}$$

Definition 1.8 *The* packing dimension *of set A is*

$$\dim_P(A) = \inf\{\alpha \,:\, P^\alpha(A) = 0\} = \sup\{\alpha \,:\, P^\alpha(A) = \infty\}. \tag{1.43}$$

The packing dimension is no more difficult to calculate than the Hausdorff dimension, it has also the same properties. In particular it does not exhibit the pathologies of the box-counting dimensions. These days the packing dimension and measure receive more and more attention and seem to become another set of basic tools of the fractal geometry. This is why we felt a mention of these constructions is appropriate even in such a short introduction as the present text.

1.1.4 Basic properties of geometric dimensions

Following Falconer [76] we list here the basic properties of dimensions. Sets A, B are subsets of $\mathbb{R}^n$.

1. Monotonicity: If $A \subset B$ then $\dim A \leq \dim B$. (HPUL)

2. Stability: $\dim(A \cup B) = \max\{\dim A, \dim B\}$. (HPU)

3. Countable stability: $\dim(\bigcup_{i=1}^\infty A_i) = \sup_{i\in\mathbb{N}} \dim A_i$. (HP)

4. Geometric invariance: dim is invariant under geometric transformations of $\mathbb{R}^n$ like translations, rotations, similarities or affinities. (HPUL)

5. Lipschitz invariance: $\dim A = \dim f(A)$ if f is bi-Lipschitz, i.e.

$$\exists c_1, c_2\, \forall \mathbf{x}, \mathbf{y} \in A \qquad c_1|\mathbf{x} - \mathbf{y}| \leq |f(\mathbf{x}) - f(\mathbf{y})| \leq c_2|\mathbf{x} - \mathbf{y}|. \tag{1.44}$$

   (HPUL)

6. Countable sets: $\dim A = 0$ for finite or countable A. (HP)

7. Open sets: $\dim A = n$ if A is an open subset of $\mathbb{R}^n$. (HPUL)

8. Smooth manifolds: $\dim A = m$ if A is a smooth m-dimensional manifold. (HPUL)

The letters HPUL in the parentheses stand for dimensions that have given property, respectively Hausdorff, packing, lower and upper box-counting dimensions. Most of these properties are shared by all the dimensions, with two exceptions.

The upper box-counting dimension is stable, but not countably stable. This is why countable sets can have non-zero box-counting dimension. The lower box-counting dimension is not even stable. Both Hausdorff and packing dimensions of the sets considered in examples 1.1.1, 1.1.2 are 0 because these sets are countable.

The last two properties (dimension of manifolds) mean that the fractal dimensions are extensions of the ordinary definition.

Bi-Lipschitz functions seem to play a similar role in the theory of fractal dimensions to the role of homeomorphisms in topology. Fundamental geometric transformations, like rotations, translations etc. are bi-Lipschitz, thus property 5 implies 4.

One can also show the following inequalities [76]:

$$\dim_H(A) \leq \underline{\dim}_B(A) \leq \overline{\dim}_B(A), \tag{1.45}$$

$$\dim_H(A) \leq \dim_P(A) \leq \overline{\dim}_B(A). \tag{1.46}$$

Thus whenever the upper box-counting dimension is equal to the Hausdorff dimension, all the above definitions give the same number.

1.1.5 Potential theoretic method of calculating dimensions

An important method of calculating Hausdorff dimension is the potential method. We will need it later on to calculate the dimension of a typical Brownian path. We present it for the reader's convenience closely following presentation of Falconer [76] where the proofs can be found.

Take a probability or mass distribution μ on $\mathbb{R}^n$. The *s-potential* induced by μ is

$$\varphi_s(x) = \int \frac{d\mu(y)}{|x-y|^s}.$$

This is the gravitational potential for $s = 1$. The *s-energy* of μ is

$$I_s = \int \varphi_s(x)d\mu(x) = \int\int \frac{d\mu(y)d\mu(x)}{|x-y|^s}. \tag{1.47}$$

If one can distribute mass on a set A so that its s-energy is finite, than the Hausdorff dimension (thus also the box-counting dimension) is at least s.

Theorem 1.1 *Let A be a subset of $\mathbb{R}^n$.*

1. *If there is a mass distribution μ on A with $I_s(\mu) < \infty$ then*

$$H^s(A) = \infty, \qquad \text{and} \qquad \dim_H(A) \geq s.$$

2. *If A is a Borel set with $H^s(A) > 0$ then there exists a mass distribution μ on A satisfying*

$$I_s(\mu) < \infty \qquad \text{for all} \qquad t < s.$$

1.2 Fractal dimensions of measures and multifractal spectra

Fractal dimensions introduced so far are convenient characteristics of sets. It often happens, however, that our object of study is some measure concentrated on a (fractal

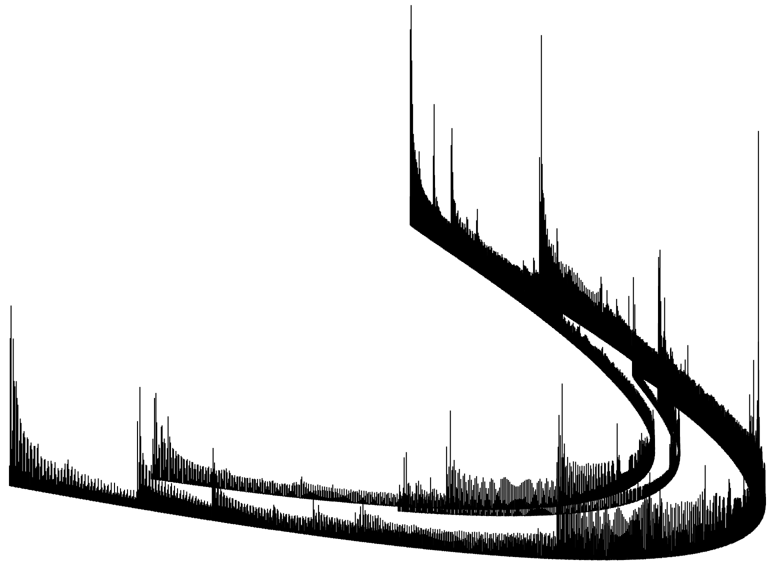

Figure 1.2: Invariant measure of the Hénon system.

or not) set. For instance, in the study of dynamical systems one is usually interested in the structure and properties of the invariant measure located on an attractor of the system (figure 1.2). In growth processes one studies the distribution of mass of an aggregate which can be very complicated. One can also study the distribution of electric potential or current in random resistor networks, distribution of stress, or chemical composition, and so on.

None of the introduced so far dimensions takes account of the weights induced on various parts of the set by the measure. To improve these definitions two approaches were proposed. Rather straightforward generalization of the box-counting dimension led to the Rényi dimensions. These were known since late fifties [11, 189] but gained wider recognition after publication of the papers by Grassberger, Hentschel and Procaccia [93, 114, 98, 99].

Another idea was to decompose the support of the measure into a family of sets with the same local scaling behavior and examine their dimensions. This approach led to the so-called f_α spectrum [107, 86].

In many cases the two spectra of dimensions, D_q spectrum of Rényi dimensions and f_α spectrum, are connected. In case of invariant measures of hyperbolic dynamical systems the theory has taken particularly beautiful structure with the application of so-called "thermodynamic formalism" [210, 35, 194, 16].

1.2.1 Rényi dimensions

Let us take a partition of $\mathbb{R}^n$ into boxes of equal volume δ^n induced by a δ-grid. For a probability measure μ located on a subset $U \subset \mathbb{R}^n$ ($\operatorname{supp}\mu = U$) let

$$p_i = \mu(i - \text{th cell}) = \int_{i-\text{th cell}} d\mu(x).$$

One defines the *Rényi dimensions* as

$$D_q(\mu) := \begin{cases} \lim\limits_{\delta\to 0} \dfrac{1}{q-1}\dfrac{\ln \sum_i p_i^q}{\ln \delta}, & \text{for } q \in \mathbb{R}\setminus\{1\}, \\ \lim\limits_{\delta\to 0} \dfrac{1}{q-1}\dfrac{\sum_i p_i \ln p_i}{\ln \delta}, & \text{for } q = 1, \end{cases} \tag{1.48}$$

where the sum is taken over all cells with $p_i \neq 0$.

It is easy to check that for $q = 0$ we regain the definition (1.1). Thus D_0 is the box-counting dimension. Of particular importance are also D_1 — the *information dimension* or the *dimension of the measure* [190, 79], which describes how the entropy $S = -\sum_i p_i \ln p_i$ increases with the change of the scale, and D_2 — the *correlation dimension* [98, 99], which can be most easily extracted from data, usually treated as a lower estimate of D_1 since $D_{q_1} \le D_{q_2}$ for $q_1 \ge q_2$ (see below).

It may happen that the limit invoked in the definition (1.48) of the Rényi dimensions does not exist, because it depends on the way we choose δ-partitions. In this case we can refine the definition [107] by taking infima or suprema (depending on q) over all the possible δ-partitions, which leads to a generalization of the Hausdorff dimension. Alternatively we can take the lower and upper Rényi dimensions defined by

$$\begin{aligned} \underline{D_q} &= \liminf_{\delta\to 0}\left(\frac{1}{q-1}\frac{\ln\sum_i p_i^q}{\ln\delta}\right), \\ \overline{D_q} &= \limsup_{\delta\to 0}\left(\frac{1}{q-1}\frac{\ln\sum_i p_i^q}{\ln\delta}\right), \end{aligned}$$

which generalize lower and upper box-counting dimensions [76].

It is generally believed, however, that most physical objects have the dimensions, i.e. the limit in definition (1.48) does not depend on particular choice of partitions and the lower and upper dimensions coincide.

The function D_q is often continuous or even differentiable but not always. Let us consider three specific examples.

Example 1.2.1: Uniform measures. Consider a measure smeared out uniformly on an n-dimensional cube of side a ($[0,a]^n$). Thus

$$\mu(d\mathbf{x}) = \varrho(\mathbf{x})d\mathbf{x} = 1/a^n\, d\mathbf{x}. \tag{1.49}$$

Therefore, for i-th box of δ-grid we have $p_i = \delta^n/a^n$ if the box is a subset of the cube, or 0 if it is not. Contributions from the boundary boxes can be neglected in the limit. From the definition (1.48) we obtain

$$D_q = \lim_{\delta\to 0}\frac{1}{q-1}\frac{\ln\sum_i(\delta^n/a^n)^q}{\ln\delta} \tag{1.50}$$

But one needs approximately $(a/\delta)^n$ boxes to cover the cube thus

$$\begin{aligned} D_q &= \lim_{\delta\to 0}\frac{1}{q-1}\frac{\ln[(a/\delta)^n(\delta^n/a^n)^q]}{\ln\delta} && (1.51)\\ &= \lim_{\delta\to 0}\frac{1}{q-1}\frac{\ln[(\delta/a)^{n(q-1)}]}{\ln\delta} && (1.52)\\ &= n. && (1.53)\end{aligned}$$

We see that for uniform measures on open sets the Rényi dimensions are all equal to the dimension of the set ($\equiv$ to the dimension of the space).

Example 1.2.2: Ulam map. Consider a paradigmatic dynamical system, Ulam map $f(x) = 4x(1-x)$ on $[0,1]$ [240]. Density of its invariant measure[2] is

$$\varrho(x) = \frac{1}{\pi\sqrt{x(1-x)}}. \qquad (1.54)$$

Divide the interval $[0,1]$ into $2N$ boxes of length $\delta = 1/2N$. Probability to find the system in the i-th box is

$$p_i = \int_{(i-1)\delta}^{i\delta}\varrho(x)dx. \qquad (1.55)$$

For $x < 1/2$ we have

$$\frac{1}{\pi\sqrt{x}} \le \frac{1}{\pi\sqrt{x(1-x)}} \le \sqrt{2}\frac{1}{\pi\sqrt{x}}. \qquad (1.56)$$

Thus

$$p_i = c_i\frac{2}{\pi}\sqrt{\delta}(\sqrt{i}-\sqrt{i-1}), \qquad (1.57)$$

where c_i is bounded $1 \le c_i \le \sqrt{2}$. But

$$\frac{1}{2\sqrt{i}} \le \sqrt{i}-\sqrt{i-1} = \frac{1}{\sqrt{i}+\sqrt{i-1}} \le \frac{1}{\sqrt{i}}, \qquad (1.58)$$

therefore

$$p_i = d_i\frac{1}{\pi}\sqrt{\delta/i}, \qquad (1.59)$$

with $d_i \in [1, 2\sqrt{2}]$. Since the density is symmetric with respect to $x = 1/2$ we have

$$\begin{aligned} \sum_{i=1}^{2N} p_i^q &\sim \sum_{i=1}^{N}(\delta/i)^{q/2} \sim \int_1^{1/(2\delta)}(\delta/i)^{q/2}di && (1.60)\\ &= \frac{\delta^{q/2}}{q/2-1}[1-(2\delta)^{q/2-1}]. && (1.61)\end{aligned}$$

[2] Invariant measures of dynamical systems are described in every good textbook on dynamical systems and chaos, e.g. [168, 206, 169, 207]. The recommended source for a serious reader is [138, 139] (these are two editions of the same book). We give a brief description in chapter 3.

Thus

$$
\begin{aligned}
D_q &= \lim_{\delta\to 0}\frac{1}{q-1}\frac{\ln\dfrac{\delta^{q/2}-2^{q/2-1}\delta^{q-1}}{q/2-1}}{\ln\delta} && (1.62)\\
&= \begin{cases} 1, & \text{for } q\le 2,\\ \dfrac{q}{2(q-1)}, & \text{for } q\ge 2. \end{cases} && (1.63)
\end{aligned}
$$

Thus in this case the spectrum of Rényi dimensions is continuous but not differentiable in $q = 2$ [171, 15, 206]. This is behavior analogous to phase transitions [129, 222].

It is often believed that most dimensions of attractors are invariant under smooth transformations of the underlying dynamics. This case shows one must be cautious in such assumptions. A smooth and one-to-one on $t \in [0, 1]$ transformation $x = \sin^2(\frac{\pi}{2}t)$ transforms the logistic map into a tent map and the invariant measure goes over into a constant measure with density $\varrho(x) = 1$. In this case $D_q(\mu) = 1$ for every q, which is different from (1.63) for $q > 2$. For discussion see [16, 171].

Example 1.2.3: Spikes. Take a normalized measure [15] on $[0, 1]$

$$\varrho(x) = \beta + (1-\beta)\delta(x), \tag{1.64}$$

where parameter $\beta \in [0, 1]$. Divide $[0, 1]$ into N boxes of length ε. The fraction of the measure in the i-th box is

$$
\begin{aligned}
p_1 &\approx 1-\beta, && (1.65)\\
p_i &= \beta/N, \qquad \text{for } i > 1. && (1.66)
\end{aligned}
$$

Therefore one can easily see that

$$D_q = \begin{cases} 1, & q < 1,\\ \beta, & q = 1,\\ 0, & q > 1. \end{cases} \tag{1.67}$$

Thus in this case the Rényi spectrum of dimensions D_q is not only non-differentiable but also discontinuous. Thus in general

$$D_1 \neq \lim_{q\to 1} D_q. \tag{1.68}$$

△

Function D_q cannot be arbitrary. The following bounds have been obtained [114, 15]

$$
\begin{aligned}
D_{q'} &\ge D_q \ge 0 \qquad \text{for } q \ge q', && (1.69)\\
\frac{q-1}{q}D_q &\ge \frac{q'-1}{q'}D_{q'} \qquad \text{for } q \ge q',\ qq' \ge 0. && (1.70)
\end{aligned}
$$

The first inequality means D_q is a monotonic non-increasing function of q. The second inequality is non-trivial only for $q > q' > 1$ and $0 > q > q'$. In particular (1.69) and (1.70) yield the following bounds on D_q for $q \ge 2$

$$D_2 \ge D_\infty \ge \frac{1}{2}D_2, \tag{1.71}$$

and for $q \leq -1$

$$2D_{-1} \geq D_{-\infty} \geq \ D_{-1}. \tag{1.72}$$

Inequalities (1.69) and (1.70) follow essentially from convexity of p^q. The proofs are not difficult and are in the spirit of our proofs of similar inequalities in chapter 3.

1.2.2 f_α spectrum of dimensions

An equivalent description of multifractal measures is f_α spectrum [107, 86]. We shall give here its crude description. The original idea was to decompose the support of measure into a family of fractals each of different dimension by choosing these boxes from δ-grid whose content scales similarly. In order to do it we introduce for $\alpha \in \mathbb{R}$

$$N_\delta(\alpha) := \#\{i \ : \ \mu(i - \text{th cell}) \geq \delta^\alpha\},$$

where $\#A$ is the number of points in set A. It is natural to examine

$$\lim_{\delta\to 0}[-\ln N_\delta(\alpha)/\ln\delta]$$

but it needs not be a dimension of any particular set, since the boxes counted for small δ need not be contained in boxes counted when δ is large. Nevertheless, we can define

$$f_\alpha := \lim_{\varepsilon\to 0}\lim_{\delta\to 0}\frac{\ln[N_\delta(\alpha+\varepsilon) - N_\delta(\alpha-\varepsilon)]}{\ln 1/\delta}, \tag{1.73}$$

if the above limits exist. Thus for a given η for sufficiently small δ, ε we have

$$\delta^{-f_\alpha+\eta} \leq N_\delta(\alpha+\varepsilon) - N_\delta(\alpha-\varepsilon) \leq \delta^{-f_\alpha-\eta}.$$

The f_α curve is called a *multifractal spectrum* or *spectrum of singularities* or simply f_α *spectrum.*

We also introduce

$$S_\delta(q) := \sum_i \mu(i - \text{th cell})^q.$$

We used $S_\delta(q)$ to define the Rényi dimensions in the previous subsection, thus we expect that for small δ it scales as

$$S_\delta(q) \propto \delta^{(q-1)D_q}.$$

From the above definitions we can see that the number of δ-boxes whose content scales as δ^α is approximately δ^{-f_α}, therefore we have approximately

$$\begin{aligned} S_\delta(q) &\approx \int_0^\infty \delta^{-f_\alpha}(\delta^\alpha)^q d\alpha \\ &= \int_0^\infty \delta^{q\alpha - f_\alpha} d\alpha. \end{aligned}$$

Under certain assumptions from the saddle-point method we infer the dominant contribution to this integral comes from the value of α for which the exponent $q\alpha - f_\alpha$ is greatest, thus we expect

$$S_\delta(q) \sim \delta^{\sup_\alpha(q\alpha - f_\alpha)} \sim \delta^{(q-1)D_q}.$$

Indeed, if f_α exists (1.73) one can show

$$(q-1)D_q = \sup_{0 \le \alpha < \infty} (q\alpha - f_\alpha).$$

When f_α and D_q are continuous functions of their parameters there is a much richer structure of the theory. It turns out the two spectra are Legendre transforms of each other. We will not develop this theory because we will not use it anywhere. There are numerous works and reviews on multifractals, some of which excellent. A sample reference list is given at the end of this chapter.

1.3 Box-counting dimension of fractal graphs of functions

Until recently it was universally assumed that a single valued continuous function of a real variable always had a first derivative whose value could become undefined or infinitely large only at isolated points. To my knowledge, even in the writings of Gauss, Cauchy, and Dirichlet there is no remark from which one can infer without doubt that these mathematicians, who in their science were accustomed to exercise the severest criticism, held any other opinion. (...) One can, however, easily construct continuous functions of a real argument x, for which it is possible to show by the simplest of means that these functions do not have a well-defined differential quotient for any value of x.

Karl Weierstraß, *"On continuous functions of a real argument that do not have a well-defined differential quotient", [247] transl. B. Sawhill, reprinted in [68].*

The second half of the XIX-th century was the time when the foundations of analysis were clarified, and the distinction between continuous and differentiable functions was made. The question of existence of functions which are continuous but nowhere differentiable was inevitable. According to sources [247], the first person to consider this problem was Georg Friedrich Bernhard Riemann (1826–1866). Around 1861 he conjectured the function

$$r(x) = \sum_{n=1}^{\infty} \frac{\sin(n^2 x)}{n^2} \tag{1.74}$$

was continuous but non-differentiable. However, he was not able to show this. Thus in 1872 Carl Weierstrass (1815-1897) proposed another function which is now referred to by his name [247, 108]:

$$W(x) = \sum_{n=0}^{\infty} a^n \cos(b^n x\pi). \tag{1.75}$$

He proved it is non-differentiable at any x for certain values of a and b. These results were not published during Weierstrass's life and appeared only in his collected works. The next step was made by Godfrey Harold Hardy (1877-1947) who proved non-differentiability of $W(x)$ for all the values of a, b satisfying $b > 1 > a > 0,\ ab \geq 1$. He also provided a proof of non-differentiability of $r(x)$ for any irrational x. It was later shown that $r(x)$ is differentiable at some rational values of x [92, 212].

In fact, Hardy did not only show non-differentiability of $W(x)$ but also quantified it, namely he proved

$$\sup\{|f(x) - f(y)| : |x - y| \leq \delta\} \sim \delta^H, \tag{1.76}$$

where

$$H = \frac{\ln(1/a)}{\ln b}.$$

From this it easily follows as we show in the next sections that the box-counting dimension of the graph of the Weierstrass function $W(x)$ is

$$D_W = 2 + \frac{\ln a}{\ln b} = 2 - \left|\frac{\ln a}{\ln b}\right|. \tag{1.77}$$

Functions whose graphs have non-integer box-counting dimension will be called *fractal functions*.

We are interested in fractal functions because in chapter 4 we will construct Weierstrass-like fractal solutions of the Schrödinger equation. In order to show their fractality we need to establish the theory of the box-counting dimension of fractal functions. We do it in the next few sections.

1.3.1 Oscillations, variations and box-counting dimensions

Consider a continuous function on a closed interval $f : [a, b] \to \mathbb{R}$. Its graph is a curve in the plane. To calculate its box-counting dimension divide the axes into δ-grid $[n\delta, (n+1)\delta] \times [m\delta, (m+1)\delta]$ and calculate the number of boxes $N(\delta)$ intersecting the graph.

Choose one of the columns in the grid containing all the points (x, y) such that $x \in [n\delta, (n + 1)\delta]$. Since the curve is continuous the number of the boxes in this column intersecting the graph of f is at least

$$\left[\sup_{x\in[n\delta,(n+1)\delta]} f(x) - \inf_{x\in[n\delta,(n+1)\delta]} f(x)\right] /\delta \tag{1.78}$$

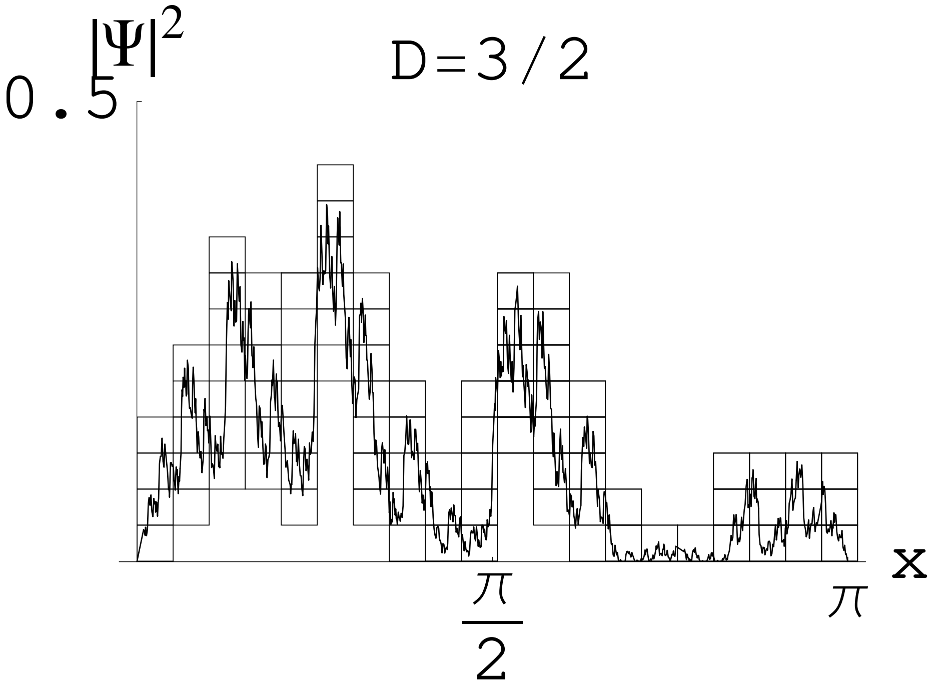

Figure 1.3: Graph of a continuous function (square of (4.8) at $t = 0$) covered by boxes of the δ-grid.

and no more than the same plus 2. If f was a record of a signal then the difference between the maximum and minimum value of f on the given interval quantifies how the signal oscillates on this interval. That's why we call it *oscillation*.

Definition 1.9 δ-oscillation *of f in x is*

$$\begin{aligned} \mathrm{osc}_\delta(x)(f) &:= \sup_{|y-x|\le\delta} f(y) - \inf_{|y-x|\le\delta} f(y) && (1.79)\\ &= \sup\{|f(y)-f(z)| \,:\, y,z\in[a,b]\cap[x-\delta,x+\delta]\}. && (1.80)\end{aligned}$$

We will skip (f) if it is clear from the context which function we consider.

From (1.78) we obtain the following estimate on the total number of boxes covering the graph of f:

$$\sum_{m=1}^{M} \mathrm{osc}_{\delta/2}(x_m)/\delta \le N(\delta) \le 2M + \sum_{m=1}^{M} \mathrm{osc}_{\delta/2}(x_m)/\delta, \tag{1.81}$$

where $x_m = a + (m-1/2)\delta$ is the middle of the mth column from the cover of the graph and $M = \lceil \frac{b-a}{\delta} \rceil$ is the number of columns in the cover ($\lceil x \rceil$ stands for the smallest integer greater or equal to x). Thus

$$N(\delta) \approx M\, \overline{\mathrm{osc}}_{\delta/2}/\delta. \tag{1.82}$$

If the graph of f has the box-counting dimension D, $N(\delta)$ scales as δ^{-D}. This implies the following scaling of the oscillations

$$\begin{aligned}\overline{\mathrm{osc}}_{\delta/2} &\approx N(\delta)\delta/M &(1.83)\\ &\approx \frac{c\delta^{-D}\cdot\delta}{\left(\frac{b-a}{\delta}\right)} &(1.84)\\ &\propto \delta^{2-D}. &(1.85)\end{aligned}$$

We have thus established a connection between the box-counting dimension of the graph and the scaling exponent of the local oscillation of the function f.

Functions with regular oscillations, i.e. such that $\mathrm{osc}_\delta(x)(f) \approx c\delta^H$ with c independent of x are called *Hölderian of exponent H*. Thus

$$\dim_B \mathrm{graph} f = 2 - H \tag{1.86}$$

for such functions. We will make it more precise and general in the next section. Combining this observation with Hardy's result (1.76) we immediately get the dimension of the Weierstrass function

$$\dim_B \mathrm{graph} W(x) = 2 - H = 2 - \frac{\ln(1/a)}{\ln b} \in]1, 2[. \tag{1.87}$$

We can use the notion of average oscillation not only for Hölder functions. To give it a definite meaning we introduce the following

Definition 1.10 δ-variation *of function f is*

$$\begin{aligned}\mathrm{Var}_\delta(f) &:= \int_a^b \mathrm{osc}_\delta(x)(f)\,dx &(1.88)\\ &=: (b-a)\overline{\mathrm{osc}}_\delta(f). &(1.89)\end{aligned}$$

Geometrically, variation is the area of the set scanned by the graph of f moved horizontally $\pm\delta$ and truncated at $x = a$ and $x = b$, thus it is a kind of δ-Minkowski sausage constructed with horizontal intervals of length 2δ. This observation leads to another convenient means of calculating the dimension.

Theorem 1.2 *Let $f(x)$ be a non constant continuous function on $[a, b]$, then*

$$\dim_B \mathrm{graph} f = \lim_{\delta\to 0}\left(2 - \frac{\ln \mathrm{Var}_\delta(f)}{\ln \delta}\right). \tag{1.90}$$

For proof see [238], p. 148. Another convenient condition which we will use in its simplest version ($\alpha = 1$) is connected with analysis of the structure function $S_\alpha(x) = \int_a^b |f(x+\delta) - f(x-\delta)|^\alpha dx$.

Theorem 1.3 (Tricot) *Let $f(x)$ be a continuous function defined on $[a, b]$. We assume there exist two parameters $\alpha \geq 1$, $0 < H < 1$ and two constants c_1 and c_2 such that*

1.

$$\sup_{x\in[a,b]} |f(x+\delta) - f(x-\delta)| \le c_1\delta^H, \tag{1.91}$$

2.

$$\left[\int_a^b |f(x+\delta) - f(x-\delta)|^\alpha dx\right]^{1/\alpha} \ge c_2\delta^H. \tag{1.92}$$

Then

$$\boxed{\dim_B \mathrm{graph} f = 2 - H.}$$

For proof see [238], p. 158.

The definitions we have introduced so far carry over to functions on $\mathbb{R}^n$. We need them to consider behavior of the fractal solutions of the Schrödinger equation in time and space (see chapter 4).

Let $\Omega = [a_1, b_1] \times \ldots \times [a_n, b_n]$ and $f : \mathbb{R}^n \supset \Omega \to \mathbb{R}$ — continuous. The volume of Ω is $\mathrm{vol}^n(\Omega) = \prod_{k=1}^n (b_k - a_k)$.

Definition 1.11 *δ-oscillation of f in $\mathbf{x} = (x^1, \ldots, x^n)$ is*

$$\mathrm{osc}_\delta(\mathbf{x})(f) := \sup\{|f(\mathbf{y}) - f(\mathbf{z})| \,:\, y^k, z^k \in [x^k - \delta, x^k + \delta] \cap [a_k, b_k]\}. \tag{1.93}$$

Generalizing the definition of oscillation we have some freedom. We chose supremum over n-dimensional box. Sometimes it is convenient to use supremum over balls, we then write sup symbol explicitly.

Definition 1.12 δ-variation *of function f is*

$$\mathrm{Var}_\delta(f) := \int_\Omega \mathrm{osc}_\delta(\mathbf{x})(f)\, d^n\mathbf{x} \tag{1.94}$$

$$=: \mathrm{vol}^n(\Omega)\overline{\mathrm{osc}}_\delta(f). \tag{1.95}$$

Theorem 1.4 *Let $f(x)$ be a non constant continuous function on Ω, then*

$$\dim_B \mathrm{graph} f = \lim_{\delta\to 0}\left(n + 1 - \frac{\ln \mathrm{Var}_\delta(f)}{\ln\delta}\right). \tag{1.96}$$

We will prove this theorem in case of Hölderian functions in the next section.

Now that we have some understanding of the local structure of fractal functions, in the next section we will discuss the case of Hölderian functions, then we calculate the box-counting dimension of a Weierstrass-like function. Finally we consider the connection between the dimension of the graph of a function and of the graph of its square.

1.3.2 Hölderian functions and their dimensions

Let $\Omega = [a_1, b_1] \times \ldots \times [a_n, b_n]$ and $f : \mathbb{R}^n \supset \Omega \to \mathbb{R}$ — continuous.

Definition 1.13 *Function f is* Hölderian of exponent H *if one of the following equivalent conditions holds:*

1. $\exists c > 0\ \forall \mathbf{x}, \mathbf{y} \in X: \qquad |f(\mathbf{x}) - f(\mathbf{y})| \leq c|\mathbf{x} - \mathbf{y}|^H.$
2. $\exists c > 0\ \forall \delta > 0: \qquad \sup_{|\mathbf{x}-\mathbf{y}| \leq \delta} |f(\mathbf{x}) - f(\mathbf{y})| \leq c\delta^H.$
3. $\exists c > 0\ \forall \delta > 0: \qquad \mathrm{osc}_\delta(\mathbf{x})(f) \leq c\delta^H.$

Proof: Equivalence of 2. and 3. is obvious, because one can both inscribe and circumscribe n-dimensional ball into n-dimensional box. Implication 2.$\Rightarrow$1. is obvious. To see the implication from 1. to 2. assume

$$|f(\mathbf{x}) - f(\mathbf{y})| \leq c|\mathbf{x} - \mathbf{y}|^H$$

for every $\mathbf{y}$. Let $\mathbf{y}_1, \mathbf{y}_2$ be defined by

$$\begin{aligned} f(\mathbf{y}_1) &= \sup_{|\mathbf{x}-\mathbf{y}| \leq \delta} f(\mathbf{y}), \\ f(\mathbf{y}_2) &= \inf_{|\mathbf{x}-\mathbf{y}| \leq \delta} f(\mathbf{y}). \end{aligned}$$

Then

$$\begin{aligned} \sup_{|\mathbf{x}-\mathbf{y}| \leq \delta} |f(\mathbf{x}) - f(\mathbf{y})| &= f(\mathbf{y}_1) - f(\mathbf{y}_2) \\ &= f(\mathbf{y}_1) - f(\mathbf{x}) + f(\mathbf{x}) - f(\mathbf{y}_2) \\ &\leq 2c\delta^H. \end{aligned}$$

□

If f is differentiable, the ratio $[\mathrm{osc}_\delta(x)(f)]/2\delta$ tends to the derivative of f in x: $f'(x)$. When the derivative does not exist, the Hölder exponent measures the degree of irregularity of the function. It is therefore convenient to introduce the notion of *semi-fractals*. A semi-fractal is an n times continuously differentiable function $f : \mathbb{R}^n \to \mathbb{R}^m$ such that its n-th derivative is fractal. For instance, if you integrate the Weierstrass-function from 0 to x you will obtain once differentiable function whose first derivative is fractal. Thus the obtained integral is a semi-fractal. Another example is given in chapter 4.

Definition 1.14 *Function f is* anti-Hölderian of exponent H *if one of the following equivalent conditions holds:*

1. $\exists c > 0\ \forall \delta > 0: \qquad c\delta^H \leq \sup_{|\mathbf{x}-\mathbf{y}| \leq \delta} |f(\mathbf{x}) - f(\mathbf{y})|.$
2. $\exists c > 0\ \forall \delta > 0: \qquad c\delta^H \leq \mathrm{osc}_\delta(\mathbf{x})(f).$

Definition 1.15 *Function f is* bi-Hölderian of exponent H *if*

$$\exists c_1, c_2 > 0 \; \forall \mathbf{x}, \mathbf{y} \in \Omega : \qquad c_1 |\mathbf{x} - \mathbf{y}|^H \leq |f(\mathbf{x}) - f(\mathbf{y})| \leq c_2 |\mathbf{x} - \mathbf{y}|^H. \tag{1.97}$$

Definition 1.16 *Function f is* bi-sup-Hölderian of exponent H *if one of the following equivalent conditions holds:*

1. $\exists \delta_0 \; \forall \delta < \delta_0 \; \exists c_1, c_2 > 0 \; \forall x : \qquad c_1 \delta^H \leq \sup_{|\mathbf{x}-\mathbf{y}| \leq \delta} |f(\mathbf{x}) - f(\mathbf{y})| \leq c_2 \delta^H.$

2. $\exists \delta_0 \; \forall \delta < \delta_0 \; \exists c_1, c_2 > 0 \; \forall x : \qquad c_1 \delta^H \leq \mathrm{osc}_\delta(\mathbf{x})(f) \leq c_2 \delta^H.$

Note the asymmetry in the definitions of Hölderian and anti-Hölderian functions.

We shall now try to establish some facts useful in estimating the box-counting dimension of graphs.

Theorem 1.5 *Let $1 > H > 0$. If function f is*

1. *Hölderian of exponent H, then* $\dim_B \mathrm{graph} f \leq n + 1 - H$.

2. *anti-Hölderian of exponent H, then* $\dim_B \mathrm{graph} f \geq n + 1 - H$.

3. *bi-sup-Hölderian of exponent H, then* $\dim_B \mathrm{graph} f = n + 1 - H$.

This is intuitively clear. The number of n-dimensional boxes of the δ-grid covering the domain of f is proportional to $1/\delta^n$. The number of $n+1$ dimensional boxes in a typical column over the domain covering the graph is $\overline{\mathrm{osc}}_{\delta/2}/\delta$. Thus

$$\begin{aligned} N_\delta &\approx \left(\frac{1}{\delta}\right)^n \overline{\mathrm{osc}}_{\delta/2}(\mathbf{x})/\delta \\ &\approx c\delta^{H-n-1} \\ &\propto \delta^{-D}, \end{aligned}$$

and $D = n + 1 - H$.

Proof: Without restricting generality we may assume

$$f : [0,1]^n \to \mathbb{R}.$$

Divide $[0,1]$ in every direction into a δ-mesh. Let $m = \lceil 1/\delta \rceil$, where $\lceil x \rceil$ is the smallest integer greater or equal to x. Let $N(\delta)$ be the number of δ-boxes crossing the graph of f. Then

$$\delta^{-1} \sum_{i_1,\ldots,i_n=1}^{m} \mathrm{osc}_{\delta/2}\left(\left(i_1 - \frac{1}{2}\right)\delta, \ldots, \left(i_n - \frac{1}{2}\right)\delta\right) \leq N(\delta) \leq$$
$$2m^n + \delta^{-1} \sum_{i_1,\ldots,i_n=1}^{\lceil m \rceil} \mathrm{osc}_{\delta/2}\left(\left(i_1 - \frac{1}{2}\right)\delta, \ldots, \left(i_n - \frac{1}{2}\right)\delta\right).$$

1. If f is Hölderian, than

$$\begin{aligned}
N_\delta &\leq 2\left(\frac{1}{\delta}+1\right)^n + \delta^{-1}\left(\frac{1}{\delta}+1\right)^n c(\delta/2)^H \\
&\leq (2/\delta)^n[2+c\delta^{H-1}] \\
&\leq (2+c)2^n\delta^{H-1-n}
\end{aligned}$$

Therefore

$$\overline{\dim}_B \mathrm{graph} f = \limsup_{\delta\to 0}\frac{\ln N_\delta}{-\ln\delta} \leq n+1-H. \tag{1.98}$$

2. If f is anti-Hölderian, than

$$\begin{aligned}
N_\delta &\geq \delta^{-1}m^n c(\delta/2)^H \\
&\geq \frac{c}{2^H}\delta^{-1-n+H}
\end{aligned}$$

Therefore

$$\underline{\dim}_B \mathrm{graph} f = \liminf_{\delta\to 0}\frac{\ln N_\delta}{-\ln\delta} \geq n+1-H. \tag{1.99}$$

□

1.3.3 Dimensions of cross-sections and the dimension of the graph

It is interesting to ask what is the dimension of the graph of f given all the dimensions of its cross-sections, namely given

$$\dim_B \mathrm{graph} f(x^1 = \mathrm{const}, \ldots, x^i, \ldots, x^n = \mathrm{const}), \tag{1.100}$$

what is

$$\dim_B \mathrm{graph} f(x^1, \ldots, x^n)? \tag{1.101}$$

For functions bi-sup-Hölderian in every direction we will calculate it. The proof can be extended to arbitrary functions using average oscillation (i.e. variation) instead. We will need this fact in chapter 4 to calculate the dimensions of the fractal quantum carpets.

Theorem 1.6 *Let $f : [a_1, b_1] \times \ldots \times [a_n, b_n] \to \mathbb{R}$ — continuous. Let $f_i(x^i)$ be a restriction of f to the one-dimensional line going through $(x^1 = x^1_0, \ldots, x^n = x^n_0)_i$, where we left out x^i. Suppose that*

1. *at every point $(x^1_0, \ldots, x^n_0)_i$, f_i is Hölderian of exponent H_i,*
2. *at almost every point $(x^1_0, \ldots, x^n_0)_i$, f_i is anti-Hölderian of exponent H_i.*

Then

1. *at almost every point $(x^1_0, \ldots, x^n_0)_i$*

$$s_i := \dim_B \mathrm{graph} f_i(x^i) = 2 - H_i, \tag{1.102}$$

2.

$$\begin{aligned}
\dim_B \mathrm{graph} f(x^1,\ldots,x^n) &= n-1+\max\{s_1,\ldots,s_n\} && (1.103)\\
&= n+1-\min\{H_1,\ldots,H_n\}. && (1.104)
\end{aligned}$$

Put simply, consider a function $f:\mathbb{R}^2\to\mathbb{R}$. Its graph is like a profile of a birthday cake. Now the question is, what is its dimension when the dimension of the profile of a typical thin slice is known. It is clear that the direction of greatest folding will determine the folding of the whole profile.

The reason we put "almost every" at the second condition is that this is the typically encountered situation, for instance in chapter 4 we will consider solutions of the Schrödinger equation $\Psi:\mathbb{R}^2\ni(x,y)\to\Psi(x,y)\in\mathbb{C}$ with the property, that almost every cross-section along the time axis of the graph of probability density $|\Psi|^2\in\mathbb{R}$ has the dimension $D_t>1$ but there is a dense set of values of x such that if we cut the graph at them we get a smooth function of dimension 1.

Proof:

1. At almost every point $(x_0^1,\ldots,x_0^n)_i$, f_i is bi-sup-Hölderian of exponent H_i.
2. (a) We will show that f is Hölderian of exponent $\min(H_1,\ldots,H_n)$:

$$\begin{aligned}
&|f(x^1,\ldots,x^n)-f(y^1,\ldots,y^n)|\\
&= |f(x^1,x^2,\ldots,x^n)-f(y^1,x^2,\ldots,x^n)+\\
&\quad +f(y^1,x^2,x^3\ldots,x^n)-f(y^1,y^2,x^3\ldots,x^n)+\ldots\\
&\quad +f(y^1,\ldots,y^{n-1},x^n)-f(y^1,\ldots,y^n)|\\
&\le \sum_{k=1}^{n}|f(y^1,\ldots,y^{k-1},x^k,x^{k+1},\ldots,x^n)+\\
&\quad -f(y^1,\ldots,y^{k-1},y^k,x^{k+1},\ldots,x^n)|.
\end{aligned}$$

Therefore

$$\begin{aligned}
&\mathrm{osc}_\delta(x^1,\ldots,x^n)(f)\\
&\le \sum_{k=1}^{n}\sup_{t^i\in[x^i-\delta,x^i+\delta]}\mathrm{osc}_\delta(x^k)(f(t^1,\ldots,t^{k-1},\cdot,t^{k+1},\ldots,t^n))\\
&\le \sum_{k=1}^{n}c_k\delta^{H_k}\\
&\le \left(\sum_{k=1}^{n}c_k\right)\delta^{\min(H_1,\ldots,H_n)}\\
&= c\delta^{2-\max(s_1,\ldots,s_n)},
\end{aligned}$$

where $c=\sum_{k=1}^{n}c_k$ is a constant.

(b) We will show that f is anti-Hölderian of exponent $\min(H_1,\ldots,H_n)$:

$$\mathrm{osc}_\delta(x^1,\ldots,x^n)(f)$$

$$\begin{aligned}
&\geq \max_k \sup_{t^i \in [x^i-\delta, x^i+\delta]} \mathrm{osc}_\delta(x^k)(f(t^1,\ldots,t^{k-1},\cdot,t^{k+1},\ldots,t^n)) \\
&\geq \max_k c_k \delta^{H_k} \\
&= c_{\tilde{k}} \delta^{\min(H_1,\ldots,H_n)} \\
&= c_{\tilde{k}} \delta^{2-\max(s_1,\ldots,s_n)},
\end{aligned}$$

where $\tilde{k}$ is the index of the most oscillating variable (with the lowest Hölder exponent H_k).

We have thus shown that f is bi-sup-Hölderian, therefore from Theorem 1.5 we obtain

$$\begin{aligned}
\dim_B \mathrm{graph} f(x^1,\ldots,x^n) &= n+1-\min\{H_1,\ldots,H_n\} \\
&= n+1-(2-\max\{s_1,\ldots,s_n\}).
\end{aligned}$$

□

1.3.4 Dimension of Weierstrass-like functions

We will show that the box-counting dimension of the function

$$\sum_{k=0}^{\infty} q^{(s-2)k} \sin(q^k x + \varphi_k),$$

is s. In order to do this we will first show that it is Hölder in every point with the exponent $2-s$, which implies $\dim_B \mathrm{graph} f \leq s$. Then we will show $\mathrm{Var}_\delta f \geq \delta^{2-s}$ which implies $\dim_B \mathrm{graph} f \geq s$. This is essentially the proof given by Tricot ([238], p. 156) for $\sum_{n=0}^{\infty} q^{(s-2)n} \cos(q^n x + \varphi_n)$. We present here these calculations, because all the proofs of fractality in chapter 4 are based on the same reasoning.

Proof:

1. Let

$$W_n(x) := \sum_{k=0}^{n} q^{(s-2)k} \sin(q^k x + \varphi_k).$$

It is a smooth function whose derivative at every point satisfies

$$\begin{aligned}
|W_n'(x)| &\leq \sum_0^n q^{(s-2+1)k} = \sum_0^n q^{(s-1)k} \\
&= \frac{q^{(s-1)(n+1)}-1}{q^{s-1}-1} \leq d_1(s) q^{(s-1)n},
\end{aligned}$$

where $d_1(s) = \frac{q^{s-1}}{q^{s-1}-1}$. Let $\delta = q^{-n}$. Then the δ-oscillation of W_n is bounded by

$$2\delta d_1 q^{(s-1)n} = 2 d_1 \delta^{2-s}.$$

On the other hand, the δ-oscillation of

$$W - W_n = \sum_{k=n+1}^{\infty} q^{(s-2)k} \sin(q^k x + \varphi_k)$$

is less than

$$2\sum_{k=n+1}^{\infty} q^{(s-2)k} = 2q^{(s-2)(n+1)}\frac{1}{1-q^{s-2}} \leq d_2 q^{(s-2)n} = d_2\delta^{2-s},$$

where $d_2 = \frac{2q^{s-2}}{1-q^{s-2}}$. Therefore, for all x and δ we have

$$\operatorname{osc}_\delta(x)(W) \leq \operatorname{osc}_\delta(x)(W_n) + \operatorname{osc}_\delta(x)(W - W_n) \leq (2d_1 + d_2)\delta^{2-s}.$$

From the fact 1.5 it follows, that

$$\dim_B \operatorname{graph} f \leq 2 - (2-s) = s.$$

2. We will estimate the δ-variation

$$\operatorname{Var}_\delta = \int_a^b \operatorname{osc}_\delta(x)\, dx$$

using the obvious inequality

$$\operatorname{osc}_\delta(x)(f) \geq |f(x+\delta) - f(x-\delta)|.$$

Thus

$$\begin{aligned} \operatorname{Var}_\delta &\geq \int_a^b |f(x+\delta) - f(x-\delta)|\, dx \\ &\geq \int_a^b |h(x)||f(x+\delta) - f(x-\delta)|\, dx, \end{aligned}$$

where $h(x)$ is an arbitrary function satisfying $|h(x)| \leq 1$. But

$$|f(x+\delta) - f(x-\delta)| = 2\sum_{k=0}^{\infty} q^{(s-2)k}\sin(q^k\delta)\cos(q^k x + \varphi_k),$$

therefore

$$\operatorname{Var}_\delta \geq \left|\int_a^b dx\, h(x)\, f_N(x)\right| - \sum_{k\neq N}\left|\int_a^b dx\, h(x)\, f_k(x)\right|,$$

where

$$f_k(x) = q^{k(s-2)}\cos(q^k x + \varphi_k)\sin(q^k\delta).$$

Fix N, choose $\delta = q^{-N}$ and $h(x) = \cos(q^N x + \varphi_N)$. Then

$$\begin{aligned} \left|\int_a^b h(x) f_N(x) dx\right| &= q^{N(s-2)}\sin(1)\int_a^b \cos^2(q^N x + \varphi_N)\, dx \\ &\geq \frac{1}{2} q^{N(s-2)}\int_a^b \cos^2(q^N x + \varphi_N)\, dt \\ &\geq \frac{1}{2}\delta^{2-s}\left[\frac{b-a}{2} + \frac{\sin(2(q^N b + \varphi_n)) - \sin(2(q^N a + \varphi_n))}{4q^N}\right] \\ &\geq \frac{1}{2}\delta^{2-s}\left[\frac{b-a}{2} - \frac{2}{4q^N}\right] \\ &= \frac{1}{2}\delta^{2-s}\left[\frac{b-a}{2} - \frac{\delta}{2}\right] \\ &\geq \frac{1}{8}\delta^{2-s}(b-a). \end{aligned}$$

On the other hand

$$\begin{aligned}
\left|\int_a^b h(x) f_k(x) dx\right| &= q^{k(s-2)} \sin(q^{k-N}) \int_a^b \cos(q^k x + \varphi_k) \cos(q^N x + \varphi_N)\, dx \\
&\leq q^{k(s-2)} \cdot \\
&\cdot \left| \frac{\sin((q^N - q^k)b + \varphi_N - \varphi_k) - \sin((q^N - q^k)b + \varphi_N - \varphi_k)}{2(q^N - q^k)} + \right. \\
&\left. \frac{\sin((q^N + q^k)b + \varphi_N + \varphi_k) - \sin((q^N + q^k)b + \varphi_N + \varphi_k)}{2(q^N + q^k)} \right| \\
&\leq 2q^{k(s-2)} \left[\frac{1}{|q^N - q^k|} + \frac{1}{q^N + q^k}\right] \\
&\leq 2q^{k(s-2)} \left[\frac{1}{q^N - q^{N-1}} + \frac{1}{q^N}\right] \\
&\leq 5 \cdot q^{k(s-2)} \delta.
\end{aligned}$$

Therefore

$$\begin{aligned}
\mathrm{Var}_\delta &\geq \frac{1}{8}\delta^{2-s}(b-a) - \sum_k 5\, q^{k(s-2)} \delta \\
&\geq \frac{1}{8}\delta^{2-s}(b-a) - 5\frac{1}{1-q^{s-2}}\delta.
\end{aligned}$$

But $2 - s < 1$, thus for large enough N (small enough δ) the first term dominates the other, therefore

$$\mathrm{Var}_\delta \geq c\delta^{2-s},$$

one can put $c = \frac{b-a}{16}$, for example.

From theorem 1.3 it follows that

$$\dim_B \operatorname{graph} f = s.$$

□

1.3.5 Dimension of a square of a function

Given a function whose graph has box-counting dimension s, what is the dimension of the graph of its square? We show that for a bi-sup-Hölder functions it is the same.

Suppose f is a bi-sup-Hölder function on an interval $[a, b]$ (this consideration carries over to arbitrary dimension). Thus

$$\forall t \in [a, b]: \qquad c_1 \delta^H \leq \sup_{x,y \in [t-\delta, t+\delta]} |f(x) - f(y)| \leq c_2 \delta^H.$$

For every t, δ there must be some x_0, y_0 such that

$$\sup_{x,y \in [t-\delta, t+\delta]} |f(x) - f(y)| = f(x_0) - f(y_0),$$

because the domain is compact and the function continuous. We then have the cases:

1. the graph of function f on $[t-\delta, t+\delta]$ does not cross the abscissa axes: $f(x_0) > f(y_0) \geq 0$ and $0 \geq f(y_0) > f(x_0)$

$$\begin{aligned} \sup|f^2(x) - f^2(y)| &= |f^2(x_0) - f^2(y_0)| \\ &= (|f(x_0)| + |f(y_0)|) \sup|f(x) - f(y)|, \end{aligned}$$

thus

$$\begin{aligned} \sup|f(x)| \sup|f(x) - f(y)| &\leq \sup|f^2(x) - f^2(y)| \\ &\leq 2\sup|f(x)| \sup|f(x) - f(y)|. \end{aligned}$$

2. the graph of function f on $[t-\delta, t+\delta]$ crosses the abscissa axes: $f(x_0) \geq 0 > f(y_0)$

$$\sup|f^2(x) - f^2(y)| = \max\{|f^2(x_0)|, |f^2(y_0)|\} = (\sup|f(x)|)^2.$$

But in this case

$$\sup|f(x) - f(y)| = f(x_0) - f(y_0) = |f(x_0)| + |f(y_0)|$$

which gives

$$\sup|f(x)| \leq \sup|f(x) - f(y)| \leq 2\sup|f(x)|.$$

Thus

$$\begin{aligned} 1/2\sup|f(x)| \sup|f(x) - f(y)| &\leq \sup|f^2(x) - f^2(y)| \\ &\leq \sup|f(x)| \sup|f(x) - f(y)|. \end{aligned}$$

One can do even better in this case:

$$(\sup|f(x) - f(y)|)^2/4 \leq \sup|f^2(x) - f^2(y)| \leq (\sup|f(x) - f(y)|)^2.$$

Therefore, whatever the case, we get the following set of inequalities:

$$\begin{aligned} 1/2\sup|f(x)| \sup|f(x) - f(y)| &\leq \sup|f^2(x) - f^2(y)| \\ &\leq 2\sup|f(x)| \sup|f(x) - f(y)| \end{aligned}$$

which leads to

$$\begin{aligned} \frac{1}{2}c_1 \sup_{x\in[t-\delta,t+\delta]} |f(x)|\ \delta^H &\leq \sup_{x,y\in[t-\delta,t+\delta]} |f^2(x) - f^2(y)| \\ &\leq 2c_2 \sup_{x\in[t-\delta,t+\delta]} |f(x)|\ \delta^H. \end{aligned}$$

To show that the dimension of graph of f^2 is s we need to have on both sides constants independent of the box in δ-partition (i.e. of t). It is easy to do on the right-hand side, because

$$\sup_{x\in[t-\delta,t+\delta]} |f(x)|\ \leq \sup_{x\in X} |f(x)|\ < \infty,$$

it's not so obvious on the left-hand side. Therefore we will estimate the variation from below.

$$\begin{aligned}
\mathrm{Var}_\delta(f^2) &= \int_a^b \mathrm{osc}_\delta(x) f^2\,dx \\
&\geq \int_a^b 1/2 \sup_{x\in[t-\delta,t+\delta]} |f(x)| \sup_{x,y\in[t-\delta,t+\delta]} |f(x)-f(y)|dt \\
&\geq \frac{1}{2}c_1\delta^H \int_a^b \sup_{x\in[t-\delta,t+\delta]} |f(x)|dt \\
&\geq \frac{1}{2}c_1\delta^H \int_a^b |f(t)|dt.
\end{aligned}$$

Thus

$$\mathrm{Var}_\delta(f^2) \geq c\delta^H$$

where $c = \frac{1}{2}c_1 \int_a^b |f(t)|dt$ is a constant independent of the box. From theorem 1.3 we obtain

$$\dim_B \mathrm{graph} f^2 = 2 - H = \dim_B \mathrm{graph} f.$$

1.3.6 Dimension of graph of sum of two functions

The dimension of the graph of a sum of functions whose graphs have the same dimensions D can be anything from 1 to D. The decrease of dimension happens when the two functions added are too correlated.

For example, let f_1 and f_2 be functions with graphs having dimensions, respectively, $1 \leq d_1 < d_2 \leq 2$. Let $g_1 = f_1 + f_2$, $g_2 = f_1 - f_2$. Then the box-counting dimension of both the graph of g_1 and g_2 is d_2, but the dimension of the graph of their sum $g_1 + g_2 = 2f_1$ is $d_1 \in [1, d_2[$.

1.3.7 Dimension of graphs of typical paths of stochastic stationary processes

In chapter 4 we criticize Berry's use of arguments giving the dimension of typical trajectories of certain stochastic processes. To give the reader some flavor of the type of argument we have in mind we recall here the most basic fact of this type. We will consider the dimension of the graph of a typical Brownian trajectory.

If we observe the dynamics of a particular Brownian particle it can be described by a function $f : \mathbb{R} \to \mathbb{R}^n$. Depending on needs one can consider dimensions of a *sample path* or *trail* or *trajectory* which is

$$f([t_1, t_2]) = \{f(t) \;:\; t_1 \leq t \leq t_2\} \subset \mathbb{R}^n,$$

or the dimensions of its *graph*

$$\{(t, f(t)) \;:\; t_1 \leq t \leq t_2\} \subset \mathbb{R}^{n+1}.$$

These dimensions are different.

We are interested here in the dimensions of graphs of functions. The simplest relevant result is:

Theorem 1.7 *With probability 1, the graph of a Brownian sample function* $X : [0,1] \to \mathbb{R}$ *has Hausdorff and box-counting dimension* $3/2$.

To obtain the upper bound one shows that with probability one a sample Brownian path is Hölderian with exponent $0 < \alpha < 1/2$, thus (subsection 1.3.2)

$$\dim_H \mathrm{graph} X(t) \leq \dim_B \mathrm{graph} X(t) \leq 2 - \alpha \to 3/2.$$

To obtain the lower bound one uses the potential method (subsection 1.1.5). The idea is to lift the Lebesgue measure from the t axis to get a mass distribution μ_f on the graph of function of f, so the measure of a set A is given by

$$\mu_f(A) := \mathrm{vol}^1(\{t \ : \ 0 \leq t \leq 1 \text{ and } (t, f(t)) \in A\}).$$

This idea works fine in this case because we may *average* the value of measure over all the the Brownian paths since the probability distribution is Gaussian. To use such an argument for a deterministic function seems very hard (here we allude to our discussion of Berry's result in chapter 4).

To get the lower bound we calculate the s-energy for the mass distribution μ_X and average it over the space of all the sample paths ($x, y \in \mathrm{graph} X(t) \subset \mathbb{R}^2$)

$$\left\langle \int\!\!\int \frac{d\mu_X(x) d\mu_X(y)}{|x-y|^s} \right\rangle = \int_0^1 dt \int_0^1 du \left\langle \frac{1}{\left(\sqrt{|X(t) - X(u)|^2 + |t-u|^2}\right)^s} \right\rangle.$$

If this is finite for some s then $\dim_B \mathrm{graph} X(t) \geq s$. But the process is Gaussian so

$$\begin{aligned} \left\langle \frac{1}{\left(\sqrt{|X(t+h) - X(t)|^2 + h^2}\right)^s} \right\rangle &= \int_0^\infty \left(\frac{1}{\sqrt{r^2+h^2}} \right)^s dp(r) \\ &= ch^{-1/2} \int_0^\infty \left(\frac{1}{\sqrt{r^2+h^2}} \right)^s \exp\left(\frac{-r^2}{2h} \right) dr \\ &\leq c_1 h^{1/2-s}. \end{aligned}$$

This implies

$$I_s(\mu_X) \leq \int_0^1 dt \int_0^1 du \; c_1 |t-u|^{1/2-s},$$

which is finite for $s < 3/2$ which ends the proof.

The details can be found for instance in [76]. See also a very complete review of dimensional properties of sample paths of stochastic processes by Taylor [226].

1.4 Notes and references

The subject of fractal dimensions is very broad and we have only been able to touch upon some most fundamental facts. If a single work should be recommended as a source for this chapter it would certainly be the excellent textbook by Kenneth Falconer [76]. The best book on fractal curves is Claude Tricot's [238]. The essential reading is still Benoit Mandelbrot's [146] but bear in mind this is an essay (words of the author), not a textbook.

The dimension theory of dynamical systems has recently been published by Yakov Pesin [178]. Iterated functions systems, another important notion of the fractal geometry got a monograph from Michael Barnsley [13] (see especially the second, extended edition). The third Falconer's book [77] should also be consulted, especially for the discussion of multifractals and other fresh topics.

All the above sources are accessible for a physicist. I found Gerald Edgar's books slightly more hermetic [67, 69]. They are the source for instance for the packing dimensions (but see also Falconer [77]) and for random fractals. And do not overlook the collection of original papers edited by Edgar, they have many good annotations [68]! If the reader is not satisfied she may consult some books on geometric measure theory [75, 149]. This is not a bedtime reading.

A thorough discussion of the properties of D_q and f_α spectra falls beyond the scope of this work. Good introductory descriptions can be found for instance in [227, 74]. Beck and Schlögl book is highly recommended [16]. We followed here Falconer's presentation in [76] but he has much more to say about multifractal spectra and the dimensions of measures in [77]. A popular review by Paladin and Vulpiani is also recommended [173]. Most good books on chaos and dynamical systems contain some discussion of multifractal spectra [168, 206, 169, 207]. Other good physical descriptions can be found in [157, 83, 154, 153, 136, 8, 31].

Mathematically precise definitions of multifractal spectra can be found in [164] (generalized Hausdorff and packing dimensions) and in [178] (generalized Caratheodory construction).

The references to original work can be found in these reviews.

Chapter 2

Elements of nonlinear time series analysis: estimating fractal dimensions

A number of methods for estimating fractal dimensions have been developed in the last twenty years. Some of them have wide applicability, some can be applied only in specific situations. Our choice of a particular method is first determined by the type of the object we want to quantify — is it a "solid" object, like a rough surface, a fractal aggregate, a percolation structure, etc. or is it an object in the phase space of a dynamical system, usually an attractor — and on available data.

In this chapter we concentrate on the methods used to estimate dimensions of attractors when a time series of measurements is given. We will need them in chapter 3. To illustrate described methods we decided to base the examples on a set of unpublished data obtained in an experiment designed to check the applicability of our method (presented in the next chapter) in real life systems (courtesy Y. Hluschchuk, N. Savitsky, S. Bauch, L. Sirko, from the Institute of Physics, Polish Academy of Sciences). The system analyzed in the experiment consists of two coupled Chua circuits similar to those examined in [160] (see also [147]), however, we used only the signal from the driver which is one Chua circuit. Full details of the experiment together with careful analysis of results will be published in the future [257].

A typical situation in analysis of real deterministic systems is that we can access only a fraction of the dynamical variables. It often happens that only one variable is available experimentally. Therefore, before one ventures to estimate the dimension of the attractor of the system (or of the invariant measure) one has to first *reconstruct* the dynamics in the full phase space. Several reconstruction methods have been proposed and used depending on experimental context [172, 104, 223, 37]. Undoubtedly, the greatest popularity gained the *delay reconstruction* method, which we describe in some detail in section 2.1.

Several algorithms have been proposed to estimate various fractal dimensions once the dynamics has been reconstructed. The most widely studied is the Grassberger-Procaccia algorithm in its multiple variants leading to an estimate on D_2 — the correlation dimension. We present this and other algorithms in section 2.2.

2.1 Embedology

The problem of representing the dynamics of the experimental system from limited data lies in the heart of nonlinear time series analysis. Before the calculation of any of the invariants (like Lyapunov exponents, generalized entropies or dimensions) one needs a reasonably faithful representation of the original phase space. The first and most often used method is the *delay reconstruction* method proposed in 1980 independently by Takens [223] and Packard, Crutchfield, Farmer and Shaw [172]. The idea is, in fact, very simple.

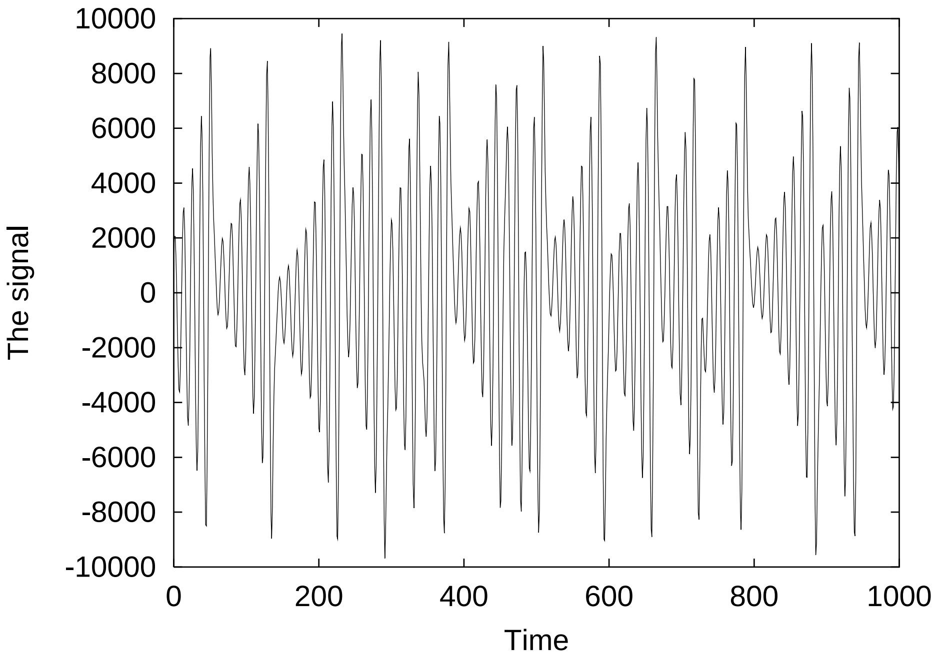

Figure 2.1: A time series of the variable x from analyzed system. All the subsequent figures in this chapter are derived from these data.

Given an experimental time series of one variable $x(n)$ (figure 2.1) one constructs a set of d-dimensional *delay vectors*

$$\tilde{\mathbf{x}}(n) = (x(n), x(n+\tau), \ldots, x(n+(d-1)\tau)), \tag{2.1}$$

where the *delay* τ and the *embedding dimension* d must be appropriately chosen. It has been shown by Takens [223] and by Sauer, Yorke and Casdagli [201] that for infinite, clean time series when the embedding dimension d is greater than twice the box-counting dimension of the attractor of the system

$$N > 2D_0(\operatorname{supp}\mu),$$

almost every delay τ is allowed and thus most functions (2.1) are embeddings. In practice one has finite and noisy data. Therefore, some delays are better than other.

We discuss the choice of delay in subsection 2.1.1. Essentially, if the delay is too short, the succeeding variables do not bring enough information to extract the other dimensions and the reconstructed measure is located near the diagonal ($x(n) \approx x(n-\tau)$). On the other hand, if it is too long, the omnipotent noise destroys determinism.

Example 2.1.1: Consider a system whose asymptotic dynamics for the given set of parameters is periodic, thus it is given by the following equations:

$$\begin{aligned} x(t) &= A\sin(\omega t+\varphi), \\ y(t) &= A\cos(\omega t+\varphi). \end{aligned}$$

Suppose the experimentally accessible variable is x. Thus if we take a vector

$$\begin{aligned} \tilde{\mathbf{x}}(t) &= (x(t), x(t+\tau)) \\ &= (A\sin(\omega t+\varphi), A\sin(\omega t+\omega\tau+\varphi)) \\ &= (x(t), A\cos(\omega\tau)\sin(\omega t+\varphi)+A\sin(\omega\tau)\cos(\omega t+\varphi)) \\ &= (x(t), ax(t)+by(t)), \end{aligned}$$

where $a=\cos(\omega\tau)$, $b=\sin(\omega\tau)$ are delay-dependent constants. Clearly, the new equations lead to attractor topologically equivalent to the original one whenever τ is not a multiple of half of the period ($b=\sin(\omega\tau)\neq 0$).

Of course, in fact we do not have $x(t)$ but rather $x(t_0+n2\pi/\omega_s)$. It is clear that the sampling frequency ω_s should be much greater than ω and incommensurate with it.

$\triangle$

Certainly, the embedding dimension d is unknown beforehand, since we do not know the dimension of the attractor. One can therefore either perform several reconstructions with increasing embedding dimension and stop as soon as obtained estimates of the quantity one seeks no longer change [193, 93]. This is often used for instance in dimension calculations, in particular this was our approach. Its main disadvantage is that the larger the embedding dimension, the worse the statistics, because the same number of points spreads out in more and more dimensions. For instance, 4096 points in $\mathbb{R}^1$ is a lot, but it gives 64 points a direction already when $d=2$, 16 points a direction in $d=3$ and so on. Thus it is of interest to know the optimal embedding dimension before the reconstruction is performed in order to reject spurious results. There are methods to obtain the embedding dimension, for instance false nearest neighbors method [130]. We will consider it in section 2.1.2.

Apart from the delay embedding method other methods have been proposed. For instance, Packard et al. [172] proposed to use successive derivatives of the time series as an embedding. For instance given $x(t)$ we construct the vectors

$$(x(t), \dot{x}(t), \ddot{x}(t), \ldots).$$

Unfortunately even small noise in $x(n)$ translates into large fluctuations of time series $\frac{d^k}{dt^k}x(n)$ approximating $\frac{d^k}{dt^k}x(t)$ which is a serious drawback.

(a)

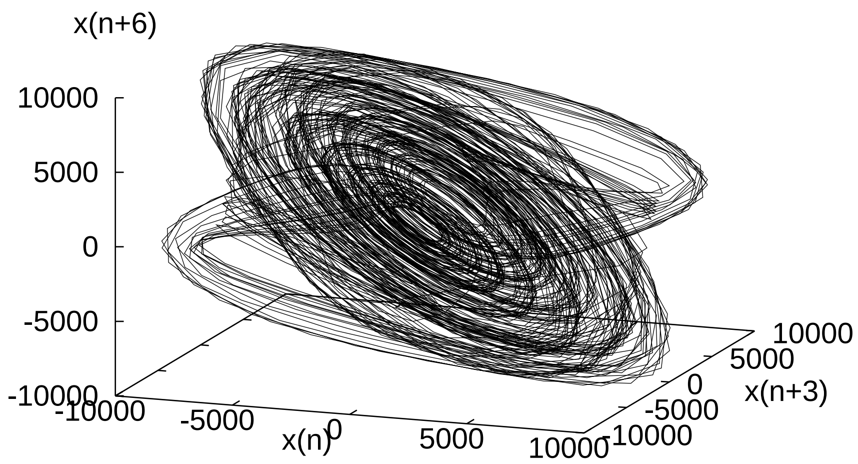

(b)

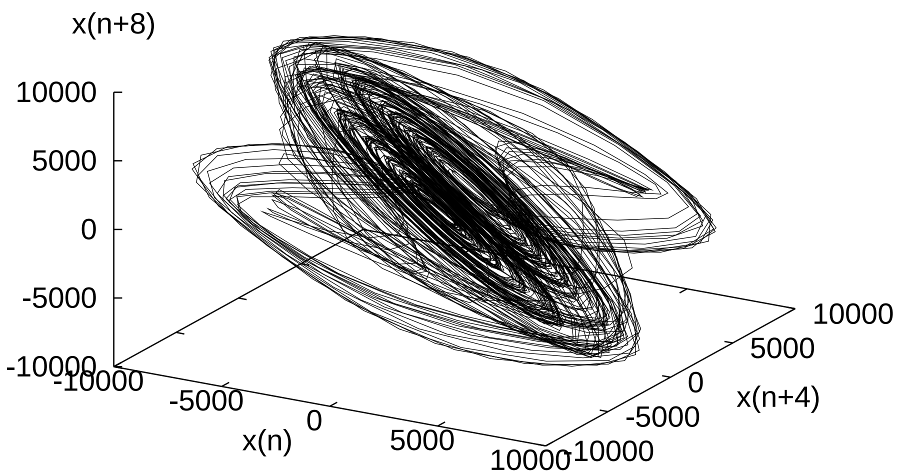

Figure 2.2: Two delay reconstructions with time delay 3 (a) and 4 (b). This values come from the subsequent analysis of autocorrelation function and average mutual information. 3000 points were used in the reconstruction.

Broomhead and King advocated the use of singular value or Karhunen-Loewe decomposition of the delayed variables $\tilde{\mathbf{x}}(n)$. The idea is to project the reconstructed vectors (2.1) onto a fewer dimensional subspace in such a way that the error is minimized. The simplest way to do it is to compute the covariance matrix

$$C_{ij} = \langle \tilde{\mathbf{x}}_i \tilde{\mathbf{x}}_j \rangle = \langle x(k + i\tau)x(k + j\tau) \rangle$$

and calculate its eigenvalues. The eigenvectors of C_{ij} are orthogonal (C_{ij} is real and symmetric) and define a new coordinate system in the space of delay vectors (2.1). The eigenvalues of C_{ij} are the squared lengths of the ellipsoid that fits best the scattered data. Most information is carried by the components corresponding to the largest eigenvalues. If there are very small eigenvalues, the corresponding components can be dropped out resulting in no significant loss of information. In fact, it is not so obvious which components can be dropped because nonlinearity may introduce coupling between modes of different amplitude.

A method of reconstructing an attractor of a spatiotemporal system suggested by Guckenheimer and Buzyna [104] is to use the information from several probes placed in various points of the experimental system. Thus instead of delay vectors (2.1) the phase space is reconstructed through

$$(h(x_1, t), \ldots, h(x_n, t)),$$

where $h(x_i, t)$ is the field measured on the i-th probe, it can be one component of velocity, temperature etc. Of course, one can also use variables with different physical meaning.

In our work we used only time delay reconstruction on which we shall now concentrate. Thorough discussion of reconstruction problems can be found in several good reviews, we recommend [44, 112, 125] but see also [1, 2].

2.1.1 Choice of delay

To obtain a good embedding the *time delay* τ (sometimes also called the *time lag*) should be the smallest possible to escape the decorrelating effect of noise. The instability of chaotic dynamics amplifies the noise over the long time scales rendering the delay variables uncorrelated, which is undesirable. On the other hand, too small a delay leads to the collapse of the reconstructed attractor on the diagonal because all the variables are approximately the same (this effect is most pronounced when the signal is sampled very fast in comparison with the natural frequency of the system). Such a reconstruction is useless because inevitable noise prevents one from disentangling the examined structure.

The simplest idea to choose something between the two extremes is to take the first zero of the autocorrelation function. This choice gives the smallest delay providing linearly uncorrelated variables, so that the pair $(x(t), x(t + \tau))$ gives maximum information. In fact, if we do not want total decorrelation because of noise, a rule of thumb is to take the time at which the autocorrelation function decays to $1/e$ (for mixing systems autocorrelation function decays exponentially).

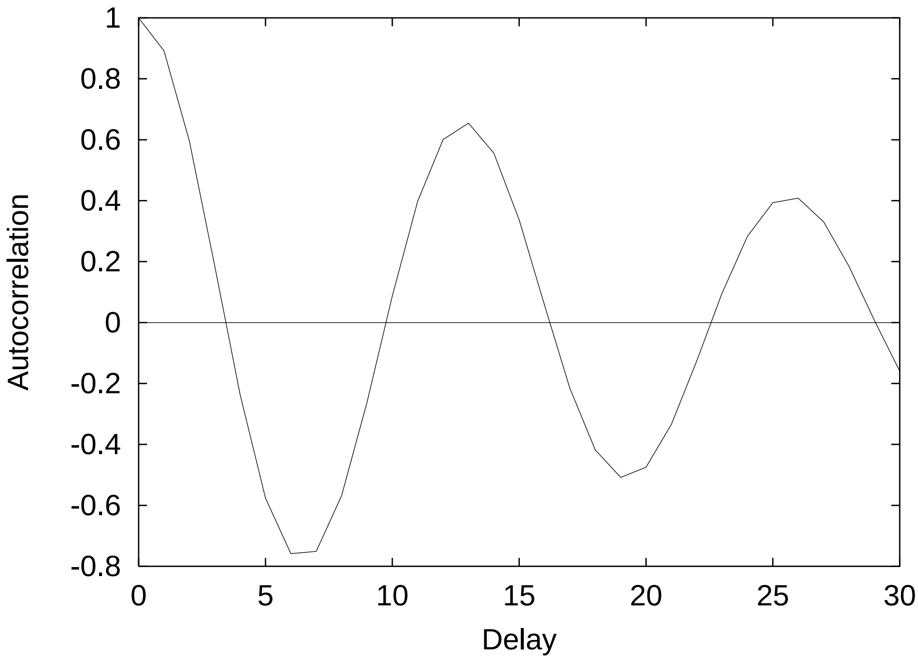

Figure 2.3: Autocorrelation function of the analyzed time series. The first 0 is between 3 and 4. These values seem to be optimal time delays in this case.

The basic objection against this approach is that is is conceived within the framework of linear systems theory and therefore does not take into account nonlinear correlations. Fraser and Swinney [85] proposed to look instead for the first minimum of the *average mutual information*. It is the information we already have about the value of $x(t+\tau)$ when we know $x(t)$. The *mutual information* or *redundancy* of two probability distributions is

$$\begin{aligned} I &:= \sum_{i,j} s_{ij} \ln s_{ij} - \sum_i p_i \ln p_i - \sum_j r_j \ln r_j \\ &= \sum_{i,j} s_{ij} \ln \frac{s_{ij}}{p_i r_j}, \end{aligned}$$

where p_i and r_j are the two probability distributions and s_{ij} is the joint probability distribution. Thus

$$p_i = \sum_j s_{ij}, \qquad r_j = \sum_i s_{ij}.$$

In particular, when p_i and r_j are independent we have

$$s_{ij} = p_i r_j$$

and $I = 0$, on the other extreme there are equal distributions $p_i = r_i$ thus

$$s_{ij} = p_i \delta_{i,j} = r_j \delta_{i,j} \tag{2.2}$$

which gives $I = -\sum_i p_i \ln p_i = H$ — the *Shannon information* or *information entropy* of the distribution p_i. While the information entropy depends on the coordinates, the mutual information usually does not (except for the case (2.2)).

In case of probability distributions induced by experimental time series I takes the form of

$$I(\tau) = \sum_{i,j} s_{ij}(\tau) \ln s_{ij}(\tau) - 2 \sum_i p_i \ln p_i,$$

where the $s_{ij}(\tau)$ is the probability to find $x(t+\tau)$ in ith bin and $x(t)$ in bin j, and p_i the probability to find $x(t)$ in bin i. The first minimum of $I(\tau)$ gives the delay for which $x(t+\tau)$ adds maximal information to the knowledge we have from $x(t)$. This is why it is often used as a good candidate for the delay time to use for the reconstruction, however, it seems there is no theoretical justification why one should take a minimum.

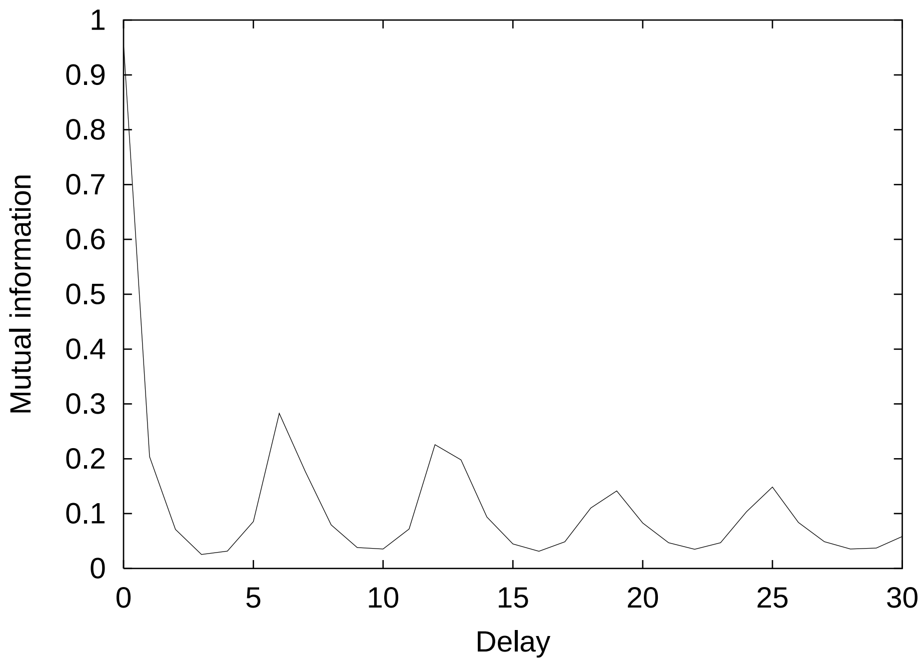

Figure 2.4: Average mutual information for the analyzed time series. The first minimum is obtained for delay 3, but the value at 4 is almost the same. Thus for this time series both the autocorrelation and the average mutual information indicate the same values of delay for optimal reconstruction.

Several other algorithms to choose the optimal delay time have been proposed [39, 44, 141]. Most of them, however, render values of the same order. On the other hand, the reconstruction procedure should be stable with respect to reasonable changes of parameters. Thus in our analysis in chapter 3 we always chose the delay as the minimum of the time delayed average mutual information in the simple implementation by Hegger et al. [112]. Discussion of other choices of delay can be found in [44, 112, 125]. In any case we recommend some experimentation with parameters.

2.1.2 Embedding dimension

A very intuitive idea to find out the optimal embedding dimension has been suggested by Kennel, Brown and Abarbanel [130]. Consider two points close on the attractor. During a short time their separation slowly increases. The same property have near neighbors on the reconstructed attractor if the embedding dimension is sufficiently large. If we now decrease the embedding dimension some points from distant parts of the attractor will be projected into the same small neighborhoods. Therefore, in the course of one step in time some close neighbors will follow the reference point while the others will immediately wander towards other parts of the projected attractor.

In the first case we call the two points *true neighbors* in the other they are *false neighbors*. When the attractor has been properly reconstructed all the neighbors are true. Thus to find the embedding dimension we calculate the percentage of false nearest neighbors as a function of embedding dimension, when it no longer drops we consider this as a signature of good reconstruction.

In practice, for each reconstructed point $\tilde{\mathbf{x}}_i$ one finds its nearest neighbor $\tilde{\mathbf{x}}_j$. If the ratio of the distance between the iterates to the distance between the neighbors

$$R_i = \frac{|\tilde{\mathbf{x}}_{i+1} - \tilde{\mathbf{x}}_{j+1}|}{|\tilde{\mathbf{x}}_i - \tilde{\mathbf{x}}_j|}$$

exceeds some threshold value R one considers the two points as false nearest neighbors.

This procedure is not free from ambiguity because one usually does not know the relevant scales for the problem so it is not clear what is the difference between a large and a small increase of distance. A rule of thumb is to consider the neighbors as false when the distance increased about 10-15 times ($R \approx$10–15).

In chapter 3 where we used nonlinear time series analysis we were not so much interested in the minimal embedding dimension but rather in estimating the dimension. Therefore we just estimated the correlation integrals for succeeding values of embedding dimension and looked for the saturation in the plots of local slope values (cf. figure 3.9).

2.2 Dimension estimates

Most definitions of fractal dimensions can be implemented. Often the algorithms obtained are rather demanding in terms of data quality and number, they can also lead to spuriously low or high estimates of dimensions. Multitude of equivalent definitions of the same quantities serves as a source of various inequivalent algorithms — the reason is that the equivalence of definitions is established in the limit of infinitely fine resolution while all the algorithms work on finite amounts of data.

2.2.1 Correlation dimension

Probably the most successful algorithms and certainly the most often used is the Grassberger-Procaccia algorithm of computing the second Rényi dimension D_2 —

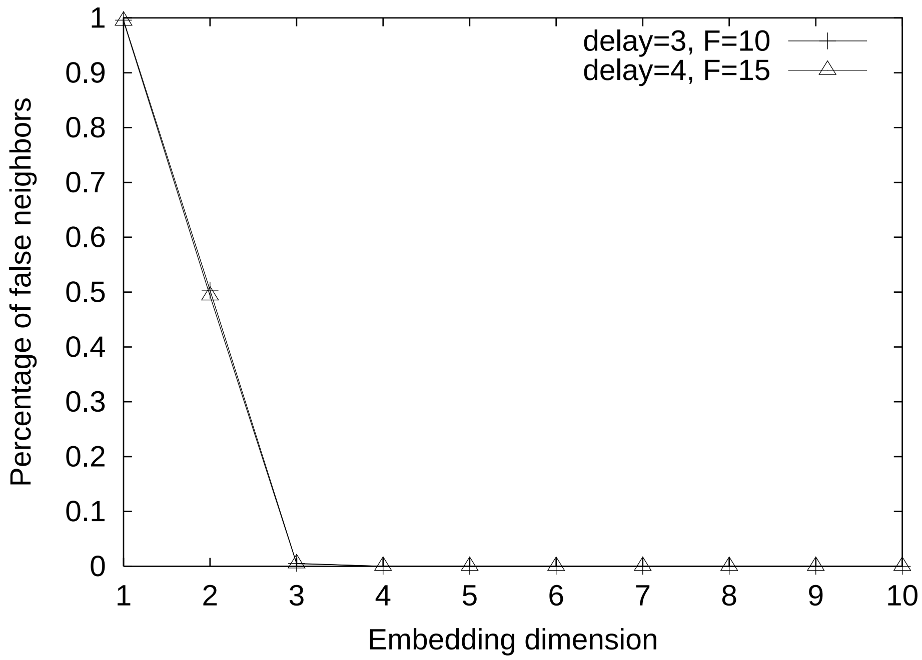

Figure 2.5: Percentage of false nearest neighbors for our time series. Embedding dimension varies from 1 to 10. Two plots are shown, one for reconstruction with delay $\tau = 3$ and the threshold $R = 10$, the other with delay $\tau = 4$ and the threshold $R = 15$. No difference can be seen. The plot suggests that already in 3 dimensions reconstruction is a faithful representation of the dynamics. This is why the attractors in figure 2.2 look so natural.

so-called *correlation dimension* [98, 99]. Grassberger and Procaccia showed that the scaling exponent of the *correlation integral*

$$\begin{aligned} C(r) &= \lim_{N\to\infty} \frac{1}{N(N-1)} \sum_{\substack{i,j=1 \\ i\neq j}}^{N} \Theta(r - |\mathbf{x}_i - \mathbf{x}_j|) \\ &= \int d\mu(\mathbf{x}) p(\mathbf{x}) \\ &= \int_0^r d^d\mathbf{x} c(\mathbf{x}), \end{aligned}$$

where $\Theta(x)$ is Heaviside step function, d the dimension of the space, and $c(\mathbf{r})$ is the *correlation function*

$$c(\mathbf{r}) = \lim_{N\to\infty} \frac{1}{N(N-1)} \sum_{\substack{i,j=1 \\ i\neq j}}^{N} \delta(\mathbf{x}_i - \mathbf{x}_j - \mathbf{r})$$

is equal to D_2. They also showed its relevance when $\mathbf{x}_i$ are the delay reconstructed vectors.

A lot of variants and improvements have been proposed over the years, improving the estimates or reducing the order of the algorithm. Algorithms used today are fast, stable and reliable and can provide a lot of information if one knows how to interpret the results. The amount of literature on the subject is overwhelming so we do not even try to properly review it but rather skip over some of the most important precautions one must take in order to avoid spurious results. Our favorite review on estimating fractal dimensions is [231]. Other reviews are [150, 151, 91, 52, 60, 124]. Good discussion of many issues can also be found in [66, 2, 1, 125, 112].

The correlation dimension in Grassberger-Procaccia setting is

$$D_2 = \lim_{\varepsilon \to 0} \lim_{N \to \infty} d(N, \varepsilon), \tag{2.3}$$

where the *local dimensions* $d(N, \varepsilon)$ are

$$\begin{aligned} d(N, \varepsilon) &= \frac{d \ln C(\varepsilon, N)}{d \ln \varepsilon} \\ &= \frac{dC(\varepsilon, N)/d\varepsilon}{C(\varepsilon, N)/\varepsilon}. \end{aligned} \tag{2.4}$$

and the *correlation sum*

$$C(\varepsilon, N) = \frac{1}{N(N-1)} \sum_{\substack{i,j=1 \\ i \neq j}}^{N} \Theta(\varepsilon - |\tilde{\mathbf{x}}_i - \tilde{\mathbf{x}}_j|) \tag{2.5}$$

is the estimate of the correlation integral in the delay space ($\Theta(x)$ is the Heaviside function). In practice we can perform neither of the two limits in (2.3) because we have a finite set of data and finite resolution. The definition seems to imply the small resolution values of $d(N, \varepsilon)$ are good estimates of D_2 but they lead to $D_2 = 0$ which is the true dimension of the discrete set of points. On the other hand, for ε comparable with the size of the whole attractor we again obtain $d(N, \varepsilon) \approx 0$ because from far away every bounded object looks like a point. Thus we usually look for some plateau in the plots of $d(N, \varepsilon)$ versus resolution $\ln \varepsilon$. If the level of the plateau becomes independent of N we interpret it as the dimension of the attractor underlying the measured dynamics.

If the time series analyzed comes from a frequently sampled flow there is a strong bias towards $d(N, \varepsilon) \approx 1$ coming from the temporal correlations (the contribution from the close neighbors along the trajectory is dominant in the correlation sum (2.5)). To avoid this effect one usually skips the pairs of points too close in time and replaces (2.5) with

$$C(\varepsilon, N) = \frac{2}{(N-w)(N-w-1)} \sum_{i=1}^{N} \sum_{j=w+1}^{N} \Theta(r - |\tilde{\mathbf{x}}_i - \tilde{\mathbf{x}}_j|), \tag{2.6}$$

where w is called *Theiler window* [228, 231]. Usually w of the order of several delays τ is enough and do not destroy the statistics. One can also use space time separation plots to infer the value of w [187].

(a)

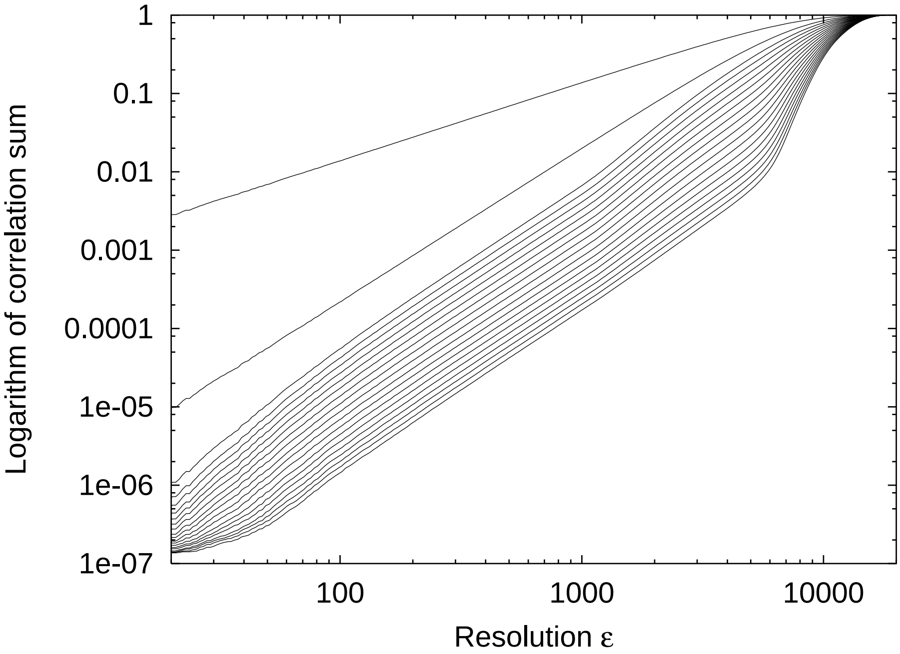

(b)

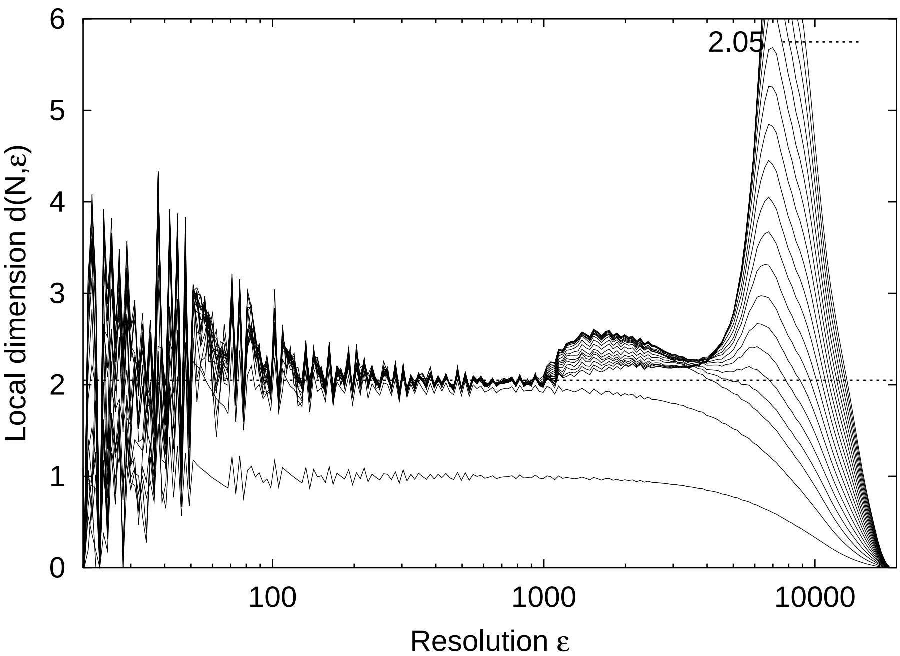

Figure 2.6: (a) Correlation sum for the analyzed time series. Embedding dimension varies from 1 to 20. Theiler window is 100, delay 4. (b) Local dimension in the same case.

(c)

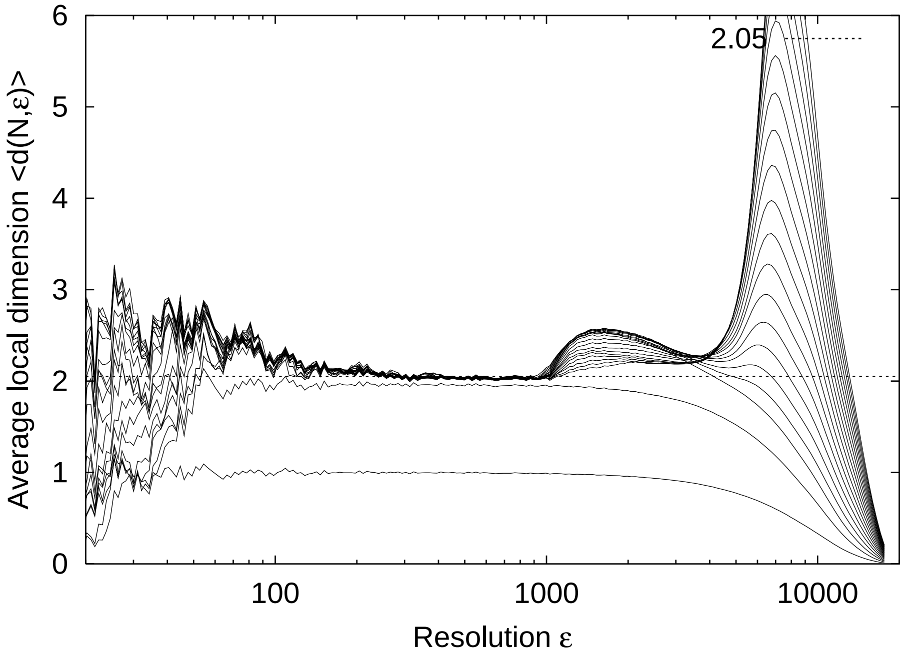

(d)

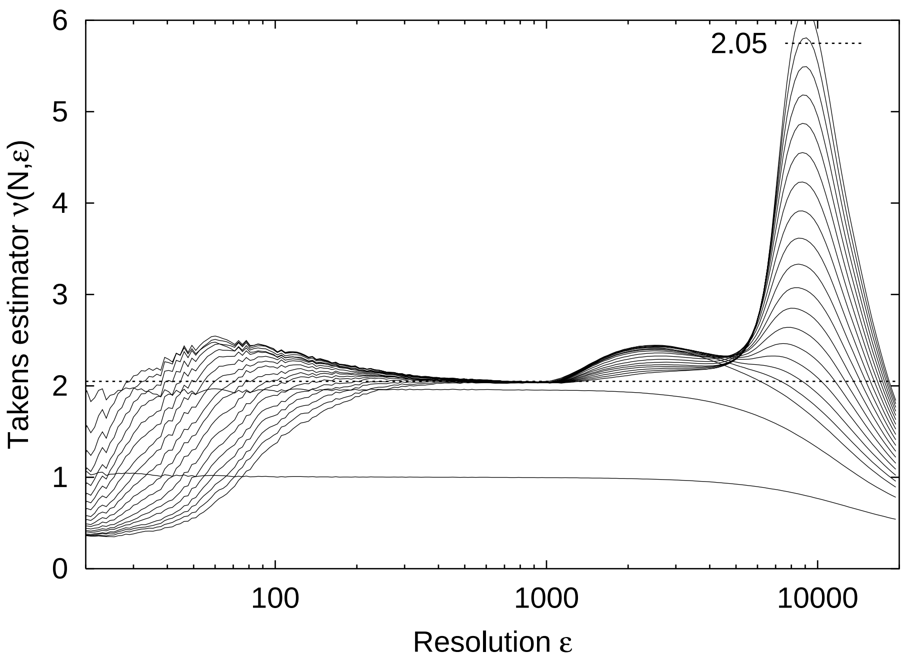

Figure 2.7: (c) Average local dimension, obtained by fitting straight lines to the sets of five succeeding points in the log-log plot of correlation sum and plotting their slopes. (d) Takens estimator in this case.

None of the dimension algorithms can be used without prejudices. *Even if we find a scaling region it is not an indication of determinism.* It is well known that delay reconstruction method can lead to a finite correlation dimension in case of stochastic signals with power-law spectra [166, 232]. Therefore one must usually *first* establish determinism (using for example Kaplan-Glass test [127], or checking the nonlinear predictability [81, 78, 42, 219]) before one can speak of the dimension of the attractor underlying observed dynamics. Otherwise one measures fractality of curves in space (cf. section 1.3) which can also be of interest but is something different.

The original implementation suggested by Grassberger and Procaccia is rather time consuming. Nowadays most algorithms make use of K-d-trees [28] or box-assisted search [229, 95].

An often used procedure to estimate the correlation dimension consists of plotting the logarithm of the correlation sum versus logarithm of resolution and fitting a straight line in the region where some scaling has been identified. This procedure has been much criticized [231] for the lack of theoretical justification. In particular it involves choosing lower and upper cut-offs. An improvement which gained some popularity has been proposed by Floris Takens [224] and advocated by James Theiler [230, 231]. On the basis of the theory of best estimators Takens and Theiler suggest to estimate

$$\begin{aligned}\tilde{\nu}(\varepsilon_0) &= \frac{C(\varepsilon_0, N)}{\displaystyle\int_0^{\varepsilon_0} \frac{C(\varepsilon, N)}{\varepsilon} d\varepsilon} \\ &= \frac{\displaystyle\int_0^{\varepsilon_0} \frac{dC(\varepsilon, N)}{d\varepsilon} d\varepsilon}{\displaystyle\int_0^{\varepsilon_0} \frac{C(\varepsilon, N)}{\varepsilon} d\varepsilon}\end{aligned} \tag{2.7}$$

(compare with (2.4)), where $\tilde{\nu}(\varepsilon_0)$ is usually called *Takens* [231] or *Takens-Theiler estimator* [125]. In this approach one formally needs only one cut-off. In practice, one usually plots $\tilde{\nu}(\varepsilon_0)$ as a function of $\ln(\varepsilon_0)$ and when $\tilde{\nu}(\varepsilon_0)$ does not change for a range of resolutions one takes its value at some ε_0 as the estimated correlation dimension. It is not clear how optimal is this estimate for real life data when one may have several scaling ranges and one can never reach the smallest scales, which give large contributions to $\tilde{\nu}(\varepsilon_0)$. Nevertheless, since all the methods face this problem we usually used this approach to estimate correlation dimension in chapter 3.

2.2.2 Other algorithms

The first numerical computations of fractal dimension used the box-counting algorithm [198, 172, 87, 103]. The impracticality of this algorithm was obvious in these early studies. The reason is that the dimension is obtained in the limit of small resolution but in this limit the number of boxes is seriously underestimated. The small measure regions of the attractor are not represented sufficiently in the experimental realization. The correlation dimension algorithm which weighs the boxes according to the natural measure has the best statistical properties.

An alternative that was used since the early 80s was estimating information dimension D_1 from the Lyapunov exponents [66], following the conjecture of Kaplan and Yorke [128]. However, the status of this conjecture for non-uniform attractors in more than two dimensions is not clear.

Other multifractal dimensions can also be obtained numerically from data of sufficient quality. Biased estimates follow from the generalized correlation sum

$$C_q(\varepsilon, N) = \frac{1}{N(N-1)^{q-1}} \sum_{i=1}^{N} \left[\sum_{i \neq j} \Theta(\varepsilon - |\tilde{\mathbf{x}}_i - \tilde{\mathbf{x}}_j|) \right]^{q-1}. \qquad (2.8)$$

The most serious problems occur for $q \leq 1$, where due to the power $(q-1)$ regions of small measure introduce singularity. The leading finite sample corrections that remove the singularity are known [94], but there is a much better approach in this case: the fixed mass algorithm [6, 242].

The idea is to examine the scaling of radii of neighborhoods of equal measure instead of scaling of measure for fixed size neighborhoods, which we did previously. In particular this approach leads to a robust estimate of the information dimension

$$D_1 = \lim_{p \to 0} \frac{\ln p}{\langle \ln \varepsilon_p \rangle},$$

where ε_p is a radius of a neighborhood of measure p.

2.3 Notes and references

The topics of nonlinear time series analysis and of numerical estimating dimension in simulations and from data are very broad. Our presentation only marks some of the topics which are indispensable for understanding our computations in chapter 3. One could go from here in several directions.

One is nonlinear time series analysis. The recommended critical reviews are [125, 204]. For an approach assuming determinism consult [1, 2]. Statisticians' point of view is represented by [236, 185].

The most important omissions in this field are probably the methods of nonlinear noise reduction [78, 134, 82, 45, 200, 133, 97, 53], prediction [81, 51, 42, 43, 213, 248] and surrogate data [233, 184, 234]. We have not mentioned methods of estimating Lyapunov exponents [20, 259, 90, 188] and generalized entropies [84, 48, 89] because we do not need these notions in the following parts of our work.

Another direction is estimating dimensions from field data, not necessarily from time series. For example scattering data are often used in analysis of porous surfaces or fractal aggregates [211, 120, 83, 239, 61, 62]. A rather comprehensive review has recently been published [157].

An interesting issue is also calculating dimension in simulations, when the dynamical equations are known. Availability of Jacobian leads to various algorithms making use of Kaplan-Yorke type relationships. Some important papers in this respect are [214, 100, 96, 7, 170].

Chapter 3

Dimension of interaction dynamics

3.1 Introduction

Given two time series can one tell if they originated from interacting or non-interacting systems? We show that with the help of embedding methods [172], Takens theorem [223, 201] and some facts concerning Rényi dimensions which we prove, one can succeed in case of chaotic systems. Moreover, one can quantify the common part of the dynamics, which we call dynamics of interaction.

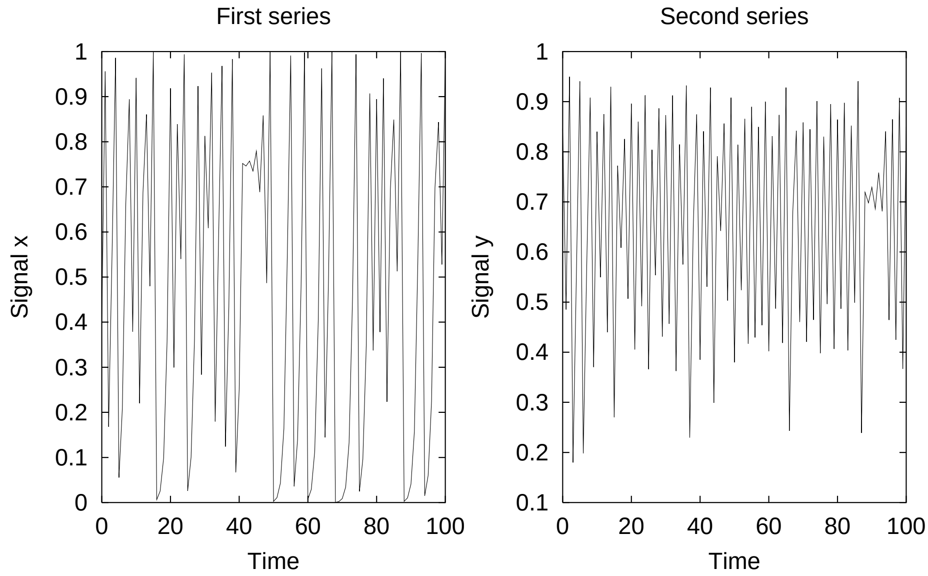

Figure 3.1: Fragments of two time series from systems coupled nonlinearly (data shown are x_n and y_n coming from the system (3.12)).

It happens sometimes, especially in simple systems like electronic circuits or coupled mechanical oscillators, that one knows whether the systems under investigation are coupled or not, what is the direction and sometimes strength of the coupling. However, there are many complex phenomena in nature where one is unable to verify directly the existence of coupling between parts of the system in which the phenomenon takes place.

Especially in complex spatiotemporal systems, like fluid systems, brain, neuronal tissue, social systems etc. one often faces the problem of characterization of interdependence of parts of the system of interest and quantifying the strength of interactions between the parts.

Recent research in neurology, for example, has shown that temporal coordination between different, often distant neural assemblies plays a critical role in the neurophysiological underpinnings of such cognitive phenomena as the integration of features in object representation (cf. [218] for a review) and the conscious experience of stimuli [237]. The critical empirical question, therefore, is which of the neural assemblies synchronize their activity. Since coordination may take many forms, including complex non-linear relations, simple correlational methods may not be sufficient to detect it. The detection of nonlinear forms of coordination is also critically important for issues in cognitive science [183], developmental psychology [235], and social psychology [163, 241].

The method traditionally used for this purpose is correlation analysis. Given two time series one studies their autocorrelation functions and cross-correlations. Large cross-correlations are usually attributed to large interdependence between the parts. Small cross-correlations are considered as the signature of independence of the variables.

Unfortunately, the linear time series analysis gives meaningful results only in case of linear systems or stochastic time series. It is well-known that spectral analysis alone cannot discriminate between low-dimensional non-linear deterministic systems and stochastic systems [125], even though the properties of the two kinds of systems are different.

Methods based on entropy measures represent one viable approach for detecting nonlinear relations between the activity of different neural assemblies [237].

Recently another approach based on nonlinear mutual prediction has been proposed and used in an experiment. Pecora, Caroll and Heagy [176] developed a statistics to study the topological nature of functional relationship between coupled systems. Schiff et al. [203] used it as a basis of their method. The idea is as follows: if there exists a functional relationship between two systems, it is possible to predict state of one system from the known states of the other. This happens if the coupling between two systems is strong enough so that generalized synchronization occurs [176, 197, 177]. The average normalized mutual prediction error is used to quantify the strength and directionality of the coupling [203].

The method we introduced in [258] does not assume generalized synchrony. We introduce the notion of the *dimension of interaction*, which measures the size of the dynamics responsible for the coupling between the two systems. More precisely, it is the dimension of the part of the attractor of the whole system, which is acted on by the dynamics of both subsystems. We also show how to obtain information concerning the strength and directionality of the coupling.

The idea is, in fact, very simple. Given two time series from subsystems of interest we construct another one which probes the whole system, for instance adding the two series. If the subsystems do not interact, dimension of the whole system is the sum of the dimensions of the two subsystems, all of which can be estimated from data. On the other hand, if the subsystems have some common degrees of freedom, dimension of the whole system will be smaller than the sum of the dimensions of the two subsystems.

Our method can also be used to find out if two response systems have a common driver. We discuss this application in Section 3.3.

Similar ideas have been considered in [182, 152] and used for instance to distinguish temporal from spatiotemporal chaos in dynamics of Bloch walls in thin magnetic films [260]. We thank Prof. J. Żebrowski for this communication.

The structure of this chapter is as follows. In Section 3.2 we formulate three theorems which form the basis of our method. The, rather straightforward, proofs have been relegated to appendix 3.A, since they are not crucial for understanding the method itself and can be omitted by readers whose main interest is in applications. We formulate our method in section 3.3. Classification of all the possible interaction schemes is given in Section 3.4. A simple way of verifying the kind and direction of the coupling is provided. Results from the simulations of coupled logistic and Hénon maps are collected in Section 3.5. Final comments and outlook are given in the last section.

3.2 Theoretical considerations

Our method presented in Section 3.3 is based on three theorems relating dimensions of subsystems to the dimension of the whole system. The first one states the intuitively obvious fact that the dimension of a system consisting of two non-interacting parts is the sum of the dimensions of the subsystems. A less trivial Theorems 2 and 3 establish interdependencies among the dimensions of the system and its interacting parts.

3.2.1 Non-interacting systems

Consider two non-interacting dynamical systems (U_1, φ_1, μ_1), (U_2, φ_2, μ_2), where $U_i \subset \mathbb{R}^{n_i}$ is the phase space, φ_i is a flow or a map on U_i, and μ_i is an ergodic φ_i-invariant natural measure on U_i. Below we shall concentrate on the case of continuous systems. Changes needed for the discrete time case are mostly notational.

By natural measure μ we mean the measure defined as the average over a trajectory

$$\mu = \mu_{x_0} := \lim_{T\to\infty} \frac{1}{T} \int_0^T \delta(x - \varphi_t(x_0))dt, \tag{3.1}$$

if it converges (in the weak sense) for μ-almost every x_0 and is independent of the trajectory (of the starting point x_0). That is, (3.1) is natural measure if the limit

$$\int f \, d\mu_{x_0} \quad := \quad \lim_{T\to\infty} \frac{1}{T} \int_0^T \delta(x - \varphi_t(x_0)) f(x) \, dt$$

$$= \lim_{T\to\infty} \frac{1}{T} \int_0^T f(\varphi_t(x_0))\,dt$$

exists for every continuous function f and is the same for μ-almost every x_0 (all x_0 except for the set A such that $\mu(A) = 0$). In other words, the average of f along a typical trajectory is independent of the trajectory, thus time averages are equal to ensemble averages. One usually thinks of some physical measure, like Sinai-Ruelle-Bowen measure [66], for which the set of x_0 such that $\mu = \mu_{x_0}$ is of non-zero Lebesgue measure.

The composite non-interacting system has a product structure $(U_1 \times U_2, \varphi_1 \times \varphi_2, \mu_1 \times \mu_2)$. Its dynamics can be written as

$$\begin{cases} \dot{\mathbf{u}}_1 &= f_1(\mathbf{u}_1), \\ \dot{\mathbf{u}}_2 &= f_2(\mathbf{u}_2), \end{cases} \quad \text{or} \quad \begin{cases} \mathbf{u}_1(t) &= \varphi_1(\mathbf{u}_1(0), t), \\ \mathbf{u}_2(t) &= \varphi_2(\mathbf{u}_2(0), t), \end{cases}$$

where

$$\begin{cases} \frac{\partial\varphi_1}{\partial t}(\mathbf{x}, t) &= f_1(\varphi_1(\mathbf{x}, t)), \\ \frac{\partial\varphi_2}{\partial t}(\mathbf{y}, t) &= f_2(\varphi_2(\mathbf{y}, t)), \end{cases} \quad \text{and} \quad \begin{cases} \varphi_1(\mathbf{x}, 0) &= \mathbf{x}, \\ \varphi_2(\mathbf{y}, 0) &= \mathbf{y}. \end{cases}$$

Theorem 3.1 *Suppose $D_q(\mu_1), D_q(\mu_1), D_q(\mu_1 \times \mu_2)$ exist. Then*

$$D_q(\mu_1 \times \mu_2) = D_q(\mu_1) + D_q(\mu_2). \tag{3.2}$$

This means, as should be intuitively obvious, the dimensions of non-interacting subsystems add up to the dimension of the whole system. The proof is given in appendix 3.A.

This is in fact one of the long-standing problems in the dimension theory, namely finding the conditions under which the equality holds for various dimensions for arbitrary measures. Some results for Olsen's version of multifractal formalism with a discussion of previous results can be found in [165].

3.2.2 Interacting systems

Take two interacting subsystems U_1 and U_2 of system U. It may happen that all the variables in U_1 couple with all those in U_2 but this is not necessary. For many-dimensional systems the structure of the equations of dynamics can be very complicated.

Consider the following decomposition of variables of U_i. Let $\mathbf{y}_1$ be the largest set of variables in U_1 satisfying the condition that if you change their state whatsoever, it will not influence the future evolution of U_2. Similarly define $\mathbf{y}_2$. Put all the remaining variables of U_1, U_2 in vector $\mathbf{x}$. They form a dynamical system V — the part of the whole system which is responsible for the interaction. Then the dynamics of the whole system U can be written as

$$\begin{cases} \dot{\mathbf{x}} &= f(\mathbf{x}), \\ \dot{\mathbf{y}}_1 &= g_1(\mathbf{x}, \mathbf{y}_1), \\ \dot{\mathbf{y}}_2 &= g_2(\mathbf{x}, \mathbf{y}_2). \end{cases} \tag{3.3}$$

Thus the dynamics of the interacting systems U_1 and U_2 is formally equivalent to dynamics of three systems: X (interaction part) driving Y_1 and Y_2. We pursue this analogy deeper in the next section. An example when such decomposition arises naturally is given in appendix 3.B.

System	variables	equations of dynamics	measure
V	$(\mathbf{x})$	$\dot{\mathbf{x}} = f(\mathbf{x})$	$\mu_V(\mathbf{x})$
U_1	$(\mathbf{x}, \mathbf{y}_1)$	$\begin{cases} \dot{\mathbf{x}} = f(\mathbf{x}) \\ \dot{\mathbf{y}}_1 = g_1(\mathbf{x}, \mathbf{y}_1) \end{cases}$	$\mu_1(\mathbf{x}, \mathbf{y}_1)$
U_2	$(\mathbf{x}, \mathbf{y}_2)$	$\begin{cases} \dot{\mathbf{x}} = f(\mathbf{x}) \\ \dot{\mathbf{y}}_2 = g_2(\mathbf{x}, \mathbf{y}_2) \end{cases}$	$\mu_2(\mathbf{x}, \mathbf{y}_2)$
U	$(\mathbf{x}, \mathbf{y}_1, \mathbf{y}_2)$	$\begin{cases} \dot{\mathbf{x}} = f(\mathbf{x}) \\ \dot{\mathbf{y}}_1 = g_1(\mathbf{x}, \mathbf{y}_1) \\ \dot{\mathbf{y}}_2 = g_2(\mathbf{x}, \mathbf{y}_2) \end{cases}$	$\mu_U(\mathbf{x}, \mathbf{y}_1, \mathbf{y}_2)$

Table 3.1: Notation.

Let $\mu_U, \mu_1, \mu_2, \mu_V$ be natural measures of dynamical systems, respectively, U, U_1, U_2, V.

Theorem 3.2 *Suppose $D_1(\mu_1)$, $D_1(\mu_2)$, $D_1(\mu_V)$, $D_1(\mu_U)$ exist. Then*

$$D_1(\mu_V) \leq d_{\mathsf{int}} := D_1(\mu_1) + D_1(\mu_2) - D_1(\mu_U). \tag{3.4}$$

(We shall call d_{int} dimension of interaction*). The equality holds when $\mathbf{y}_1$ and $\mathbf{y}_2$ are asymptotically independent.*

Asymptotical independence means essentially lack of generalized synchronization between the $\mathbf{y}$s and their common driver $\mathbf{x}$. We relegate further discussion to appendix 3.A, where we make this condition precise and show where it is needed[1].

If we think of dimensions as estimates on the number of degrees of freedom, the Theorem 3.2 means intuitively that if the system can be considered as composed of interacting parts, some of the degrees of freedom — perhaps even all — are common for both of the parts. Therefore, dimension of the whole system is equal to the sum of the number of the common degrees of freedom, those degrees of freedom which belong to U_1 and do not belong to U_2, and the other way round. Thus if we add the

[1] One would like to establish a similar inequality in case of other Rényi dimensions, however, in general, even when $\mathbf{y}_1$ and $\mathbf{y}_2$ are asymptotically independent

$$D_q(\mu_V) + D_q(\mu_U) - D_q(\mu_1) - D_q(\mu_2)$$

can have arbitrary sign (cf. appendix 3.A). Nevertheless, we expect this difference for typical physical systems to be small in comparison with the dimensions involved, and typically

$$D_q(\mu_V) \leq d_q^{\mathsf{int}} = D_q(\mu_1) + D_q(\mu_2) - D_q(\mu_U).$$

dimensions of the subsystems U_1 and U_2, we count the common degrees of freedom twice. We must therefore subtract them if we want to get the dimension of the whole system U.

In the above Theorem we show that this intuition can be made precise in case of the information dimension D_1 and with an additional assumption. The notions of the dimension of interaction we define in equation (3.4) and that of generalized dimensions of interaction defined below are crucial for our method.

In the special case, when one (or both) of $U_i = V$, (all the variables of U_i couple with some of the variables of the other subsystem), say $U_2 = V$, we may establish

Theorem 3.3 *Suppose $D_q(\mu_1)$, $D_q(\mu_2)$, $D_q(\mu_V)$ exist and $U_2 = V$. Then*

$$D_q(\mu_V) = d_q^{\mathsf{int}} := D_q(\mu_1) + D_q(\mu_2) - D_q(\mu_U). \tag{3.5}$$

The proof is obvious, for in this case $U_2 \equiv V$ and $U_1 = U$. This also means that the above intuitions in this case are precise for arbitrary generalized dimensions and no further assumptions are needed.

The generalized dimensions of interaction d_q^{int} are estimates on the number of effective degrees of freedom responsible for the interaction between the parts of the system under study. Of most interest are $d_1^{\mathsf{int}} \equiv d_{\mathsf{int}}$, which has the best analytical properties, and d_2^{int}, which can be most reliably estimated from data.

Note that

$$\begin{aligned} \max\{d_q^{\mathsf{int}}, D_q(\mu_V)\} &\leq \min\{D_q(\mu_1), D_q(\mu_2)\} \\ &\leq \max\{D_q(\mu_1), D_q(\mu_2)\} \\ &\leq D_q(\mu_U), \end{aligned} \tag{3.6}$$

(cf. appendix 3.A). Furthermore, for $q = 1$ one can show

$$0 \leq D_1(\mu_V) \leq d_1^{\mathsf{int}}.$$

We conjecture $d_q^{\mathsf{int}} \geq 0$ also for $q > 1$. We also expect typically $d_q^{\mathsf{int}} \geq D_q(\mu_V)$.

3.3 The method

Suppose we are given two time series measured in subsystems U_1 and U_2 of system U whose structure and interdependence we do not know, e.g. signals gathered on two electrodes placed in not too far away portions of brain, or measurements of velocity or temperature in various parts of moderately turbulent fluid. We would like to know, if the equations governing the dynamics of both of these variables are coupled or not, how many degrees of freedom are common and what is the direction of the coupling.

Let X_i be a function on U_i, i.e. $X_i : U_i \to \mathbb{R}$. The time series we measure are $x_1(n) := X_1(\mathbf{u}_1(t_n))$ and $x_2(n) := X_2(\mathbf{u}_2(t_n))$. Let $Y : \mathbb{R}^2 \to \mathbb{R}$ be a smooth function nontrivially depending on both variables[2]. Therefore we exclude functions for which $\partial Y/\partial \mathbf{x}_1 = 0$ or $\partial Y/\partial \mathbf{x}_2 = 0$. We construct another time series $y(n) = Y(x_1(n), x_2(n))$. Thus $Y(X_1, X_2)$ is a function on U.

Using time delay method (chapter 2) we can reconstruct the dynamics of the systems U_i and U from $x_i(n)$ and $y(n)$. Having reconstructed the attractors we can estimate their generalized dimensions and calculate the *generalized dimensions of interaction*

$$d_q^{\mathsf{int}} := D_q(\mu_1) + D_q(\mu_2) - D_q(\mu_U). \tag{3.7}$$

It is also convenient to consider normalized dimensions of interaction:

$$\begin{aligned} m_1^q &:= d_q^{\mathsf{int}}/D_q(\mu_1), \\ m_2^q &:= d_q^{\mathsf{int}}/D_q(\mu_2), \\ m_U^q &:= d_q^{\mathsf{int}}/D_q(\mu_U). \end{aligned} \tag{3.8}$$

From the values of m_i^q we can infer the information we need. All the possible cases are described in the next section. Note that if $m_i^q \neq 0$, they satisfy

$$\frac{1}{m_1^q} + \frac{1}{m_2^q} - \frac{1}{m_U^q} = 1.$$

From (3.6) we also have

$$0 \leq m_U^q \leq m_1^q, m_2^q \leq 1,$$

which provides us with a tool to check consistency of results.

Before we present the classification of all the possible schemes of interaction let us discuss heuristically four simple examples.

I If U_1, U_2 are uncoupled, the variables we see through x_1, x_2 are different, thus $\mu_U = \mu_1 \times \mu_2$. Therefore, from Theorem 3.1, $d_q^{\mathsf{int}} = 0$, as it should be for any reasonable definition of dimension of interaction for non-interacting systems.

II Consider now a system U consisting of three isolated systems V_i, which we cannot observe separately, however, but rather through U_1 and U_2, e.g. measuring $X_1(\mathbf{v}_1, \mathbf{v}_2)$ and $X_2(\mathbf{v}_2, \mathbf{v}_3)$. Reconstructing dynamics from time series of X_1 and X_2 we expect to obtain

$$\begin{aligned} D_q(\mu_1) &= D_q(\mu_{V_1}) + D_q(\mu_{V_2}), \\ D_q(\mu_2) &= D_q(\mu_{V_2}) + D_q(\mu_{V_3}). \end{aligned}$$

With a typical function $Y(x_1, x_2)$ we obtain time series $y(n)$ from which we estimate

$$D_q(\mu_U) = D_q(\mu_{V_1}) + D_q(\mu_{V_2}) + D_q(\mu_{V_3}).$$

[2] For finite noisy time series some functions are better than other. In practice we used five different functions $Y(x, y)$, namely $x+y$, $x \cdot y$, $\sin(x)\cos(y)$, $x \exp(y)$, $2x-y$, to calculate dimension of the system $D_q(\mu_U)$ and averaged the results. The variance of the obtained five estimates was usually small.

The above functions were not chosen for their particularly good numerical properties but rather to verify that the results obtained depend only weekly on the choice of the function Y.

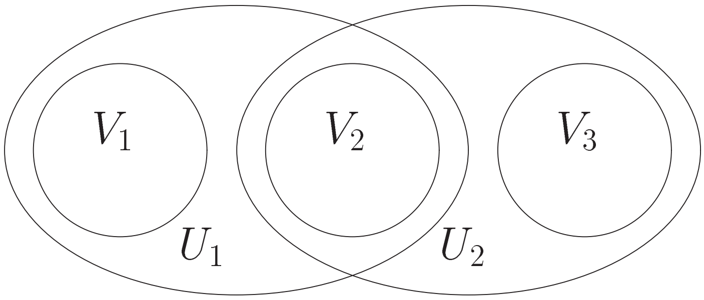

Figure 3.2: Simple interaction

Since dynamics of V_2 is responsible for the interaction between U_1 and U_2, we want to give the name of *dimension of interaction* to the dimension of μ_{V_2}. According to the definition (3.7) we have

$$\begin{aligned} d_q^{\mathsf{int}} &= D_q(\mu_1) + D_q(\mu_2) - D_q(\mu_U) \\ &= D_q(\mu_{V_1}) + D_q(\mu_{V_2}) + D_q(\mu_{V_2}) + D_q(\mu_{V_3}) + \\ &\quad -[D_q(\mu_{V_1}) + D_q(\mu_{V_2}) + D_q(\mu_{V_3})] \\ &= D_q(\mu_{V_2}). \end{aligned}$$

III Consider now the general situation described in section 3.2.2. Reconstructing dynamics from time series of typical variables from systems U_1 and U_2, say $x_1(n)$ and $x_2(n)$ we get

$$\begin{aligned} D_q(\mu_1) &\geq D_q(\mu_V), \\ D_q(\mu_2) &\geq D_q(\mu_V). \end{aligned}$$

From a typical function $Y(x_1, x_2)$ we reconstruct attractor of U and obtain

$$\begin{aligned} &\max\{D_q(\mu_1), D_q(\mu_2)\} \\ &\quad \leq D_q(\mu_U) \\ &\quad \leq D_q(\mu_V) + (D_q(\mu_1) - D_q(\mu_V)) + \\ &\qquad (D_q(\mu_2) - D_q(\mu_V)), \end{aligned}$$

where $D_q(\mu_1) - D_q(\mu_V)$ quantifies number of degrees of freedom in U_1 not coupled to U_2. From this we conclude

$$\begin{aligned} 0 < D_q(\mu_V) &\leq d_q^{\mathsf{int}} \\ &= D_q(\mu_1) + D_q(\mu_2) - D_q(\mu_U) \\ &\leq \min\{D_q(\mu_1), D_q(\mu_2)\}, \end{aligned}$$

the difference between $D_q(\mu_V)$ and d_q^{int} depending on the strength of synchronization between U_1 and U_2.

IV As the last example we shall take a system X driving two response systems Y_1 and Y_2. Suppose we also have a second copy of this setup, namely drive X' with response systems Y_1' and Y_2'. We collect simultaneously four time series of some variable from all of the response systems. Now we choose randomly two of them and want to know if the systems they come from have a common driver.

It is easy to check that if they do, then d_q^{int} is approximately the dimension of the invariant measure of the driver system $D_q(\mu_X) > 0$. If they have different drivers, then $d_q^{\mathsf{int}} = 0$.

Summarizing, from measurements involving parts of the given system and arbitrary nontrivial smooth function of two variables we can reconstruct the dimensions of measures μ_1, μ_2 and μ_U. From this we can obtain the dimension of interaction d_q^{int} (3.7). Depending on the values of $D_q(\mu_1), D_q(\mu_2), D_q(\mu_U)$ and d_q^{int} we can find out if the systems are coupled or not, and what is the direction of coupling.

3.4 Classification of possible interaction schemes

Let us thus assume that we have two subsystems and their reconstructed dimensions are $D_q(\mu_1)$ and $D_q(\mu_2)$. The dimension of the whole system $D_q(\mu_U)$ is obtained from time series $y(n)$ constructed through the procedure described in the previous section. The dimension of interaction is calculated from (3.7). The above discussion leads to the question which situations are possible. There are four non-equivalent cases:

1. $d_q^{\mathsf{int}} = 0$ suggests that the systems U_1 and U_2 do not interact;

2. $D_q(\mu_1) = D_q(\mu_2) = d_q^{\mathsf{int}}$ suggests that the systems U_1 and U_2 are the same system or we have maximal coupling;

3. $D_q(\mu_1) > D_q(\mu_2) = d_q^{\mathsf{int}}$ suggests that all the variables of U_2 couple to some of the degrees of freedom of U_1, or U_2 is the driver in the pair driver—response which is $U_1 \equiv U$;

4. The generic situation $D_q(\mu_1), D_q(\mu_2) > d_q^{\mathsf{int}}$ can be interpreted as two response systems driven by a common driver.

It is convenient sometimes to use m_1^q, m_2^q, m_U^q (3.8). We can write then the above classification as follows

1. $m_1^q = m_2^q = m_U^q = 0$ — no interaction;

2. $1 = m_1^q = m_2^q = m_U^q$ — maximal coupling: $\mu_1 \equiv \mu_2 \equiv \mu_V$;

3. $1 = m_1^q > m_2^q = m_U^q > 0$ — all the degrees of freedom of $U_2 \equiv V$ couple to some variables of U_1;

4. $1 > m_1^q \geq m_2^q > m_U^q > 0$ — interaction or double control.

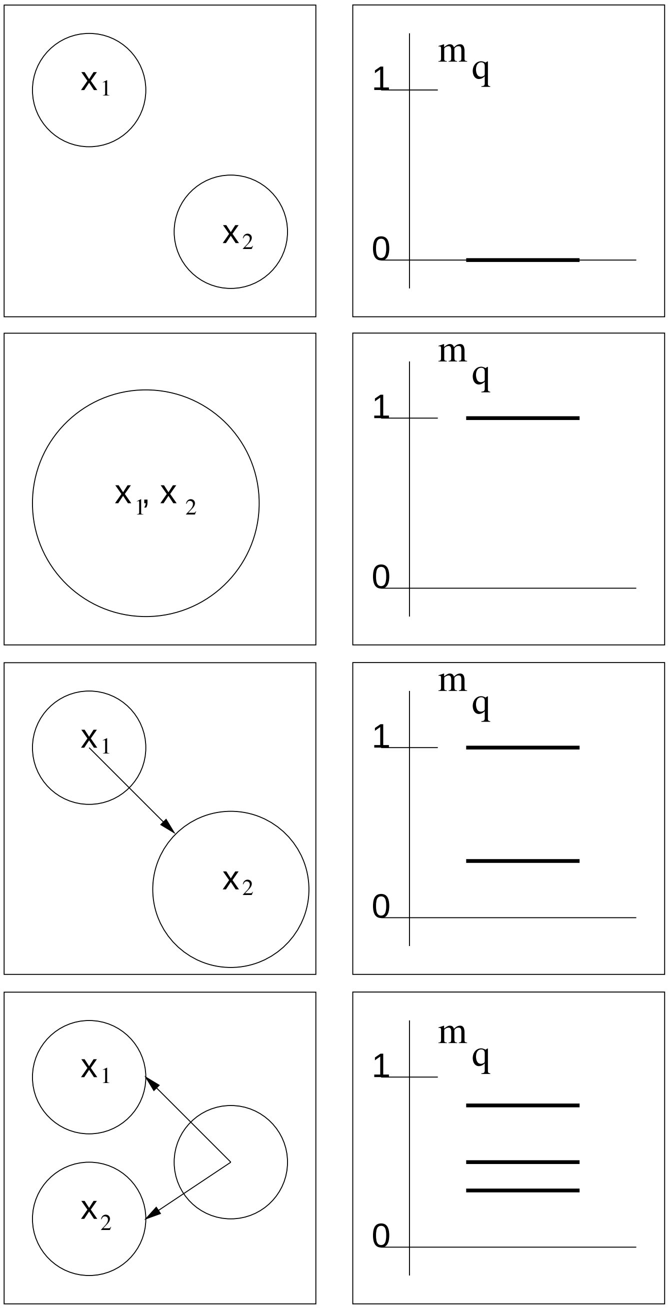

$$d_q^{\mathsf{int}} = 0$$

$$m_1^q = m_2^q = m_U^q = 0$$

$$D_q(\mu_1) = D_q(\mu_2) = d_q^{\mathsf{int}} > 0$$

$$m_1^q = m_2^q = m_U^q = 1$$

$$D_q(\mu_2) > D_q(\mu_1) = d_q^{\mathsf{int}} > 0$$

$$1 = m_2^q > m_1^q = m_U^q > 0$$

$$D_q(\mu_1), D_q(\mu_2) > d_q^{\mathsf{int}} > 0$$

$$1 > m_1^q \geq m_2^q > m_U^q > 0$$

Figure 3.3: Classification of possible interaction schemes. The first column shows symbolically the relative position in the abstract space of the subsystems in which we measure the time series x_1 and x_2. An arrow from one system to another means the future states of the second system depend on the current states of both. The second column shows the values of normalized dimensions m_1^q, m_2^q and m_U^q in each of the cases.

All the four cases are presented symbolically in Figure 3.3.

The examples considered in the previous section can easily be identified as particular cases of this classification. Namely

1. example I represents case 1;
2. example II represents case 4;
3. example III can represent cases 2, 3 or 4, depending on the values of differences $D_q(\mu_1) - D_q(\mu_V)$, $D_q(\mu_2) - D_q(\mu_V)$ (whether they are greater than or equal to 0);
4. the last example represents cases 1 or 4 depending on whether the signals analyzed come from systems coupled to the same driver or not.

3.5 Numerical results

Below we shall present some applications of our method to analysis of numerical results for several paradigmatic systems (coupled Hénon maps and logistic maps).

Throughout this section we will use d_2^{int}. The dimensions presented in the pictures are always D_2 calculated with the help of `d2` program from TISEAN package [112] with an algorithm which is an extension of algorithms published previously [98, 99, 126] improving speed of computation [112]. In every case we used 10^5 points with one exception described in the text. The functions Y used to calculate the dimension of the whole system (cf. previous sections) were $x + y$, $x \cdot y$, $\sin(x)\cos(y)$, $x\exp(y)$, $2x - y$. To estimate the dimension we smoothed output from `d2` either with the help of the Takens-Theiler estimator `c2t` or by fitting straight lines locally to the correlation sum with `c2d` (see chapter 2).

3.5.1 Two Hénon maps

Consider a system U consisting of two Hénon maps [113] coupled as follows [203]:

$$\begin{aligned} K & \left\{ \begin{array}{rcl} x_{i+1} & = & 1.4 - x_i^2 + 0.3 y_i, \\ y_{i+1} & = & x_i, \end{array} \right. \\ L & \left\{ \begin{array}{rcl} u_{i+1} & = & 1.4 - (C x_i + (1-C) u_i) u_i + B v_i, \\ v_{i+1} & = & u_i. \end{array} \right. \end{aligned} \tag{3.9}$$

Thus Hénon system K drives system L. The coupling is introduced through variable u. We consider the case of coupled identical systems ($B = 0.3$) and non-identical coupled systems ($B = 0.1$). Parameter C measures the strength of interaction.

Suppose the variables accessible experimentally are x_n and u_n. What can be said in this case about the interaction between systems K and L?

Certainly, for $C = 0$ the systems K and L do not interact (case 1. in our classification), therefore $D_q(\mu_U) = D_q(\mu_K) + D_q(\mu_L)$ and $d_q^{\mathsf{int}} = 0$. On the other hand, for positive C the influence of x should reflect in the behavior of u. From Theorem 3 we expect $D_q^{\mathsf{int}} = D_q(\mu_K)$ (case 3.). One can also expect for C raising slightly above 0, $D_q(\mu_U)$ not to change much, while $D_q(\mu_L)$ should jump from its value at 0 to the value of $D_q(\mu_U)$ at $C = 0$.

(a) (b)

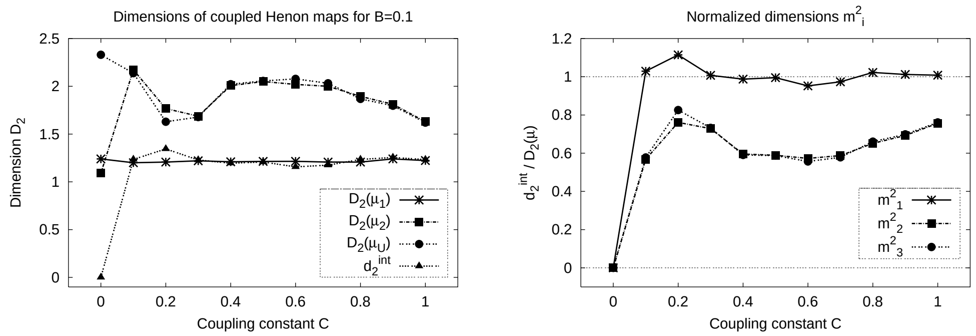

Figure 3.4: a) Dimensions $D_2(\mu_1), D_2(\mu_2), D_2(\mu_U)$ and d_2^{int} of one-way coupled non-identical Hénon maps (3.9) for $B = 0.1$. b) Normalized dimensions m_1^2, m_2^2 and m_U^2 for the same systems.

(a) (b)

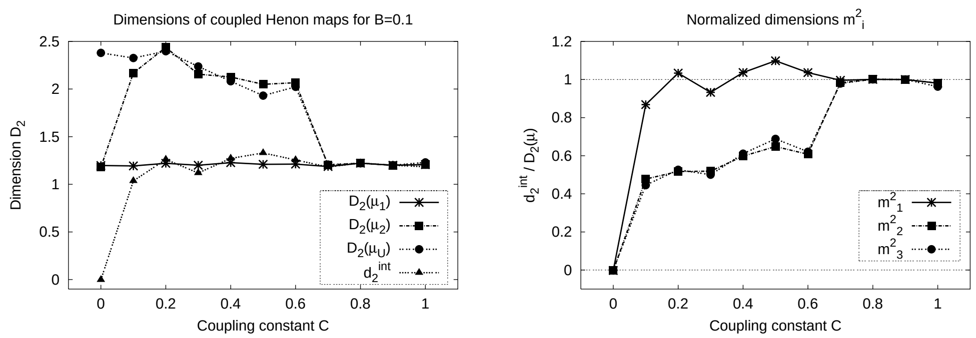

Figure 3.5: a) Dimensions $D_2(\mu_1), D_2(\mu_2), D_2(\mu_U)$ and d_2^{int} of one-way coupled identical Hénon maps (3.9) for $B = 0.3$. b) Normalized dimensions m_1^2, m_2^2 and m_U^2 for the same systems.

This behavior can indeed be seen in figure 3.4a for non-identical Hénon systems ($B = 0.1$) and in 3.5a for identical systems ($B = 0.3$). The synchronization of x and u [175, 208] visible for $C \geq 0.7$ (case 2.) can be discovered much simpler, namely if one plots several consecutive values of $x_n - u_n$ versus coupling, for these particular values all of the points fall on 0 (figure 3.6, see also figure 7 of [203]).

Looking at the normalized dimensions (fig. 3.4b and 3.5b) we easily identify lack of coupling for $C = 0$ ($m_1 = m_2 = m_3 = 0$), case 4. (maximal coupling) for $B = 0.3$ and $C \geq 0.7$ ($m_1 = m_2 = m_3 = 1$), and case 3. in all the other cases.

The drop-down of the dimension at 0.7 for identical systems is connected with the full synchronization of the systems. The equations (3.9) admit solutions symmetric

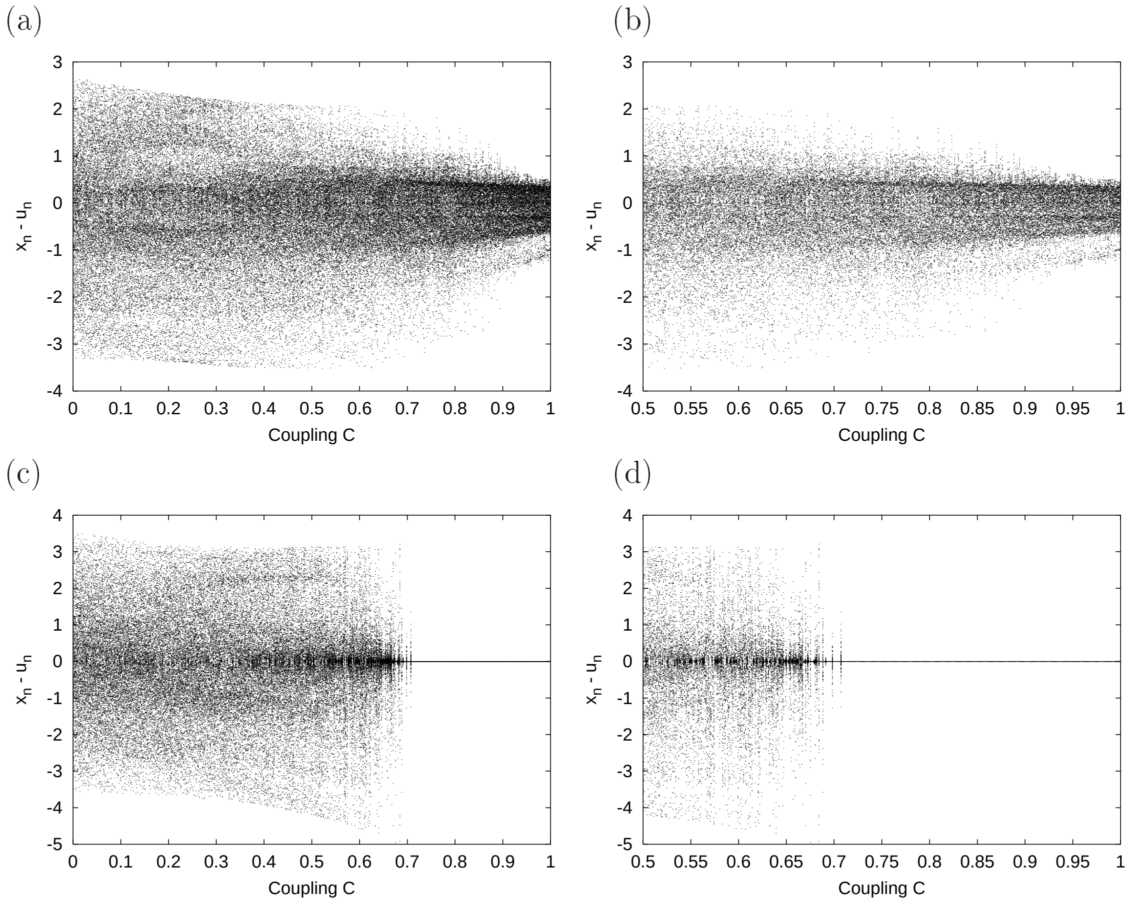

Figure 3.6: Differences between the x_n and u_n values of two coupled Hénon systems (3.9) of a 100 consecutive values. (a) and (b) show the case of non-identical systems ($B = 0.1$), (c) and (d) show the case of identical systems ($B = 0.3$).

in x and u ($x_n - u_n = 0$), which at this region become stable and the whole probability measure gets localized on a lower-dimensional manifold. For more details cf. [203].

3.5.2 Three Hénon maps

Consider now the system U consisting of three Hénon maps [113] coupled as follows [203]:

$$
\begin{aligned}
K \quad & \begin{cases} x_{i+1} = 1.4 - x_i^2 + 0.3y_i, \\ y_{i+1} = x_i, \end{cases} \\
L \quad & \begin{cases} u_{i+1} = 1.4 - (C_1 x_i + (1 - C_1)u_i)u_i + B_1 v_i, \\ v_{i+1} = u_i, \end{cases} \\
M \quad & \begin{cases} w_{i+1} = 1.4 - (C_2 x_i + (1 - C_2)w_i)w_i + B_2 z_i, \\ z_{i+1} = w_i. \end{cases}
\end{aligned}
\tag{3.10}
$$

Thus Hénon system K drives systems L and M. The coupling is introduced through variables u and w. Parameters C_1, C_2 measure the strength of interaction.

Suppose the measurements on (K, L, M) yield variables u and w. What can be said in this case about the interaction between the systems L and M?

For $C_1 = C_2 = 0$ neither system L nor M feels the influence of K. They also do not interact (case 1.). When one of C_i grows, the influence of K is immediately mirrored in the rise of the dimension of μ_L or μ_M. For both $C_i > 0$ the systems L and M interact (case 2.), and the part responsible for interaction is K. Thus the dimension of the common part is constant and equal to 1.22 in our case.

We show this behavior in figures 3.7a for non-identical systems ($B_1 = 0.3, B_2 = 0.1$) and 3.8a for identical systems ($B_1 = 0.3, B_2 = 0.3$). In both cases $C_1 = 0.5$ and C_2 is varied. In both figures one can clearly see the jump of the dimension of interaction from 0 to values equal to or greater than 1.22, the dimension of the attractor of K.

Typical behavior of local dimension $d \ln C(\varepsilon)/d \ln \varepsilon$ as a function of resolution ε is shown in figure 3.9.

Figure 3.8 is particularly interesting, since one can apparently identify all the four cases from our classification. For $C_2 = 0$ we have non-interacting systems, for $C_2 \in [0.2, 0.4]$ and $C_2 = 0.6$ we have case 2.

For $C_2 = 0.5$ the two Hénon systems L and M become identical. Since at this value of coupling constant they are in general synchrony with the driver, which means their asymptotic states are independent of their initial states, and depend only on the present state of the driver, it follows that $u_n = w_n$.

For $C_2 \geq 0.7$ the system M fully synchronizes with K, which leads to the collapse of the probability measure in K, M space on the diagonal (compare the discussion in the previous subsection).

(a) (b)

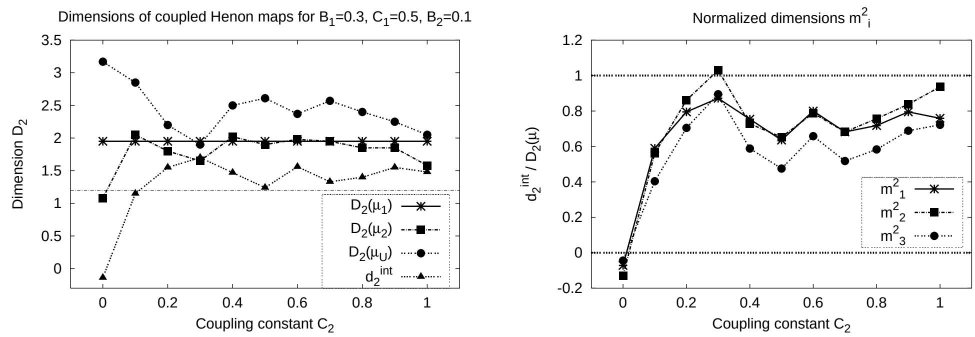

Figure 3.7: a) Dimensions $D_2(\mu_1), D_2(\mu_2), D_2(\mu_U)$ and d_2^{int} of two-way coupled Hénon maps (3.10) with different response systems ($C_1 = 0.5, B_1 = 0.3, B_2 = 0.1$). Additional line at 1.2 in the upper figure is the guide for the eye and stands for the dimension of the attractor of Hénon system K. b) Normalized dimensions m_1^2, m_2^2 and m_U^2 for the same systems.

(a) (b)

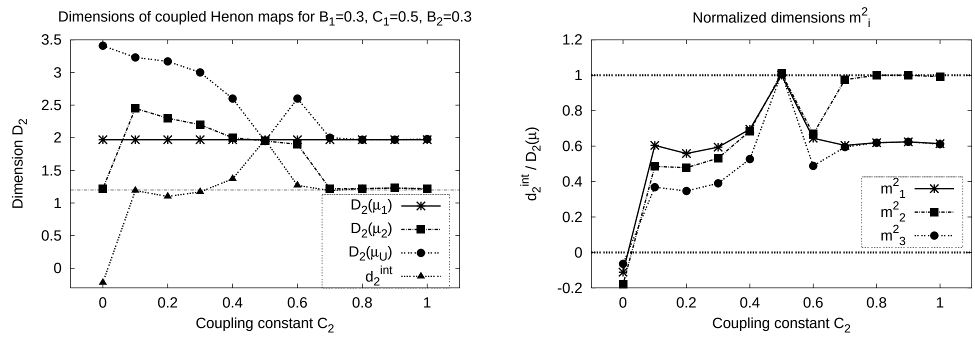

Figure 3.8: a) Dimensions $D_2(\mu_1), D_2(\mu_2), D_2(\mu_U)$ and d_2^{int} of two-way coupled Hénon maps (3.10) with identical response systems ($C_1 = 0.5, B_1 = 0.3, B_2 = 0.3$). Additional line at 1.2 in the upper figure is the guide for the eye and stands for the dimension of the attractor of Hénon system K. b) Normalized dimensions m_1^2, m_2^2 and m_U^2 for the same systems.

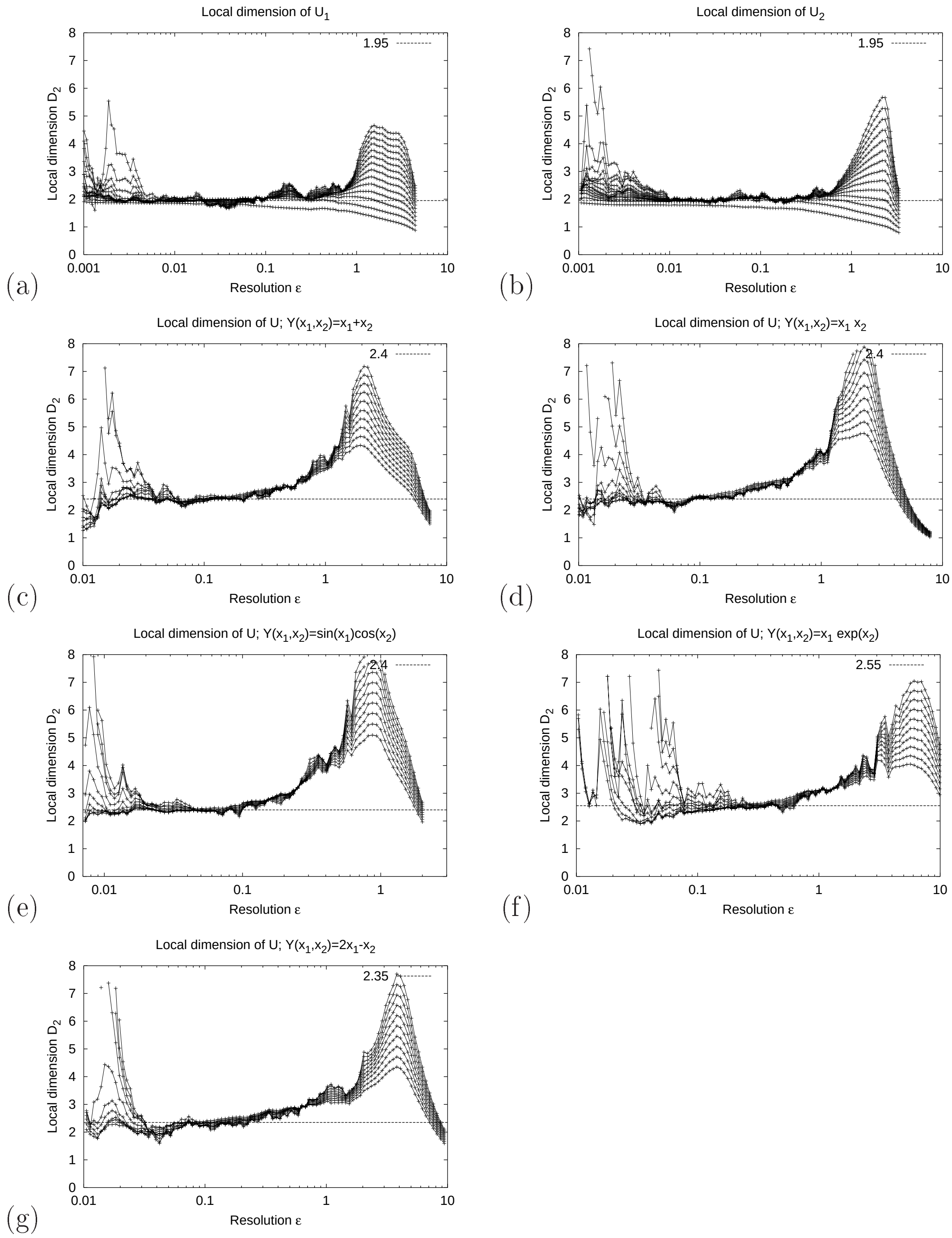

Figure 3.9: Local correlation dimension $d\ln C(\varepsilon)/d\ln\varepsilon$ as a function of resolution ε smoothed out with the Takens estimator. Data shown come from two different Hénon systems driven by the third (eq. 3.10 with parameters $B_1 = 0.3$, $C_1 = 0.5$, $B_2 = 0.1$, $C_2 = 0.6$.). Correlation dimension of subsystems U_1 and U_2 estimated from (a) and (b) is 1.95 for both. Dimension of the whole system is estimated to be 2.4 on the basis of plots (c) to (g), for which five different coupling functions were used. Dimension of interaction d_2^{int} in this case is $1.95 + 1.95 - 2.4 = 1.5 > 1.22$, which suggests partial synchronization of the two response systems with the driver.

3.5.3 Logistic maps

Let $f_\alpha(x) := \alpha x(1-x)$. Consider a system consisting of four uncoupled logistic maps

$$x^i_{n+1} = f_{\alpha_i}(x^i_n),$$

where $\alpha_1 = 3.7$, $\alpha_2 = 3.8$, $\alpha_3 = 3.9$ and $\alpha_4 = 4$. Suppose the only variables available experimentally are[3] $Y^{i,j}(n) = F^{i,j}(x^i_n, x^j_n)$, $i < j$. Given two randomly chosen time series $Y^{i,j}(n), Y^{k,l}(n)$ we want to know if they share some degrees of freedom or not (if they "interact" or not). If i or j is equal to k or l, there are only three active degrees of freedom in the compound system. Otherwise there are four.

Estimated correlation dimensions for several cases are collected in Table 3.2. In every case we used time series 10^5 points long except for the last one, for which 10^6 points were used. The estimation error was roughly 2% except for the last case for which it was about 5-10%[4].

series $x(n)$	$D(\mu_{x(n)})$
x_1	0.96
x_2	0.95
x_3	0.97
x_4	0.99
$Y^{1,2}$	1.88
$Y^{1,3}$	1.94
$Y^{1,4}$	1.95
$Y^{2,3}$	1.89
$Y^{2,4}$	1.94
$Y^{3,4}$	1.93
$f(Y^{1,2}, Y^{1,3})$	2.88
$f(Y^{1,2}, Y^{3,4})$	3.8

Table 3.2: Estimated correlation dimension for uncoupled logistic maps. The estimation error is roughly 2% except for the last number for which it is about 5-10%.

Consider now two symmetrically coupled logistic maps

$$\begin{cases} x_{n+1} &= f_\alpha(\tilde{x}_n), \\ y_{n+1} &= f_\beta(\tilde{y}_n), \end{cases} \quad \text{where} \quad \begin{cases} \tilde{x}_n &= \frac{x_n + c y_n}{1+c}, \\ \tilde{y}_n &= \frac{y_n + c x_n}{1+c}, \end{cases} \tag{3.11}$$

and parameter $c \in [0, 1]$ measures the coupling. This is slightly different from couplings discussed previously in the literature (e.g. [180, 261, 208]). The maps are

[3] The coupling functions $F^{i,j}$ were chosen randomly out of $x + y$, $x \cdot y$, $\sin(x)\cos(y)$, $x\exp(y)$, $2x - y$ and fixed.

[4] We believe there are two reasons for this. One is higher dimensionality of the system in the last case (four uncoupled logistic maps), the other is worse ergodicity in the phase space because the maps are uncoupled. Note that our procedure consists of two parts: first we make the embedding, then we calculate the dimensions. Each of the two can introduce errors. The number expected in the last case is the sum of the first four numbers, namely 3.87 ± 0.06

uncoupled for $c = 0$. For $c = 1$ (the strongest coupling) if we set $z_n := \tilde{x}_n = \tilde{y}_n$, we have $x_n = \frac{2\alpha}{\alpha+\beta} z_n$, $y_n = \frac{2\beta}{\alpha+\beta} z_n$, and $z_{n+1} = f_{\frac{\alpha+\beta}{2}}(z_n)$. Therefore dynamics is one-dimensional. Case $c > 1$ is equivalent to $c' = 1/c$.

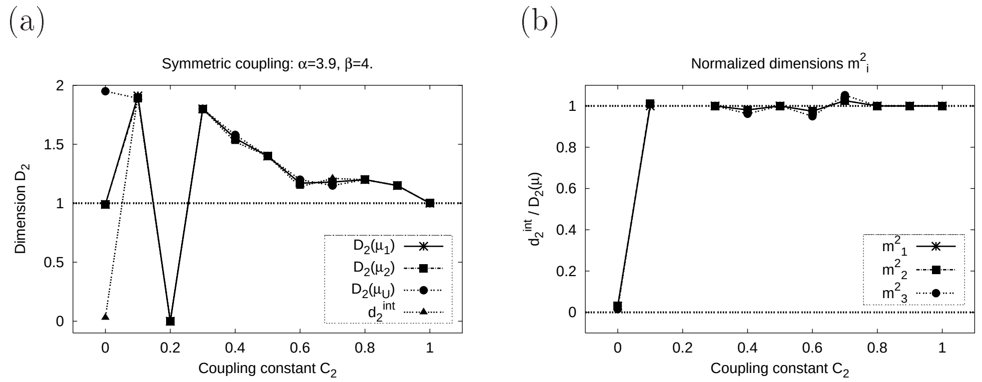

Figure 3.10: a) Dimensions $D_2(\mu_1), D_2(\mu_2), D_2(\mu_U)$ and d_2^{int} of symmetrically coupled logistic maps (3.11). b) Normalized dimensions m_1^2, m_2^2 and m_U^2 for the same systems.

Estimated correlation dimensions for several values of the coupling constant c are shown in figure 3.10. One can see the jump in the dimension of interaction from 0 at $c = 0$ to the value equal to the dimension of the whole systems for positive c indicating case 4. in our classification. For $c = 0.2$ asymptotic dynamics settles on a period two periodic orbit leading to all the dimensions equal to 0. Numerically obtained approximations to asymptotic measures for coupling constant $c = 0., 0.1, 0.2, 0.3, 0.4, 0.5$ are shown in figure 3.11. Note the increasing synchronization between x and y.

It is of interest to compare the values of dimensions for $c = 0$ and 1, because in both cases $D_1(\mu_x) \approx D_1(\mu_y) = 1$, but the dimension of the whole system, estimated from $f(x_n, y_n)$, is equal to 2 in the first case and 1 in the second, implying $D_q^{\text{int}} = 0$ and 1 in these cases, respectively. Thus the first measure has a product structure, while the other is concentrated on the diagonal $x = y$.

The last case considered is that of the double control:

$$\begin{cases} x_{n+1} &= f_\alpha(x_n), \\ y_{n+1} &= \frac{f_\beta(y_n)+c_1 x_n}{1+c_1}, \\ z_{n+1} &= \frac{f_\gamma(z_n)+c_2 x_n}{1+c_2}, \end{cases} \tag{3.12}$$

where $\alpha = 4.0$, $\beta = 3.8$, $\gamma = 3.9$, $c_1, c_2 \in [0, 1]$. Let the observed systems U_1 and U_2 be the sets of all pairs (x, y) and (x, z), respectively. Then we have essentially the case 4. If U_1 and U_2 are the sets of all points x and pairs (x, z) then we have the case 3.

Figures 3.12 and 3.13 show estimated correlation dimension in these cases. Again, one can clearly see the difference between the coupled ($c_i > 0$) and uncoupled ($c_i = 0$) systems, because the interaction dimension jumps from 0 to 1 or more, in agreement with our expectations from Theorems 2 and 3, since the dimension of the common part is 1 (x_n evolves according to Ulam map: $\alpha = 4.0$; see example 1.2.2, in particular

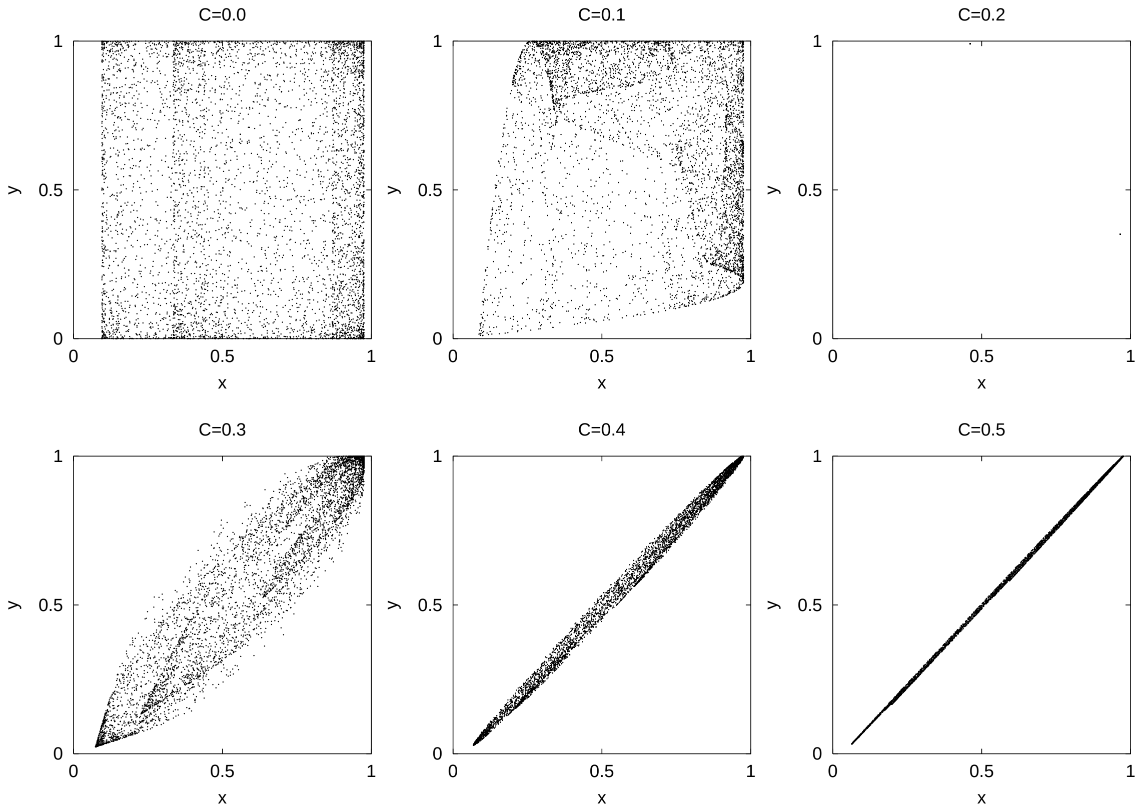

Figure 3.11: Attractors of symmetrically coupled logistic maps (3.11) for $c = 0$, 0.1, 0.2, 0.3, 0.4, 0.5 in (x, y) plane.

(a) (b)

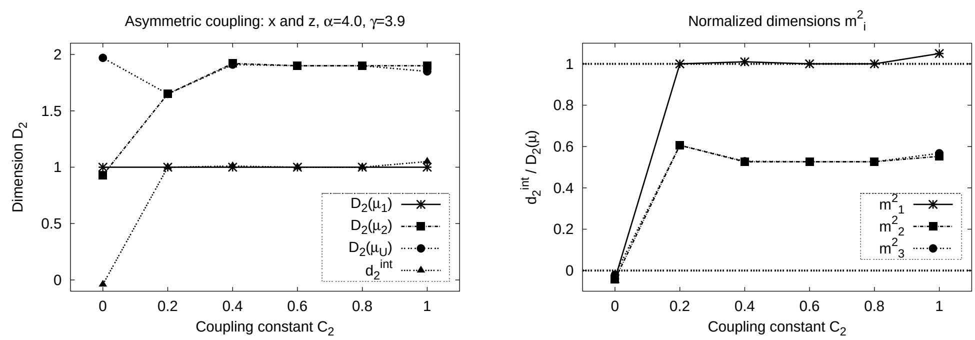

Figure 3.12: (a) Dimensions $D_2(\mu_1), D_2(\mu_2), D_2(\mu_U)$ and d_2^{int} of asymmetrically coupled logistic maps (3.12) when x and z are the observed variables. (b) Normalized dimensions m_1^2, m_2^2 and m_U^2 for the same systems.

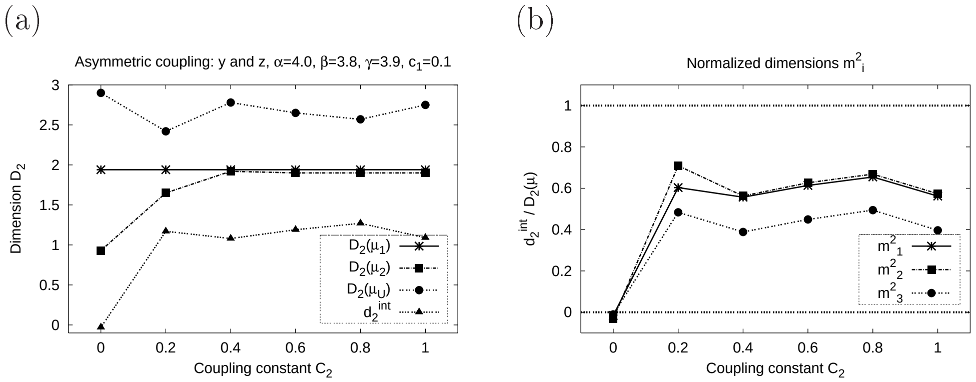

Figure 3.13: (a) Dimensions $D_2(\mu_1), D_2(\mu_2), D_2(\mu_U)$ and d_2^{int} of asymmetrically coupled logistic maps (3.12) when y and z are the observed variables. (b) Normalized dimensions m_1^2, m_2^2 and m_U^2 for the same systems.

eq. (1.63)). Figure 3.14 shows projections of the attractor of (3.12) on (x, z) and (y, z) planes for $c_1 = 0.1$ and $c_2 = 0.2$.

3.6 Conclusions and outlook

We presented a method which allows to distinguish interacting from non-interacting systems when time series of variables of the two systems are available. Partial proof of its validity was provided. Classification of all the possible interaction schemes was presented with examples of all the cases. Several simple interacting systems were analyzed.

To use our method in practice (from field data) we suggest the following procedure:

A. calculate the dimensions $D_q(\mu_1), D_q(\mu_2), D_q(\mu_U)$ and d_q^{int} (3.7) (we suggest $q = 1$ or $q = 2$). It is also good to normalize the data if they are of different orders. In this respect one might wish to use a coupling function of the type

$$Y\left(\frac{x - \langle x \rangle}{\sigma_x}, \frac{y - \langle y \rangle}{\sigma_y}\right).$$

B. repeat the calculation for several different coupling functions Y and average the results (linear combinations seem to be the best choice);

C. if they are different from 0, calculate the normalized dimensions m_i^q (3.8).

D. they may take one, two or three distinct values.

   (a) if all of them are 0, the systems do not interact (case 1.);

   (b) if all of them are greater than 0 and less than 1, this is a generic case of interacting systems (case 4.);

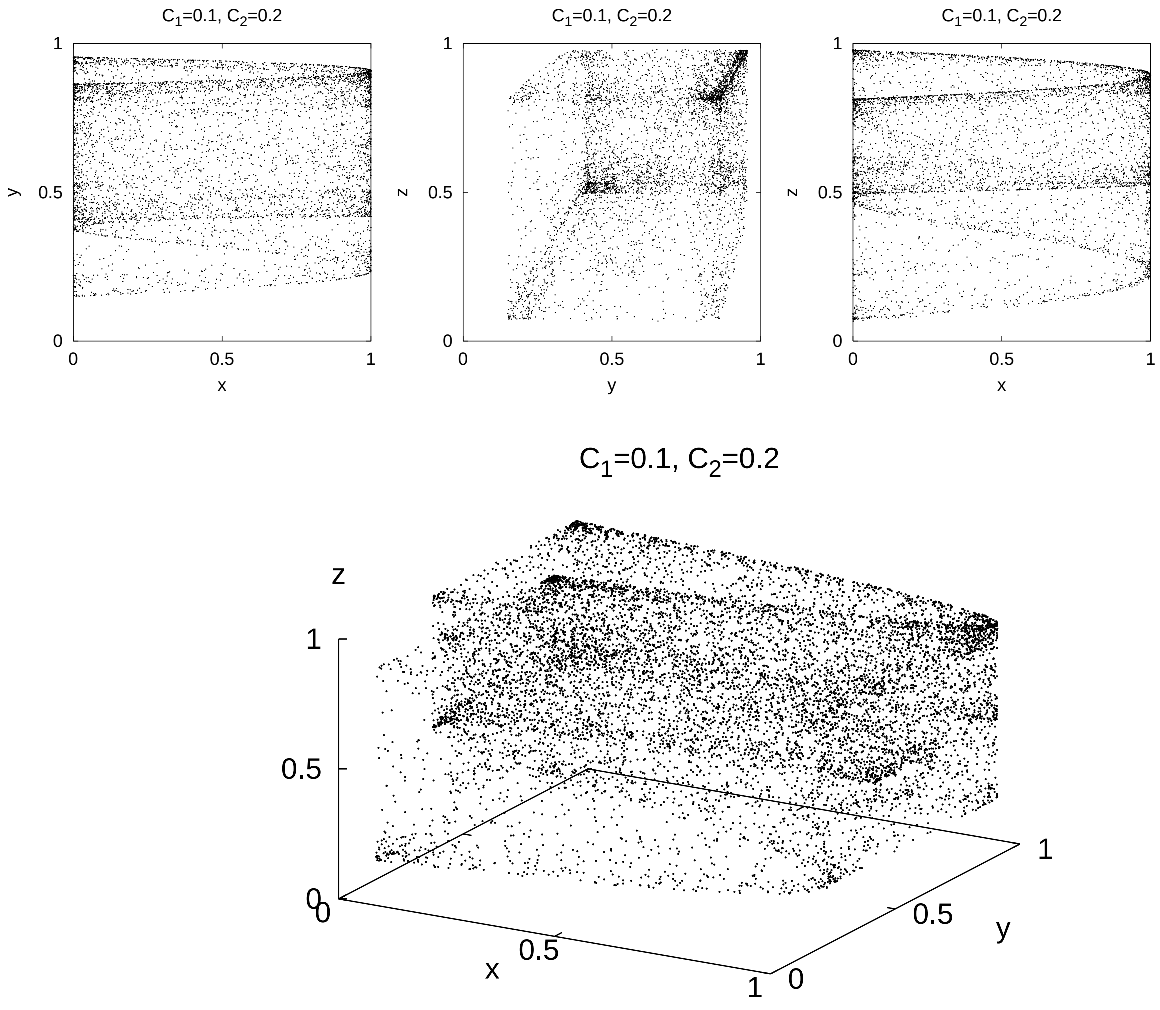

Figure 3.14: Projections of the attractor of asymmetrically coupled logistic maps (3.12) for $c_1 = 0.1$, $c_2 = 0.2$ on (x, y), (y, z) and (x, z) planes and a view of the whole structure from a distant point.

(c) if one of them is 1, the other are smaller, all the degrees of freedom of one system couple to some degrees of freedom of the other (case 3.), or we have the previous case (case 4.) but the variables of one of the systems which are not coupled to the other synchronize to the system comprising the common part of the dynamics;

(d) if they are all equal to 1, all the degrees of freedom of one system couple to all the degrees of freedom of the other (case 2.), or we have the two previous cases (3. or 4.) but the variables of the two systems which are not coupled synchronize to the system comprising the common part of the dynamics.

Appendix 3.A The Proofs.

3.A.1 Theorem 3.1

Let μ_1, μ_2 be the invariant measures of systems U_1, U_2 as defined in Section 3.2.1.

Theorem 3.1 *Suppose $D_q(\mu_1), D_q(\mu_2), D_q(\mu_1 \times \mu_2)$ exist. Then*

$$D_q(\mu_1 \times \mu_2) = D_q(\mu_1) + D_q(\mu_2).$$

Proof: Take $q \neq 1$. For every $\delta > 0$ consider partitions of $\mathbb{R}^{n_i}$ into cells of volume δ^{n_i}. This gives a partition in $\mathbb{R}^{n_1+n_2}$ into boxes of volume $\delta^{n_1+n_2}$.

Let

$$\begin{aligned} p_j &= \mu_1(j-\text{th cell from the cover of } U_1), \\ r_k &= \mu_2(k-\text{th cell from the cover of } U_2). \end{aligned}$$

Then

$$\begin{aligned} D_q(\mu_1 \times \mu_2) &= \lim_{\delta\to 0} \frac{1}{q-1} \frac{\ln \sum_{k,j} p_i^q r_j^q}{\ln \delta} \\ &= \lim_{\delta\to 0} \frac{1}{q-1} \frac{\ln \left(\sum_k p_i^q\right) \left(\sum_j r_j^q\right)}{\ln \delta} \\ &= \lim_{\delta\to 0} \left(\frac{1}{q-1} \frac{\ln \sum_k p_k^q}{\ln \delta} \right) + \\ &\quad \lim_{\delta\to 0} \left(\frac{1}{q-1} \frac{\ln \sum_j r_j^q}{\ln \delta} \right). \end{aligned}$$

But the last two limits exist and are equal to $D_q(\mu_1)$ and $D_q(\mu_2)$, respectively.

The case of $q = 1$ is straightforward and left to the reader. ☐

3.A.2 Theorem 3.2

For the next proof we need the following Lemma.

Lemma 3.1 *Let* $1 \geq c_{ij} \geq 0$, $a_i = \sum_j c_{ij}$, $b_j = \sum_i c_{ij}$, $\sum_{ij} c_{ij} = \sum_j b_j = \sum_i a_i = 1$. *Then*

$$\sum_{i,j} (c_{ij} \ln c_{ij} - a_i b_j \ln(a_i b_j)) \geq 0. \tag{3.A.1}$$

Proof: Every convex function f satisfies Jensen's inequality

$$f\left(\sum_i p_i x_i\right) \leq \sum_i p_i f(x_i), \tag{3.A.2}$$

where $\sum_i p_i = 1$. Since $f(x) = x \ln x$ is convex, one has

$$\begin{aligned}
f\left(\sum_{i,j} c_{ij}\right) &\leq \sum_{i,j} a_i b_j f\left(\frac{c_{ij}}{a_i b_j}\right), \\
f(1) &\leq \sum_{i,j} a_i b_j \frac{c_{ij}}{a_i b_j} (\ln c_{ij} - \ln a_i - \ln b_j) \\
0 &\leq \sum_{i,j} c_{ij} \ln c_{ij} - \sum_{i,j} c_{ij} \ln a_i - \sum_{i,j} c_{ij} \ln b_j \\
0 &\leq \sum_{i,j} c_{ij} \ln c_{ij} - \sum_i a_i \ln a_i - \sum_j b_j \ln b_j \\
0 &\leq \sum_{i,j} (c_{ij} \ln c_{ij} - a_i b_j \ln(a_i b_j)),
\end{aligned}$$

where we used (3.A.2) with $p_{ij} = a_i b_j$ and $x_{ij} = c_{ij}/(a_i b_j)$. □

Let μ_1, μ_2, μ_V and μ_U be the invariant measures defined in Section 3.2.2.

Theorem 3.2 *Suppose* $D_1(\mu_1)$, $D_1(\mu_2)$, $D_1(\mu_V)$, $D_1(\mu_U)$ *exist. Then*

$$D_1(\mu_V) \leq d_{\mathsf{int}} = D_1(\mu_1) + D_1(\mu_2) - D_1(\mu_U).$$

The equality holds when y_1 *and* y_2 *are asymptotically independent.*

Proof: Let n_1 be the number of variables $\mathbf{y}_1$ (section 3.2.2) of the property that any change in their present state does not influence the future states of system U_2. Let n_2 be the number of variables $\mathbf{y}_2$ of the symmetric property. Let m be the number of all the other variables ($\mathbf{x}$). Variables $\mathbf{x}$ form the part V of the compound system which is responsible for the interaction. Thus the system can be embedded in $\mathbb{R}^{n_1+n_2+m}$. Consider a partition of $\mathbb{R}^{n_1+n_2}$ into cells of size δ consistent with the structure of equations of dynamics, i.e. (i,j,k)-th cell$= A_i \times B_j \times C_k$, where A, B, C are δ-cells of dimension, respectively, m, n_1 and n_2 in spaces spanned by $\mathbf{x}$, $\mathbf{y}_1$ and $\mathbf{y}_2$.

Since the dynamics of $(\mathbf{x}, \mathbf{y}_1)$ is independent of $\mathbf{y}_2$, the invariant measure $\mu_1(A_i \times B_j)$ can be written as

$$\mu_1(A_i \times B_j) = \mu_V(A_i)\mu_{(y_1|x)}(B_j|A_i) =: p_i r_{ji},$$

where $\mu_{(y_1|x)}(B_j|A_i)$ are the conditional probabilities of finding the $\mathbf{y}_1$ in B_j under the condition $\mathbf{x}$ being in A_i. Similarly,

$$\mu_2(A_i \times C_k) = \mu_V(A_i)\mu_{(y_2|x)}(C_k|A_i) =: p_i s_{ki},$$

and

$$\begin{aligned} \mu_S(A_i \times B_j \times C_k) &= \mu_V(A_i)\mu_{(y_1,y_2|x)}(B_j, C_k|A_i). \\ &=: p_i t_{jki} \end{aligned}$$

If $\mu_{(y_1|x)}(B_j|A_i)$ and $\mu_{(y_2|x)}(C_k|A_i)$ are independent, then

$$\mu_{(y_1,y_2|x)}(B_j, C_k|A_i) = \mu_{(y_1|x)}(B_j|A_i)\mu_{(y_2|x)}(C_k|A_i), \tag{3.A.3}$$

otherwise the only thing we know is that the l.h.s. measure is the coupling of the r.h.s. measures, namely

$$\begin{aligned} \sum_k \mu_{(y_1,y_2|x)}(B_j, C_k|A_i) &= \mu_{(y_1|x)}(B_j|A_i), \\ \sum_j \mu_{(y_1,y_2|x)}(B_j, C_k|A_i) &= \mu_{(y_2|x)}(C_k|A_i), \end{aligned}$$

or

$$\begin{aligned} \sum_k t_{jki} &= r_{ji}, \\ \sum_j t_{jki} &= s_{ki}. \end{aligned}$$

Of course,

$$\sum_k s_{ki} = \sum_j r_{ji} = \sum_{jk} t_{jki} = 1,$$

if $p_i \neq 0$. Otherwise we take $\forall j, k: \ t_{jki} = 0$.

Taking this into consideration, inequality (3.4) follows:

$$\begin{aligned} & D_1(\mu_1) + D_1(\mu_2) - D_1(\mu_V) - D_1(\mu_U) = \\ & \quad \lim_{\delta \to 0} \frac{\sum_i \sum_j p_i r_{ji} \ln(p_i r_{ji})}{\ln \delta} + \\ & \quad \lim_{\delta \to 0} \frac{\sum_i \sum_k p_i s_{ki} \ln(p_i s_{ki})}{\ln \delta} + \\ & \quad - \lim_{\delta \to 0} \frac{\sum_i p_i \ln(p_i)}{\ln \delta} + \\ & \quad - \lim_{\delta \to 0} \frac{\sum_{i,j,k} p_i t_{jki} \ln(p_i t_{jki})}{\ln \delta} \\ = & \quad \lim_{\delta \to 0} \frac{\sum_i p_i \ln(p_i) \left(\sum_j r_{ji} + \sum_k s_{ki} - 1 - \sum_{j,k} t_{jki}\right)}{\ln \delta} + \\ & \quad \lim_{\delta \to 0} \frac{\sum_i p_i \sum_{j,k}(r_{ji}s_{ki} \ln(r_{ji}s_{ki}) - t_{jki} \ln(t_{jki}))}{\ln \delta} \\ \geq & \quad 0 \end{aligned}$$

where in the last line we used Lemma 5 for $c = t$, $a = r$ and $b = s$ and the fact that $\ln \delta < 0$.

Note that the equality holds if and only if

$$t_{jki} = r_{ji} s_{ki}. \tag{3.A.4}$$

This is what we call asymptotical independence of variables y_1 and y_2. In particular, when y_i are in generalized synchrony with x, this means that their asymptotic behavior is independent of their initial states and depends only on initial state of x, therefore their probability distributions cannot be independent, since they depend on the same number $x(0)$. However, we are not sure if this the only case when the equality is violated, this is why we use another name for the above condition. □

One would like to establish a similar inequality in case of other Rényi dimensions, however, in general, even when (3.A.4) is satisfied,

$$D_q(\mu_S) \neq D_q(\mu_1) + D_q(\mu_2) - D_q(\mu_x).$$

Indeed,

$$\begin{aligned} D_q(\mu_1) + D_q(\mu_2) - D_q(\mu_x) - D_q(\mu_S) &= \qquad (3.A.5)\\ = \lim_{\delta\to 0} \frac{1}{\ln\delta} \ln &\left[\frac{\left(\sum_{i,k} p_i^q r_{ki}^q\right)\left(\sum_{l,j} p_l^q s_{jl}^q\right)}{\left(\sum_l p_l^q\right)\left(\sum_{i,j,k} p_i^q s_{ji}^q r_{ki}^q\right)} \right] \\ = \lim_{\delta\to 0} \frac{1}{\ln\delta} \ln &\left[1 + \frac{\sum_{i<l,j,k} p_i^q p_l^q (r_{ki}^q - r_{kl}^q)(s_{ji}^q - s_{jl}^q)}{\sum_{i,j,k,l} p_i^q p_l^q s_{ji}^q r_{ki}^q} \right]. \end{aligned}$$

This may have arbitrary sign and needs not vanish in the limit.

Although (3.A.5) must go to 0 in the limit $q \to 1$, one can perhaps construct examples of measures for which the slope can be arbitrarily large. On the other hand, we believe such measures will not be typically observed in physical systems.

3.A.3 Inequality (3.6)

We will prove inequalities (3.6)

$$\begin{aligned} d_q^{\mathsf{int}} &\leq D_q(\mu_i), \qquad (3.A.6)\\ D_q(\mu_V) &\leq D_q(\mu_i), \qquad (3.A.7)\\ D_q(\mu_i) &\leq D_q(\mu_U). \qquad (3.A.8) \end{aligned}$$

for $q > 1$. The case of $q = 1$ is similar and partly shown in the previous subsection.

Proof: We will use the fact that for $q > 1$ and positive a_i

$$\sum_i (a_i)^q \leq (\sum_i a_i)^q$$

(inequality (2.12.1) in [109]). We have

$$\begin{aligned} \sum_{i,j} p_i^q \sum_k t_{jki}^q &\leq \sum_{i,j} p_i^q (\sum_k t_{jki})^q = \sum_{i,j} p_i^q r_{ji}^q \leq \sum_i p_i^q \leq (\sum_i p_i)^q = 1,\\ \sum_{i,k} p_i^q \sum_j t_{jki}^q &\leq \sum_{i,k} p_i^q (\sum_j t_{jki})^q = \sum_{i,k} p_i^q s_{ki}^q \leq \sum_i p_i^q \leq (\sum_i p_i)^q = 1. \end{aligned}$$

(3.A.6) Since

$$\left(\sum_{i,j} p_i^q r_{ji}^q\right) \frac{\left(\sum_{l,k} p_l^q s_{kl}^q\right)}{\left(\sum_{i,j,k} p_i^q t_{jki}^q\right)} \geq \left(\sum_{i,j} p_i^q r_{ji}^q\right)$$

and $\ln \delta$ is negative we have

$$\begin{aligned} d_q^{\mathsf{int}} &= \frac{1}{q-1} \lim_{\delta \to 0} \frac{1}{\ln \delta} \ln \left[\frac{\left(\sum_{i,j} p_i^q r_{ji}^q\right)\left(\sum_{l,k} p_l^q s_{kl}^q\right)}{\left(\sum_{i,j,k} p_i^q t_{jki}^q\right)} \right] \\ &\leq \frac{1}{q-1} \lim_{\delta \to 0} \frac{1}{\ln \delta} \ln \left(\sum_{i,j} p_i^q r_{ji}^q\right) \\ &= D_q(\mu_1). \end{aligned}$$

Similarly for $D_q(\mu_2)$.

(3.A.7) Since

$$\sum_i p_i^q \geq \sum_{i,j} p_i^q r_{ji}^q$$

we have

$$\begin{aligned} D_q(\mu_V) &= \frac{1}{q-1} \lim_{\delta \to 0} \frac{1}{\ln \delta} \ln \left(\sum_i p_i^q\right) \\ &\leq \frac{1}{q-1} \lim_{\delta \to 0} \frac{1}{\ln \delta} \ln \left(\sum_{i,j} p_i^q r_{ji}^q\right) \\ &= D_q(\mu_1). \end{aligned}$$

Similarly for $D_q(\mu_2)$.

(3.A.8) Since

$$\sum_{i,j} p_i^q r_{ji}^q \geq \sum_{i,j,k} p_i^q t_{jki}^q$$

we have

$$\begin{aligned} D_q(\mu_1) &= \frac{1}{q-1} \lim_{\delta \to 0} \frac{1}{\ln \delta} \ln \left(\sum_{i,j} p_i^q r_{ji}^q\right) \\ &\leq \frac{1}{q-1} \lim_{\delta \to 0} \frac{1}{\ln \delta} \ln \left(\sum_{i,j,k} p_i^q t_{jki}^q\right) \\ &\leq D_q(\mu_U). \end{aligned}$$

Similarly for $D_q(\mu_2)$.

$\square$

Appendix 3.B An example of partially coupled systems.

We present here a simple although abstract example of interacting systems for which one can introduce the natural decomposition (3.3).

Consider two systems U_1, U_2 interacting through a thin contact layer V. Denote variables in U_1 as $\mathbf{u}_1 = (\mathbf{v}_1, \mathbf{w}_1)$, variables in U_2 as $\mathbf{u}_2 = (\mathbf{v}_2, \mathbf{w}_2)$, and variables of the contact layer V are $(\mathbf{v}_1, \mathbf{v}_2)$. Dynamics of such a configuration can be described

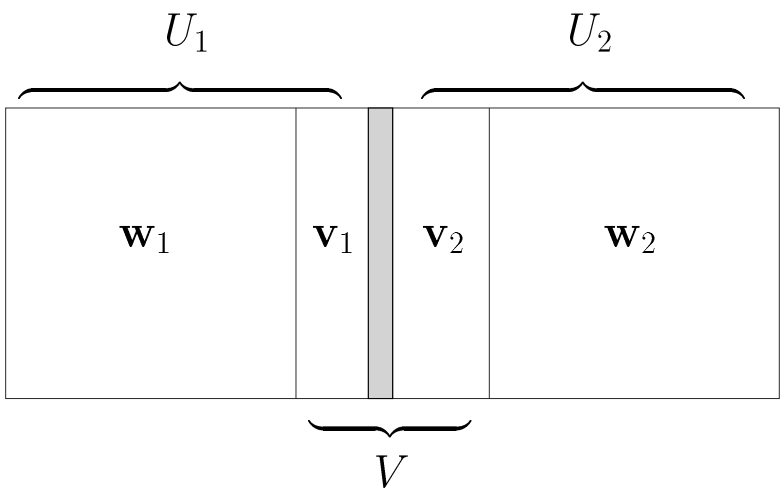

Figure 3.15: Interacting systems.

as

$$\begin{cases} \dot{\mathbf{w}}_1 &= f_1(\mathbf{v}_1, \mathbf{w}_1), \\ \dot{\mathbf{w}}_2 &= f_2(\mathbf{v}_2, \mathbf{w}_2), \\ \dot{\mathbf{v}}_1 &= g_1(\mathbf{v}_1, \mathbf{v}_2, \mathbf{w}_1), \\ \dot{\mathbf{v}}_2 &= g_2(\mathbf{v}_1, \mathbf{v}_2, \mathbf{w}_2). \end{cases}$$

If we can average the influence of $\mathbf{w}_1, \mathbf{w}_2$ on the dynamics of $\mathbf{v}_1, \mathbf{v}_2$, e.g. when the time scales involved in the dynamics of $\mathbf{v}_i$ and $\mathbf{w}_i$ are different, we obtain

$$\begin{cases} \dot{\mathbf{w}}_1 &= f_1(\mathbf{v}_1, \mathbf{w}_1), \\ \dot{\mathbf{w}}_2 &= f_2(\mathbf{v}_2, \mathbf{w}_2), \\ \dot{\mathbf{v}}_1 &= \tilde{g}_1(\mathbf{v}_1, \mathbf{v}_2, \lambda_1), \\ \dot{\mathbf{v}}_2 &= \tilde{g}_2(\mathbf{v}_1, \mathbf{v}_2, \lambda_2), \end{cases} \tag{3.B.1}$$

where λ_1, λ_2 measure the average influence of $\mathbf{w}_1, \mathbf{w}_2$ on V. Thus equations for $\mathbf{v}_1, \mathbf{v}_2$ comprise a closed system V. This part of dynamics is responsible for the interaction. Note that this scheme can also be considered as a double control configuration of three systems, where $(\mathbf{v}_1, \mathbf{v}_2)$ control $\mathbf{w}_1$ and $\mathbf{w}_2$.

If we set $\mathbf{x} := (\mathbf{v}_1, \mathbf{v}_2)$, $\mathbf{y}_i = \mathbf{w}_i$, then the equations (3.B.1) reduce to equations (3.3).

Chapter 4

Quantum fractals

And the more he looked inside, the more Piglet wasn't there.
A. A. Milne, *"The House at Pooh Corner"*

4.1 Introduction

In the introductory chapter we have presented many examples of fractals arising in various areas of science. Some of them were macroscopic objects, like fractal aggregates or percolation structures, some were abstract sets like repellers or attractors of dynamical systems. Fractals have been found not only in the classical but also in the quantum theory. For instance, several quantum models related to the problem of chaotic scattering reveal the fractal structure [63, 131, 41]. Typical Feynmann paths of a quantum mechanical particle were shown to be fractal curves of Hausdorff dimension 2 [3]. Quantum field theories in fractal spacetimes have recently been reviewed [135]. Taking this into consideration it seems strange that until very recently there were no attempts to examine possibility of existence of fractal solutions of the Schrödinger equation.

Michael V. Berry was the first to consider this problem. He constructed a *quantum fractal in a box* from solutions of the Schrödinger equation for a particle in an infinite potential well. Assuming initial probability density to be uniform in the well, $|\Psi(\mathbf{x}, t = 0)|^2$ =const, he conjectured that for almost all later times, $t > 0$, the probability function $P_t(\mathbf{x}) := |\Psi(\mathbf{x}, t)|^2$ has fractal nature and is characterized by the fractal dimension $D_x = D + 1/2 > 1$, where D is the (Euclidean) dimension of the space. Berry's wave functions are initially *discontinuous* at the boundaries of the well. Due to propagation effects these initial discontinuities cause the wave function to become fractal. We discuss the simplest (one-dimensional) example of Berry's fractal in subsection 4.2.1.

In [256] we proposed a general construction of fractal solutions of the Schrödinger equation valid for a large class of one, two, or three dimensional quantum problems. In sections 4.2.2 to 4.4 we demonstrate its usefulness for some textbook examples (infinite potential well, linear potential and harmonic oscillator). All these well known quantum problems are integrable, and our approach does not rely on *chaotic* *dynamics*. Moreover, our fractal wave functions are continuous everywhere.

4.2 Fractal wave functions in the well

"But they were in *the well," Alice said (...) "Of course they were," said the Dormouse: "well in".*

Lewis Carroll, *"Alice's adventures in Wonderland"*

Let us consider solutions of the Schrödinger equation

$$i\partial_t \Psi(x,t) = -\nabla^2 \Psi(x,t) \tag{4.1}$$

for a particle in a one-dimensional infinite potential well. The general solutions satisfying the boundary conditions $\Psi(0,t) = 0 = \Psi(\pi,t)$ have the form

$$\Psi(x,t) = \sum_{n=1}^{\infty} a_n \sin(nx) e^{-in^2 t}, \tag{4.2}$$

where

$$a_n = \frac{2}{\pi} \int_0^\pi dx\, \sin(nx)\Psi(x,0). \tag{4.3}$$

4.2.1 Berry's example

In [22] Michael Berry considered solutions of the Schrödinger equation for a particle in an infinite potential well in D space dimensions evolving from a spatially uniform initial state. He conjectured that for almost all times the graph of the spatial probability density $P(\mathbf{x}, t = \text{const})$ is fractal with box-counting dimension $D_x = D + 1/2$. For almost all positions $\mathbf{x} = (x_1, \ldots, x_D)$ the temporal probability density $P(\mathbf{x} = \text{const}, t)$ is fractal with box-counting dimension $D_t = 7/4$. In the case when the box has a fractal boundary with dimension $D - 1 + \gamma$ $(0 \le \gamma < 1)$ he suggested that the respective dimensions are $D_x = D + (1+\gamma)/2$ and $D_t = (7+\gamma)/4$.

In one dimensional well (4.2) Berry's function takes the form

$$\Psi(x,0) = \begin{cases} \frac{1}{\sqrt{\pi}} & \text{for } x \in]0,\pi[, \\ 0 & \text{for } x \notin]0,\pi[. \end{cases} \tag{4.4}$$

From (4.3) one obtains

$$a_n = \frac{2}{\pi} \int_0^\pi dx\, \sin nx \frac{1}{\sqrt{\pi}} = \begin{cases} 0 & n = 2k, \\ \frac{4}{\pi\sqrt{\pi}n} & n = 2k+1. \end{cases} \tag{4.5}$$

Therefore[1]

$$\Psi_{\text{Berry}}(x,t) = \sum_{k=0}^{\infty} \frac{4}{\pi\sqrt{\pi}(2k+1)} \sin((2k+1)x)\, e^{-i(2k+1)^2 t}. \tag{4.6}$$

[1] Just for the record, formula given by Berry for D-dimensional hyper-cubic box (eq. (22) in [22]) leads to unnormalized wave function. Normalization is obtained when one multiplies his c_q^2 by reversal of volume $1/V = 1/L^D$. Of course, it bears no influence on the dimension of the graph.

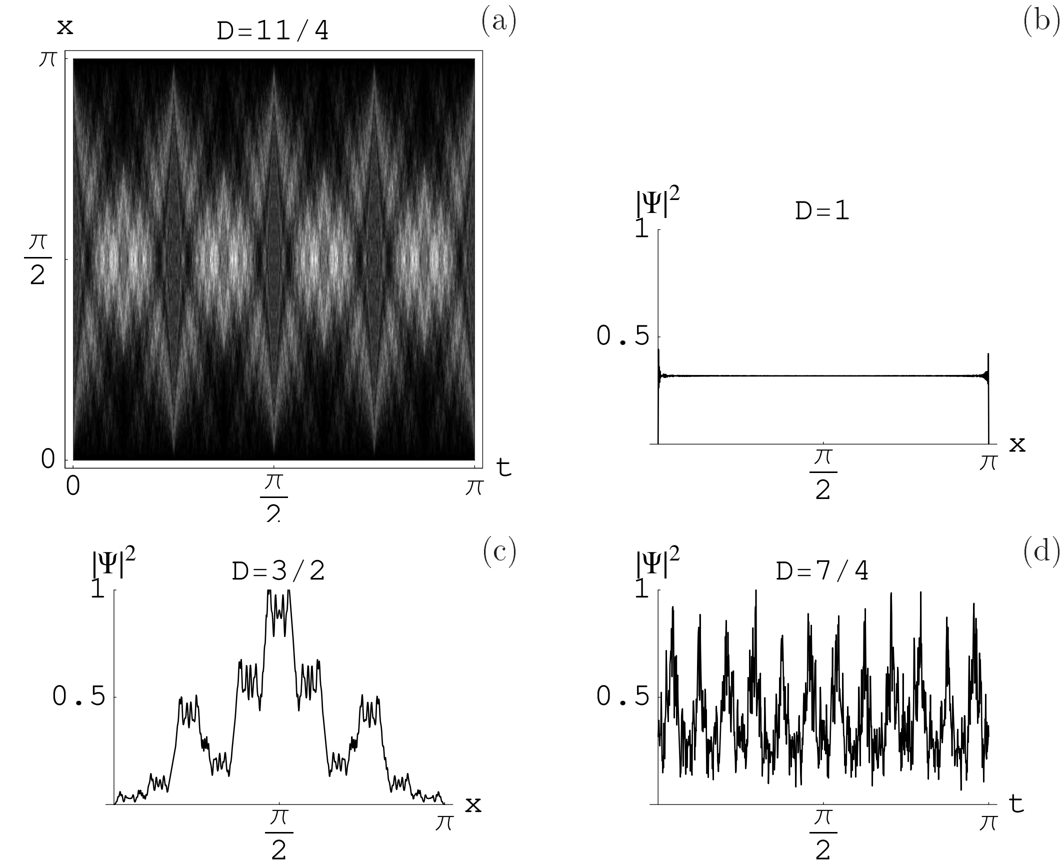

Figure 4.1: Fractal quantum carpet in a box (a; lighter shade means greater probability), space (at $t = 0$ (b), and $t = 1$ (c)) cross-sections and time (at $x = 1$ (d)) cross-section obtained by superimposing 200 terms in eq. (4.6).

Figure 4.1a shows the space-time density plot of the probability density $P(x,t)$, which we call a *fractal quantum carpet* in analogy to the term *quantum carpet* used in the past [106]. Initial probability density $P(x,0)$ is shown in figure 4.1b. Space cross-section (at $t = 1$) and time cross-section (at $x = 1$) of the probability density presented in figures 4.1c and 4.1d show generic behavior of space and time cross-sections.

The insight of Berry was very stimulating to our work, which was started in order to overcome three problems we saw in his example. Firstly, $\Psi(x,t)$ has infinite energy and is discontinuous for a dense set of times. The problem of infinity seems to be impossible to overcome: a true fractal must keep scaling to the smallest scales. This means the wave function must oscillate at every resolution, therefore it must contain eigenfunctions of arbitrarily high energy with weights large enough to render Ψ non-differentiable, what leads to divergent average energy. More precise discussion will follow in particular examples. On the other hand, discontinuity is not necessary for fractality. We have thus been able to construct continuous fractal wave functions.

Secondly, the dimension of physically interesting probability density has not been properly deduced from the dimensions of the real and imaginary parts of the wave function. Berry's argument is the following. Take a complex function $\Psi(x,t)$ such that its real and imaginary parts are fractal (i.e. their graphs are fractal, cf. section 1.3). Therefore the graphs of their squares are also fractal (cf. subsection 1.3.5). Also the graph of the sum of the two squares has the same dimension if the two functions are not too correlated. But the real and imaginary part of a wave function *are* correlated, what's more, they are known in Berry's example explicitly. Thus it could be checked whether or not this correlation induces a decrease in dimensionality of graph of $|\Psi|^2$. In general, dimension of the graph of the sum of functions whose graphs have the same dimensions is arbitrary within allowed limits (cf. subsection 1.3.6), in particular it can be 1.

Thirdly, the methods used by Berry for estimating the box-counting dimension of the graphs of various functions were introduced in analysis of typical paths of stochastic processes and are inadequate in analysis of deterministic curves. Since these methods are generally used [24, 131, 41, 22] it is one of our objectives to point out there inadequacy in certain cases and propose a correct method of analysis.

Let us recall Berry's reasoning. Take the function $\Psi(x,t)$ given by (4.6). The flow of time randomizes phases in Ψ so the fractal properties of its graph are the same as the properties of the graph of a typical trajectory of a stationary stochastic process with the same power spectrum as Ψ (cf. subsection 1.3.7).

Obviously, this argument cannot be valid for all times t, since at $t = 0$ the dimension of the graph of Ψ is 1. Moreover, there is a dense set of times when we observe *quantum revivals* [5, 140] when the graph is again smooth for almost all x which makes the dimension of the graph equal to 1. Therefore the only way to render this reasoning plausible would be to treat the family of all the graphs of $|\Psi(x,t)|^2$ at all the values of t as an ensemble and show its equivalence to the ensemble of all the paths of the stochastic process compared. This is not done by Berry and it seems to be very difficult. Analysis of dimensional properties of stochastic processes (both the ranges of paths and their graphs) is rather simple since one can use the properties of the Wiener measure (cf. subsection 1.3.7). But every deterministic function $\Psi(x,t)$ defines a different probability measure whose properties are unknown and which is therefore almost impossible to treat with these methods.

Thus we felt that the only way to correctly establish the value of the dimension of the graph of a wave function or a probability density is to directly calculate it. This is why we chose another class of examples of wave functions which admits this analysis well and what's more can be constructed for a large class of potentials. To calculate the dimension of the graph of a function we usually calculated its δ-oscillation or variation which we introduced in section 1.3.

4.2.2 Weierstrass type solutions

One of the deficiencies of Berry's example is discontinuity of his wave function. In this section we propose a solution of the Schrödinger equation (4.1) which is everywhere continuous and lends itself easily to generalizations to non-trivial potentials (cf. later sections). In analogy to the Weierstrass function (1.75) we construct fractal wave functions of the form

$$\Psi_M(x,t) = N_M \sum_{n=0}^{M} q^{n(s-2)} \sin(q^n x) e^{-iq^{2n}t}, \tag{4.7}$$

where $q = 2, 3, \ldots$, $s \in (0,2)$.

In the physically interesting case of any finite M the wave function Ψ_M is a solution of the Schrödinger equation. The limiting case

$$\Psi(x,t) := \lim_{M\to\infty} \Psi_M(x,t) = N \sum_{n=0}^{\infty} q^{n(s-2)} \sin(q^n x) e^{-iq^{2n}t}, \tag{4.8}$$

is continuous but nowhere differentiable. It represents a vector in the Hilbert space which does not belong to the domain of the Hamiltonian H. However, it does belong to the domain of the unitary evolution operator. It can also be considered as a solution of the Schrödinger equation in the weak sense: for any fixed orthonormal basis $\{|\varphi_n\rangle\}$ for every n we have

$$\langle H\varphi_n|\Psi(t)\rangle = i\hbar \frac{\partial}{\partial t}\langle \varphi_n|\Psi(t)\rangle.$$

Note that (4.8) converges for

$$|q^{s-2}| < 1 \quad \equiv \quad s < 2.$$

Later on we will show that the probability density of (4.8) shows fractal features for $s > 0$. Thus the interesting range of s is $(0,2)$. The normalization constant of (4.8) follows from

$$\begin{aligned}
1 &= \int_0^\pi |\Psi(x,0)|^2 dx \\
&= N^2 \int_0^\pi dx \sum_{n=0}^{\infty} q^{2n(s-2)} \sin^2(q^n x) \\
&= N^2 \frac{\pi}{2} \sum_{n=0}^{\infty} \left(q^{2(s-2)}\right)^n \\
&= \frac{\pi N^2}{2} \frac{1}{1 - q^{2(s-2)}}.
\end{aligned}$$

Thus $N = \sqrt{\frac{2}{\pi}(1 - q^{2(s-2)})}$.

We show that not only the real wave function $\Psi(x,t)$, but also the physically important probability density $P(x,t) := |\Psi(x,t)|^2$ exhibit fractal nature. This is not obvious, because $|\Psi(x,t)|^2$ is the sum of squares of real and imaginary part having usually equal dimensions. As we argued the dimension of the graph of a sum of functions whose graphs have the same dimensions D can be anything from 1 to D (cf. subsection 1.3.6).

Our results are summarized by

Theorem 4.1 *Let $P(x,t)$ denote the probability density of a Weierstrass-like wave function (4.8). Then*

1. *at the initial time $t=0$ the probability density, $P_0(x) = P(x,0)$, forms a fractal graph in the space variable (i.e. a* space fractal*) of dimension $D_x = \max\{s,1\}$;*
2. *the dimension D_x of graph of $P_t(x)$ does not change in time;*
3. *for almost every x inside the well the probability density, $P_x(t) = P(x = \text{const}, t)$, forms a fractal graph in the time variable (i.e. a* time fractal*) of dimension $D_t(x) = D_t := 1 + s/2$;*
4. *for a discrete, dense set of points x_d, $P_{x_d}(t) = P(x_d,t)$ is smooth and thus $D_t(x_p) = 1$;*
5. *for even q the average velocity $\frac{d\langle x\rangle}{dt}(t)$ is fractal with the dimension of its graph equal to $D_v = \max\{(1+s)/2, 1\}$;*
6. *the surface $P(x,t)$ has dimension $D_{xy} = 2 + s/2$.*

The rigorous proof of this theorem is given in appendix 4.B. It is based on the power-law behavior of the δ-oscillation of the infinite double sum present in $P(x,t) = |\Psi(x,t)|^2$ (see 4.A.1).

We will call two-dimensional density plots of the probability density $P(x,t)$ *fractal quantum carpets* in analogy to the term *quantum carpets* used in the past [106]. In figure 4.2 we show a typical fractal quantum carpet (lighter shade means greater probability) obtained for $q = 2$, $s = 3/2$, and its time and space cross-sections. Periodicity in time with the period $2\pi/3$ visible in the carpet is connected with the structure of the frequency spectrum $\omega_{m,k} = 3(4^{m-1} + \ldots + 4^{m-k})$, $m = 1,\ldots,\infty$, $k = 1,\ldots,m$ of the fractal probability density $P(x,t)$ (cf. appendix 4.A).

The dimensions D_x and D_t are the dimensions of the (generic) cross-sections of the carpet $P(x,t)$ in the space (Fig. 1c and 1d) and time (Fig. 1e) directions.

The Hölder exponent (1.13) in the x direction is $2-s$ and in the t direction is $(2-s)/2$ since the frequencies of time oscillations $\exp(-iq^{2n}t)$ grow as q^{2n}. For these results to hold it is crucial that the series in equation (4.8) is infinite. This is not the case at the points $x_d = k\pi/q^m$ ($k = 0, 1, \ldots, q^m$), for which the series (4.7) consists of at most m terms and the time dependence $P_x(t)$ is smooth ($D_t = 1$). An example of this behavior is shown in figure 1f. Thus, $D_t(x) := \dim_B \text{graph}|\Psi(x = \text{const}, t)|^2$ forms a nowhere continuous function on $[0,\pi]$; for almost all arguments $D_t(x) = D_t = 1 + s/2$, while it is equal to 1 for the dense set of points in this interval $\{k\pi/q^m\}$.

Our fractal wave functions (4.8) have infinite mean energy necessary to generate mathematical fractals with infinite scaling. In practice a few terms in the series may lead to physically interesting effects. The lack of differentiability of $\Psi(x)$ leads to the average momentum $\langle p\rangle$ being ill-defined. On the other hand, we may compute the average position $\langle x\rangle$ and define the average velocity $v = d\langle x\rangle/dt$ not equal to $\langle p\rangle/m$ for infinite series (4.8). For physical fractals (4.7) we recover the Ehrenfest theorem

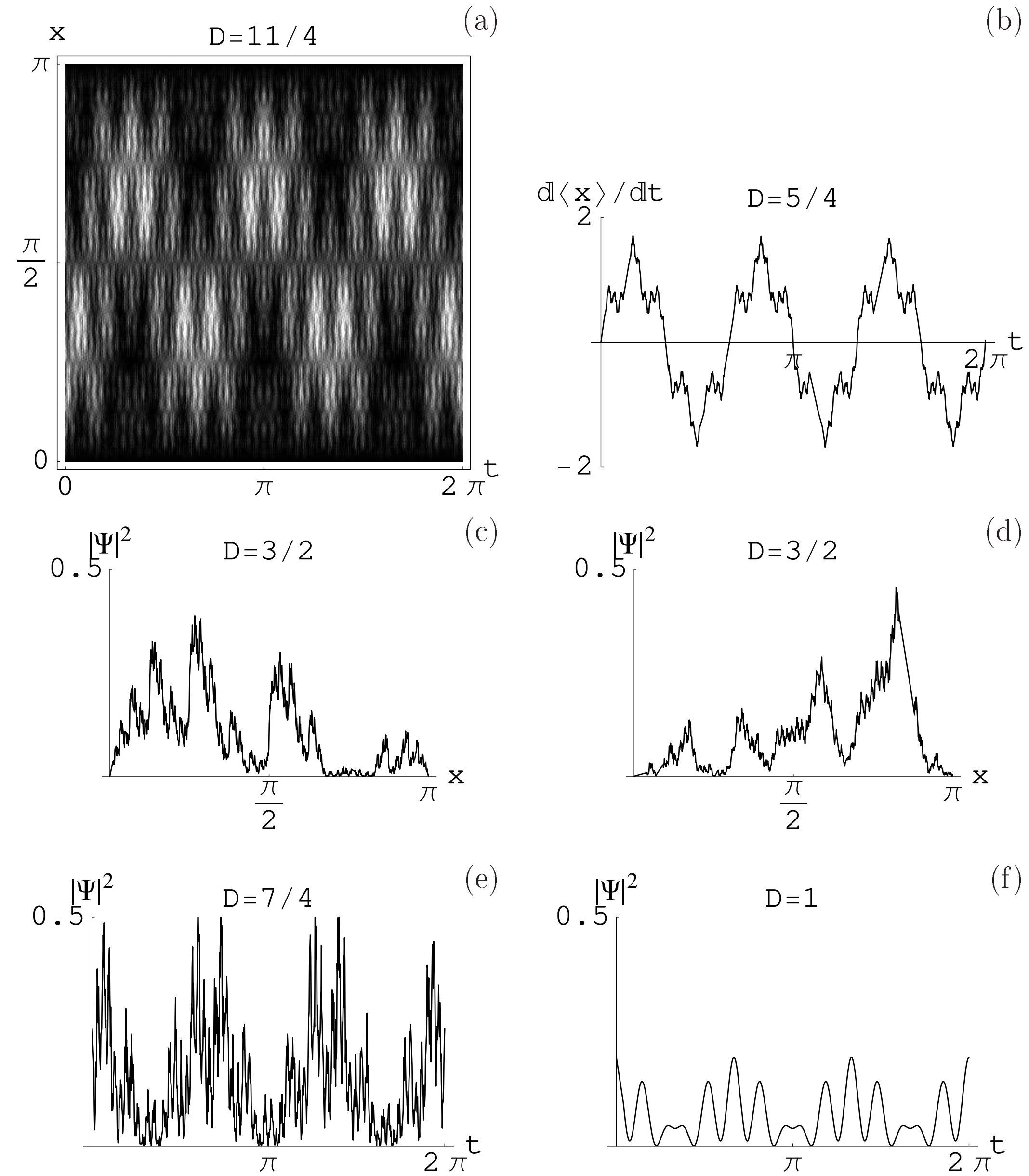

Figure 4.2: Fractal quantum carpet in a box (a), average velocity (b), space (at $t = 0$ (c), and $t = 1$ (d)) and time (at $x = 1$ (e), and $x = \pi/8$ (f)) cross-sections obtained by superimposing 20 terms in eq. (4.7) with $q = 2, s = 3/2$.

and $\langle v\rangle = \langle p\rangle/m$. Straightforward calculations (appendix 4.A) give a continuous function of the class $\mathcal{C}^1$, which for even q is

$$\langle x\rangle = \frac{\pi}{2} - \frac{16}{\pi}(1-q^{2(s-2)})\sum_{k=1}^{\infty}\frac{q^{k(s-1)}}{(q^{2k}-1)^2}\cos(q^{2k}-1)t. \tag{4.9}$$

It is a *semi-fractal* (cf. subsection 1.3.2), since its first derivative v produces a fractal graph with dimension $D_v = \max\{(1+s)/2, 1\}$ (Fig. 1b). For odd q, $\langle x\rangle = \pi/2$ and $D_v = 1$.

The reason for this peculiar dependence of fractality of the average velocity on the parity of q is connected with our very special choice of the wave function. A necessary condition for the graph of the average velocity to be fractal is the presence of both parities eigenstates (cf. appendix 4.A). For odd q all the wave functions are even (i.e. symmetric with respect to $x = \pi/2$). Obviously, if one tried to experimentally obtain states similar to those discussed here one should expect some deviations from the ideal form (4.8). Introduction of even a single state of a different parity would immediately introduce fractality into the graph of $\langle v\rangle$. Thus we expect that this is the prevalent situation for any q: the graph of average velocity of a particle described by a slightly perturbed function (4.8) will be fractal with dimension of its graph equal to $D_v = \max\{(1+s)/2, 1\}$.

In the region where all the three dimensions characterizing the fractal carpet $P(x,t)$ are non-integer ($s \in (1,2)$), they are not independent but linked by the relation

$$D_t + D_v = D_x + 3/2. \tag{4.10}$$

Comprehensive analysis of the details of the fractal wave functions in the potential well was provided in [255].

4.3 Harmonic oscillator

Let us now demonstrate how to generate fractal solutions of the Schrödinger equation for the one-dimensional harmonic oscillator

$$i\hbar\partial_t\Psi(x,t) = \left[-\frac{\hbar^2\nabla^2}{2m} + \frac{1}{2}m\omega^2\right]\Psi(x,t). \tag{4.11}$$

Let $\varphi_n(x)$ denote the eigenstates of this Hamiltonian expressed by the Hermite polynomials $H_n(x)$

$$\varphi_n(x) = (\sqrt{2\pi}2^n n!)^{-1/2}H_n(x/\sqrt{2})\exp(-x^2/4), \tag{4.12}$$

where x is measured in units $\sqrt{\hbar/2m\omega}$.

Consider the following superposition of eigenstates

$$\Psi(x,t) = N\sum_{n=1}^{\infty} q^{n(s-3/2)}\varphi_{q^{2n}}(x)e^{-i(q^{2n}+1/2)t} \tag{4.13}$$

with a natural q and a real $s \in (1, 3/2)$. On every fixed interval $[-b, b]$ sufficiently high energy eigenstates can be arbitrarily well approximated by

$$\varphi_n(x) \sim n^{-1/4} \sin[\sqrt{n+1/2}x - (n-1)\pi/2], \tag{4.14}$$

which follows from neglecting the potential in the WKB approximation. We give a simple derivation of this fact in the next section. In this case one can also obtain this result by studying the asymptotic form of Hermite polynomials (cf. for example [215] equation (24:9:2) page 221). Thus the high n contribution to the wave function (4.13) responsible for the fine scale structure of the probability density reduces to

$$\tilde{\Psi}(x,t) \approx \sum_{n=p}^{\infty} q^{n(s-2)} \sin(q^n x - \theta_{q^n}) e^{-i(q^{2n}+1/2)t}. \tag{4.15}$$

The analysis similar to the case of the infinite well allows one to obtain the dimensions of typical cross-sections of the fractal carpet $|\Psi(x,t)|^2$

$$D_x = s \qquad \text{and} \qquad D_t = 1 + s/2 = 1 + D_x/2. \tag{4.16}$$

Note that this reasoning is valid for arbitrarily large b. However, the larger b the more terms in the sum one needs to take to observe the fractal structure. An example of a fractal quantum carpet for harmonic oscillator is provided in Fig. 4.3.

4.4 Power-law potentials in one dimension

We conjecture that the relation $D_t = 1 + D_x/2$ is valid for a wide class of fractal solutions, not necessarily of our form, of every 1D potential that admits them. The reason for this is the connection between the energy and momentum $E_n \sim k_n^2$ for high energy states (when one can neglect the potential).

We provide here an explicit construction for a class of asymptotically power-law potentials, $V_H(x) \sim |x|^\alpha$ for large $|x|$. For these potentials one may establish what is one of the main results of this chapter:

Theorem 4.2 *Let $V_H(x)$ be an asymptotically power-law potential $V_H(x) \sim |x|^\alpha$ for large $|x|$, $\alpha \in (0, \infty]$, $V_H(x) = V_H(-x)$, $V_H(x) < \infty$ for any finite x. Let $\varphi_n(x)$ denote its eigenstates and E_n its eigenenergies. Choose real $q > 1$, $s \in (0, 2)$ and indices[2] $B_n = [q^{(1+2/\alpha)n}]$. Then the wave function*

$$\Psi_H(x,t) = N \sum_{n=1}^{\infty} q^{n(s-2+1/\alpha)} \varphi_{B_n}(x) \exp(-iE_{B_n} t) \tag{4.17}$$

1. *is a normalizable solution of the corresponding Schrödinger equation in a weak sense for $s < 2 - 1/\alpha$,*

[2] $[x]$ is the largest integer smaller or equal to x.

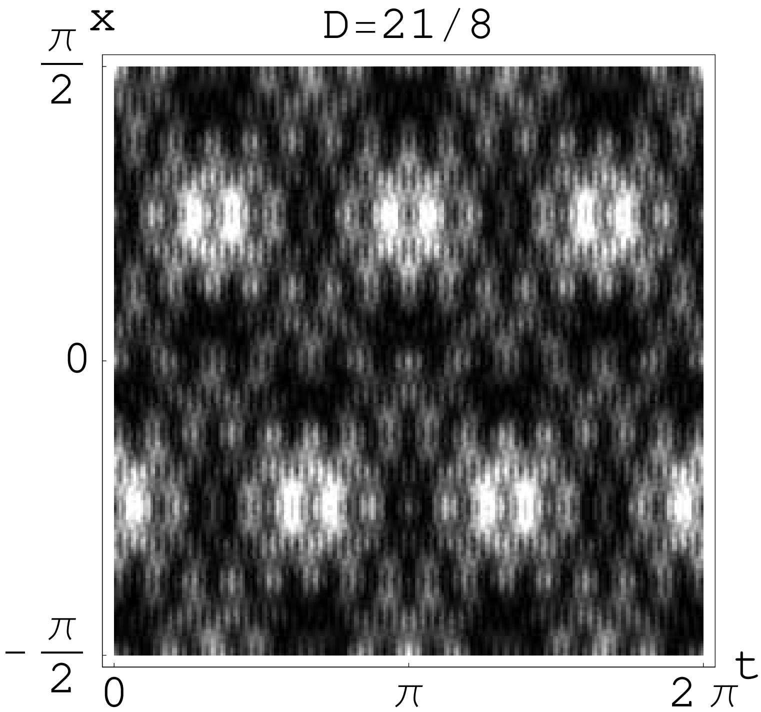

Figure 4.3: Fractal quantum carpet $|\Psi(x,t)|^2$ of dimension $D_{xt} = 21/8$ for quantum harmonic oscillator obtained for $q = 2$, $s = 5/4$, and $M = 15$ terms in (4.13).

2. *for almost all t the space dimension is constant, and*

$$\dim_B \operatorname{graph}(P_t(x)) = D_x := \max\{1, s\},$$

3. *for almost all x the time dimension is constant, and*

$$\dim_B \operatorname{graph}(P_x(t)) = D_t := 1 + s/2,$$

4. *the surface $P(x,t)$ has dimension $D_{xt} = 2 + s/2$.*

Note that potential well, square potential and linear potential are all special cases of the class of asymptotic power-law potentials $V_H(x) \sim |x|^\alpha$ for $\alpha = \infty, 2$ and 1, respectively.

Sketch of the proof. Superposition of eigenstates (4.17) is by construction a solution of the Schrödinger equation. Since the eigenfunctions $\varphi_n(x)$ are normalized, $\Psi_H(x,t)$ converges for

$$|q^{s-2+1/\alpha}| < 1 \qquad \Rightarrow \qquad s - 2 + 1/\alpha < 0,$$

thus $s < 2 - 1/\alpha$.

For large n the WKB approximation gives eigenenergies $E_n \sim n^\beta$ with $\beta = 2\alpha/(2+\alpha)$ (e.g. [191, 246]) and eigenstates $\varphi_n(x) \sim g_n \sin(k_n x - \theta_n)$, where the momentum $k_n = \sqrt{E_n} = n^{\beta/2}$.

To see it let us recall rudiments of the WKB approximation (more details can be found in most good textbooks on quantum mechanics, e.g. [202, 137, 27]; the last one has a particularly rich bibliography). We consider one-dimensional case with two classical turning points. In the stationary Schrödinger equation

$$E\Psi = \left[-\frac{\hbar^2}{2m}\frac{d^2}{dx^2} + V\right]\Psi$$

substitute an ansatz

$$\Psi = \exp\left\{\frac{\hbar}{i}\sigma\right\}.$$

The equation for σ reads

$$\frac{1}{2m}(\sigma')^2 - \frac{i\hbar}{2m}\sigma'' = E - V.$$

If we expand σ in the powers of $\hbar/i$

$$\sigma = \sigma_0 + \frac{\hbar}{i}\sigma_1 + \left(\frac{\hbar}{i}\right)^2\sigma_2 + \ldots \tag{4.18}$$

we obtain an infinite set of equations for the coefficients σ_k of the asymptotic series (4.18). Asymptotically (for large energies) a very good approximation is obtained already with the first two terms. The first two equations which define them read

$$\frac{1}{2m}(\sigma_0')^2 = E - V(x), \tag{4.19}$$

$$\sigma_0'\sigma_1' + \frac{\sigma_0''}{2} = 0. \tag{4.20}$$

In our case (we take here $V = A|x|^\alpha$ for simplicity) they imply

$$\sigma_0 = \pm\int\sqrt{2m(E - A|x|^\alpha)}\,dx, \tag{4.21}$$

$$\sigma_1 = -\frac{1}{2}\ln\sqrt{2m(E - A|x|^\alpha)}. \tag{4.22}$$

The n-th approximate eigenenergy is obtained from the condition [19, 191, 245]

$$\int_{x_-}^{x_+}\sqrt{E - V(x)}\,dx = \left(n + \frac{1}{2}\right)\pi, \tag{4.23}$$

where $x_\pm$ are the classical turning points. In our case

$$x_\pm = \pm(E_n/A)^{1/\alpha}.$$

Substituting $y = x/|x_\pm|$ into (4.23) we get the equation:

$$\left(n + \frac{1}{2}\right)\pi = \sqrt{E_n}|x_\pm| \int_{-1}^{1} \sqrt{1 - |y|^\alpha}\, dy \tag{4.24}$$

$$= CE_n^{\frac{1}{2}+\frac{1}{\alpha}}, \tag{4.25}$$

where $C = \int_{-1}^{1} \sqrt{1 - |y|^\alpha} dy$ is a constant. Thus

$$E_n \sim n^{2\alpha/(2+\alpha)} =: n^\beta,$$

with $\beta = \frac{2\alpha}{2+\alpha}$.

The approximate solution we obtain from the above considerations in the region far away from the turning points ($E_n >> V(x)$) is

$$\varphi_n \approx g_n \sin\left(\frac{1}{\hbar}\int \sqrt{2m(E_n - V(x))} dx\right) \tag{4.26}$$

$$\approx g_n \sin\left(\frac{1}{\hbar}\int \sqrt{2mE_n dx}\right) \tag{4.27}$$

$$= g_n \sin(k_n x), \tag{4.28}$$

where the wave vector k_n satisfies

$$\frac{(\hbar k_n)^2}{2m} = E_n$$

(this is the solution of a free particle problem with energy E_n).

The normalization constant scales as $g_n = n^{-\gamma}$. To determine γ consider again the classical return points $x_\pm$ which satisfy:

$$n^\beta \sim E_n \sim |x_\pm|^\alpha, \quad \text{thus} \quad |x_\pm| \sim n^{\beta/\alpha} = n^{2/(2+\alpha)}. \tag{4.29}$$

Therefore

$$\int_{x_-}^{x_+} g_n^2\, dx \sim 1, \qquad \text{so} \qquad g_n \sim 1/\sqrt{|x_\pm|} = n^{-\gamma}, \tag{4.30}$$

where $\gamma = 1/(2+\alpha) = (2-\beta)/4$. Hence, for $B_n \approx q^{(1+2/\alpha)n}$,

$$\varphi_{B_n}(x) \sim g_{B_n} \sin(k_{B_n} x - \theta_{B_n}) = q^{-n/\alpha} \sin(q^n x - \theta_{B_n}), \tag{4.31}$$

and the wave function (4.17) might be written in the Weierstrass-like form

$$\Psi_H(x,t) \approx \sum_{n=1}^{\infty} q^{n(s-2)} \sin(q^n x - \theta_{B_n}) e^{-iq^{2n}t}. \tag{4.32}$$

Repeating the reasoning used earlier for the problem of rectangular well we conclude that if $s \in (0, 2 - 1/\alpha)$ than for almost all t the space dimension of the carpet is $D_x = \max\{1, s\}$, while for almost all x the above series is infinite and the time dimension reads $D_t = 1 + s/2$ which equals to $1 + D_x/2$ for $s \geq 3/2$.

Generic	α	$\beta = 2\alpha/(2+\alpha)$	$\gamma = 1/(2+\alpha)$
Linear	1	2/3	1/3
Harm. Osc.	2	1	1/4
Well	∞	2	0

Table 4.1: The exponents α, β and γ for the linear potential, harmonic oscillator and the infinite well.

4.5 Continuous spectrum

The idea of producing fractal functions by taking a suitable superposition of eigenstates with the wavelengths of different orders of magnitude is very general and may be used for many problems. However, it cannot be easily generalized to continuous spectra. Let us consider, for example a free particle in one dimension. Following our constructions (eq. 4.8, 4.13, 4.17) we may write down a fractal superposition of the plane waves. To localize it we introduce a square integrable envelope $f(x)$. In this case the wave function is the sum of two terms of the form

$$\Psi_{\pm}(x,t) = \sum_n q^{n(s-2)} e^{\pm iq^n x - iq^{2n}t} f(x \mp 2q^n t, t), \tag{4.33}$$

where $f(x,t)$ is the solution of the Schrödinger equation satisfying $f(x,0) = f(x)$ (cf. appendix 4.A). The fractal properties of this packet will depend on the asymptotic behavior of $f(x,t)$ for large x. Fractality is destroyed if f decreases sufficiently fast. This is the case for the Gaussian envelope of variance σ^2:

$$\begin{aligned} \Psi(x,t) \quad &= \quad \frac{N_0}{\sqrt{1+it}} \exp\left[-\frac{x^2/4}{1+it}\right] \cdot \\ &\sum_{n=0}^{\infty} q^{n(s-2)} \sin\left[\frac{xq^n}{1+it}\right] \exp\left[\frac{-iq^{2n}t}{1+it}\right], \end{aligned} \tag{4.34}$$

where x is measured in units of σ and t in units of $2m\sigma^2/\hbar$.

For any non-zero value of t the absolute value of the last term decreases exponentially with n which destroys fractality. Therefore, this state (4.34) is fractal only at $t = 0$.

Appendix 4.A Auxiliary calculations

4.A.1 Probability density

Take the fractal wave function (4.8)

$$\Psi(x,t) = \sqrt{\frac{2}{\pi}\left(1 - q^{2(s-2)}\right)} \sum_{n=0}^{\infty} q^{n(s-2)} \sin(q^n x) e^{-iq^{2n}t}.$$

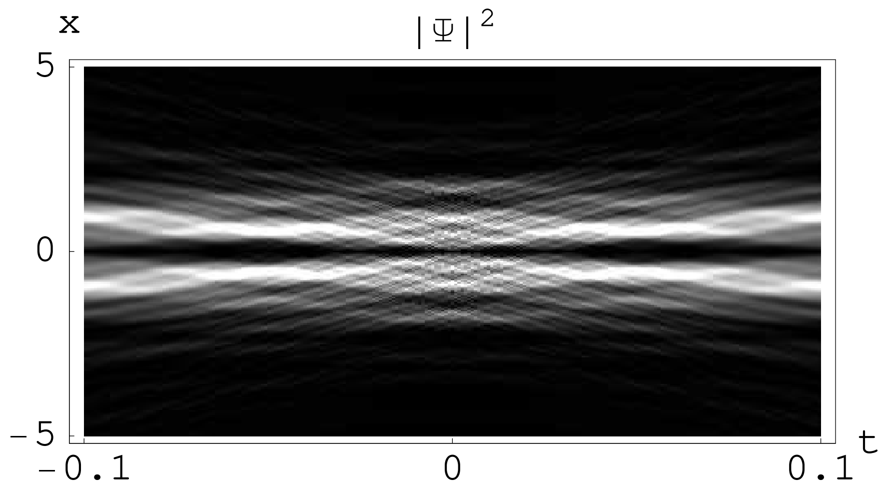

Figure 4.4: Quantum carpet for free particle (4.34) with $M = 30$ terms, $s = 3/2$ and $q = 2$ displays fractal properties ($D_x = 3/2$) only at $t = 0$. For $t \neq 0$, $D_x = 1$.

Let us calculate two useful forms of the probability density $P(x, t)$

$$\begin{aligned} P(x,t) &= |\Psi(x,t)|^2 \\ &= \frac{2}{\pi}\left(1 - q^{2(s-2)}\right) \sum_{m,n=0}^{\infty} q^{(m+n)(s-2)} \sin q^n x \sin q^m x \, e^{-i(q^{2n}-q^{2m})t}. \end{aligned}$$

Taking $k = m + n, l = n$ we obtain

$$\begin{aligned} P(x,t) &= \frac{2}{\pi}\left(1 - q^{2(s-2)}\right) \sum_{k=0}^{\infty} q^{k(s-2)} \sum_{l=0}^{k} \sin q^l x \sin q^{k-l} x \, e^{-i(q^{2l}-q^{2(k-l)})t}, \\ &= \frac{2}{\pi}\left(1 - q^{2(s-2)}\right) \sum_{k=0}^{\infty} q^{k(s-2)} \sum_{l=0}^{k} \sin q^l x \sin q^{k-l} x \cos(q^{2l} - q^{2(k-l)})t, \end{aligned} \quad (4.A.1)$$

where the imaginary part vanishes due to the symmetry of the exponent. If you take $c = m$, $d = m - n$ instead of k, l you can also write

$$\begin{aligned} P(x,t) &= \frac{2}{\pi}\left(1 - q^{2(s-2)}\right) \sum_{m=0}^{\infty} \Big\{ q^{2m(s-2)} \sin^2 q^m x + \\ &\quad +2 \sum_{n<m} q^{(m+n)(s-2)} \sin q^n x \sin q^m x \cos(q^{2m} - q^{2n})t, \Big\} \\ &= \frac{2}{\pi}\left(1 - q^{2(s-2)}\right) \Bigg\{ \sum_{m=0}^{\infty} q^{2m(s-2)} \sin^2 q^m x + \\ &\quad +2 \sum_{c=1}^{\infty} \sum_{d=1}^{c} q^{(2c-d)(s-2)} \sin q^c x \sin q^{c-d} x \cos(q^{2c} - q^{2(c-d)})t \Bigg\} \end{aligned}$$

$$
\begin{aligned}
&= \frac{2}{\pi}\left(1-q^{2(s-2)}\right)\left\{\sum_{m=0}^{\infty} q^{2m(s-2)}\sin^2 q^m x + \right.\\
&\quad +2\sum_{c=1}^{\infty} q^{2c(s-2)}\sin q^c x\,\cdot\\
&\quad \left.\cdot\sum_{d=1}^{c} q^{-d(s-2)}\sin q^{c-d}x\cos\left[(q^2-1)\cdot q^{2(c-d)}\sum_{a=0}^{d-1} q^{2a}\right]t\right\}\\
&= \frac{2}{\pi}\left(1-q^{2(s-2)}\right)\sum_{m=0}^{\infty} q^{2m(s-2)}\sin^2 q^m x + \\
&\quad +\frac{4}{\pi}\left(1-q^{2(s-2)}\right)\sum_{c=1}^{\infty} q^{2c(s-2)}\sin q^c x\,\cdot\\
&\quad \cdot\sum_{d=1}^{c} q^{-d(s-2)}\sin q^{c-d}x\cos(q^2-1)(q^{2(c-1)}+\ldots+q^{2(c-d)})t \qquad (4.A.2)\\
&=: P_x(x)+P_{xt}(x,t).
\end{aligned}
$$

Note that the time-independent part

$$
\begin{aligned}
P_x(x) &= \frac{2}{\pi}\left(1-q^{2(s-2)}\right)\sum_{m=0}^{\infty} q^{2m(s-2)}\frac{1-\cos q^m 2x}{2}\\
&= \frac{\left(1-q^{2(s-2)}\right)}{\pi}\left(\sum_{m=0}^{\infty} q^{2m(s-2)} - \sum_{m=0}^{\infty} q^{2m(s-2)}\cos q^{m+1}x\right)\\
&= \frac{1}{\pi} - \frac{\left(1-q^{2(s-2)}\right)}{\pi}\sum_{m=0}^{\infty} q^{m(2s-4)}\cos q^m 2x,
\end{aligned}
$$

is essentially a Weierstrass function with the dimension $s' = \max\{2s-2, 1\} \in [1,2)$ (i.e. for $s \in [1, 3/2]$, $s' = 1$). From the equation (4.A.2) one immediately gets the spectrum of $P(x,t)$: all the frequencies governing the time evolution are

$$
\omega_{c,d} = (q^2-1)(q^{2(c-1)}+\ldots+q^{2(c-d)}),
$$

where $c = 1, 2, \ldots$, $d = 1, 2, \ldots, c$. Thus all the frequencies divide by q^2-1 which is also the smallest frequency, so the fundamental period of $P(x,t)$ is $2\pi/(q^2-1)$. For $q = 2$ this gives $T_0 = 2\pi/3$ which is clearly visible in figures 4.2a, b, d, e and 4.3.

4.A.2 Average velocity

It is interesting to calculate the behavior of $\langle x\rangle$. Before we do it, let us first calculate some helpful integrals:

$$
\begin{aligned}
\int_0^{\pi} dx\, x\, \cos kx &= \frac{1}{k}x\sin kx\Big|_0^{\pi} - \frac{1}{k}\int_0^{\pi} dx\, \sin kx\\
&= \frac{1}{k^2}\cos kx\Big|_0^{\pi} = \frac{(-1)^k-1}{k^2}
\end{aligned}
$$

for $k \neq 0$. Let

$$F(n,m) := \int_0^\pi dx\, x\, \sin nx \sin mx.$$

If $n \neq m$, then

$$\begin{aligned}
\int_0^\pi dx\, x\, \sin nx \sin mx &= \frac{1}{2}\int_0^\pi dx\, x[\cos(n-m)x - \cos(n+m)x] \\
&= \frac{1}{2}\left[\frac{(-1)^{n-m}-1}{(n-m)^2} - \frac{(-1)^{n+m}-1}{(n+m)^2}\right] \\
&= \begin{cases} 0 & 2|n-m \qquad (n,m \text{ of the same parity}) \\ \frac{-4nm}{(n^2-m^2)^2} & 2 \not| n-m \qquad (n,m \text{ of different parity}) \end{cases}
\end{aligned}$$

otherwise

$$\int_0^\pi dx\, x\, \sin^2 nx = \int_0^\pi dx\, x\, \frac{1-\cos 2nx}{2} = \frac{\pi^2}{4} - \frac{1}{2}\int_0^\pi dx\, x\, \cos 2nx = \frac{\pi^2}{4}.$$

We can now calculate average x using the above results and the form (4.A.1) of probability density $P(x,t)$.

$$\begin{aligned}
\langle x\rangle &= \int_0^\pi dx\, x\, |\Psi|^2 \\
&= \frac{2}{\pi}\left(1-q^{2(s-2)}\right)\sum_{k=0}^{\infty} q^{k(s-2)}\sum_{l=0}^{k} F(q^l,q^{k-l})\cos(q^{2l}-q^{2(k-l)})t \\
&= \frac{2}{\pi}\left(1-q^{2(s-2)}\right)\left\{\sum_{k=1}^{\infty} q^{k(s-2)}2\cdot F(1,q^k)\cos(q^{2k}-1)t + \right. \\
&\left. \sum_{k=0}^{\infty} q^{2k(s-2)}F(q^k,q^k)\cos(q^{2k}-q^{2k})t\right\} \\
&= \frac{2}{\pi}\left(1-q^{2(s-2)}\right)\left\{\sum_{k=1}^{\infty} q^{k(s-2)}2\cdot\frac{-4\cdot q^k}{(q^{2k}-1)^2}\cos(q^{2k}-1)t + \sum_{k=0}^{\infty} q^{2k(s-2)}\frac{\pi^2}{4}\right\} \\
&= \frac{\pi}{2} - \frac{16}{\pi}\left(1-q^{2(s-2)}\right)\sum_{k=1}^{\infty}\frac{q^{k(s-1)}}{(q^{2k}-1)^2}\cos(q^{2k}-1)t.
\end{aligned}$$

The above expression is valid only for even q. For odd q we have just the first term, which is $\pi/2$.

The average $x(t)$ is of class $\mathcal{C}^1$, because its derivative is given by an absolutely convergent series:

$$\begin{aligned}
\left|\frac{d\langle x\rangle}{dt}\right| &= \left|\frac{16}{\pi}\left(1-q^{2(s-2)}\right)\sum_{k=1}^{\infty}\frac{q^{k(s-1)}}{q^{2k}-1}\sin(q^{2k}-1)t\right| \\
&\leq \frac{16}{\pi}\left(1-q^{2(s-2)}\right)\sum_{k=1}^{\infty}2\frac{q^{k(s-1)}}{q^{2k}}
\end{aligned}$$

$$
\begin{aligned}
&= \frac{32}{\pi}\left(1-q^{2(s-2)}\right)\sum_{k=1}^{\infty} q^{k(s-3)} \\
&= \frac{32}{\pi}\left(1-q^{2(s-2)}\right)\frac{q^{s-3}}{1-q^{s-3}}. \qquad (4.A.3)
\end{aligned}
$$

We show in section (4.B) that (4.A.3) is fractal, while for odd q the average velocity $|d\langle x\rangle/dt|$, of course, is not. This seemingly strange behavior is caused by the structure of $F(n,m)$ function which is non-zero only for m,n of different parity. We expect that if one slightly disturbs our function, for instance by changing an arbitrary number of terms to the next higher or lower eigenstates, the dimensions D_x and D_t will not be altered. In other words, with probability one, independently of the parity of q, the average velocity of the wave function

$$
\Phi_0(x,t) = M_0 \sum_{n=1}^{\infty} q^{n(s-2)} \sin((q^n \pm 1)x) e^{-i(q^n\pm 1)^2 t}. \qquad (4.A.4)
$$

is fractal.

If one wants an explicit example of a similar function for odd q it is

$$
\Phi_1(x,t) = M_1\left[2^{s-2}\sin(2x)e^{-i2^2t} + \sum_{n=1}^{\infty} q^{n(s-2)}\sin(q^n x)e^{-iq^{2n}t}\right]. \qquad (4.A.5)
$$

One can see the only difference between this example and the original one (4.8) is in the *first* term. This difference accounts for the smoothness or roughness of the average velocity. It is very interesting because normally one expects that it is the *asymptotic* behavior that determines the fractal dimension. Here we have exactly opposite case: a change in the first term (varying most slowly) of a series changes the dimension of a complicated function $\langle v\rangle$.

Average velocity of the wave packet (4.A.5) is smooth for even q and fractal for odd q. A function which gives fractal average velocity for both even and odd q is

$$
\begin{aligned}
\Phi_2(x,t) &= M_2\left[2^{s-2}\sin(2x)e^{-i2^2t} + \sum_{n=0}^{\infty} q^{n(s-2)}\sin(q^n x)e^{-iq^{2n}t}\right] \\
&= M_2\left[2^{s-2}\sin(2x)e^{-i2^2t} + \frac{1}{N}\Psi(x,t)\right],
\end{aligned}
$$

where M_2 is the normalization constant.

4.A.3 A step towards fractal free particles

There are several ways in which one could try to construct a fractal wave packet in an empty space. One idea is to take the solution (4.8) for an infinite well, which of course is a solution of the zero potential problem, however, in infinite space this solution is unbounded. To localize it one can multiply it by a square integrable envelope $f(x,0)$ at time $t=0$ and examine the evolution of this wave packet.

Thus
$$\Psi(x,0) := \sum_{n=0}^{\infty} q^{n(s-2)} \sin(q^n x) f(x,0).$$
The evolution equation
$$i\hbar \frac{\partial \Psi}{\partial t} = -\frac{\hbar^2}{2m}\Psi''$$
for Fourier transforms $\tilde{\Psi}(k,t)$
$$\Psi(x,t) = \frac{1}{2\pi}\int_{-\infty}^{\infty} dk\, e^{ikx}\tilde{\Psi}(k,t)$$
is
$$i\hbar \frac{\partial \tilde{\Psi}}{\partial t} = -\frac{\hbar^2 k^2}{2m}\tilde{\Psi}.$$
This can be easily solved
$$\tilde{\Psi}(k,t) = \tilde{\Psi}(k,0)e^{-i\frac{\hbar}{2m}k^2 t}.$$
In our case
$$\begin{aligned}\tilde{\Psi}(k,0) &= \int_{-\infty}^{\infty} dx\, e^{-ikx}\Psi(x,0)\\ &= \int_{-\infty}^{\infty} dx\, e^{-ikx} f(x,0)\sum_{n=0}^{\infty} q^{n(s-2)}\sin(q^n x)\\ &= \sum_{n=0}^{\infty} q^{n(s-2)}\int_{-\infty}^{\infty} dx\, e^{-ikx}\sin(q^n x) f(x,0).\end{aligned}$$
If instead of $\Psi(x,0)$ the initial condition was $f(x,0)$ itself then its Fourier transform would evolve according to
$$\tilde{f}(k,t) = \tilde{f}(k,0)e^{-i\frac{\hbar}{2m}k^2 t}.$$
Since
$$f(x,t) = \frac{1}{2\pi}\int_{-\infty}^{\infty} dk\, e^{ikx}\tilde{f}(k,t)$$
we have
$$\begin{aligned}\tilde{\Psi}(k,0) &= \sum_{n=0}^{\infty} q^{n(s-2)}\int_{-\infty}^{\infty} dx\, e^{-ikx}\frac{1}{2i}\left[e^{iq^n x} - e^{-iq^n x}\right]\frac{1}{2\pi}\int_{-\infty}^{\infty} dk' e^{ik'x}\tilde{f}(k',0)\\ &= \frac{1}{2i}\sum_{n=0}^{\infty} q^{n(s-2)}\frac{1}{2\pi}\int_{-\infty}^{\infty} dk'\int_{-\infty}^{\infty} dx\left[e^{i(k'-k+q^n)x} - e^{i(k'-k-q^n)x}\right]\tilde{f}(k',0).\end{aligned}$$
Integrating over x we obtain
$$\begin{aligned}\tilde{\Psi}(k,0) &= \frac{1}{2i}\sum_{n=0}^{\infty} q^{n(s-2)}\int_{-\infty}^{\infty} dk'\left[\delta(k'-k+q^n) - \delta(k'-k-q^n)\right]\tilde{f}(k',0)\\ &= \frac{1}{2i}\sum_{n=0}^{\infty} q^{n(s-2)}\left[\tilde{f}(k-q^n,0) - \tilde{f}(k+q^n,0)\right].\end{aligned}$$

Thus

$$\tilde{\Psi}(k,t) = \frac{1}{2i}\sum_{n=0}^{\infty} q^{n(s-2)}\left[\tilde{f}(k-q^n,0) - \tilde{f}(k+q^n,0)\right] e^{-i\frac{\hbar}{2m}k^2 t}.$$

But

$$\begin{aligned}\tilde{f}(k-q^n,t) &= \tilde{f}(k-q^n,0)\exp\left[-\frac{i\hbar(k^2+q^{2n}-2kq^n)t}{2m}\right]\\ &= \tilde{f}(k-q^n,0)e^{-i\frac{\hbar}{2m}k^2 t}e^{-i\frac{\hbar}{2m}q^{2n}t}e^{i\frac{\hbar}{2m}2kq^n t}.\end{aligned}$$

Therefore

$$\tilde{f}(k-q^n,0)e^{-i\frac{\hbar}{2m}k^2 t} = \tilde{f}(k-q^n,t)e^{i\frac{\hbar}{2m}q^{2n}t}e^{-i\frac{\hbar}{2m}2kq^n t}$$

which leads to

$$\tilde{\Psi}(k,t) = \frac{1}{2i}\sum_{n=0}^{\infty} q^{n(s-2)}\left[\tilde{f}(k-q^n,t)e^{-i\frac{\hbar}{2m}2kq^n t} - \tilde{f}(k+q^n,t)e^{i\frac{\hbar}{2m}2kq^n t}\right] e^{i\frac{\hbar}{2m}q^{2n}t}.$$

If we transform this result back we obtain

$$\begin{aligned}\Psi(x,t) &= \frac{1}{2\pi}\int_{-\infty}^{\infty}dk\, e^{ikx}\frac{1}{2i}\sum_{n=0}^{\infty} q^{n(s-2)}e^{i\frac{\hbar}{2m}q^{2n}t}\\ &\quad \left[\tilde{f}(k-q^n,t)e^{-i\frac{\hbar}{2m}2kq^n t} - \tilde{f}(k+q^n,t)e^{i\frac{\hbar}{2m}2kq^n t}\right]\\ &= \frac{1}{2i}\sum_{n=0}^{\infty} q^{n(s-2)}e^{i\frac{\hbar}{2m}q^{2n}t}\\ &\quad \frac{1}{2\pi}\int_{-\infty}^{\infty}dk\left[e^{ik(x-\frac{\hbar}{2m}2q^n t)}\tilde{f}(k-q^n,t) - e^{ik(x+\frac{\hbar}{2m}2q^n t)}\tilde{f}(k+q^n,t)\right].\end{aligned}$$

Since

$$\begin{aligned}\frac{1}{2\pi}\int_{-\infty}^{\infty}dk e^{ik(x-\frac{\hbar}{2m}2q^n t)}\tilde{f}(k-q^n,t) &= \frac{1}{2\pi}\int_{-\infty}^{\infty}dk e^{i(k-q^n+q^n)(x-\frac{\hbar}{2m}2q^n t)}\tilde{f}(k-q^n,t)\\ &= f\left(x-\frac{\hbar}{2m}2q^n t,t\right)e^{iq^n(x-\frac{\hbar}{2m}2q^n t)}\end{aligned}$$

we have

$$\begin{aligned}\Psi(x,t) &= \frac{1}{2i}\sum_{n=0}^{\infty} q^{n(s-2)}e^{-i\frac{\hbar}{2m}q^{2n}t}\\ &\quad \left[f\left(x-\frac{\hbar}{2m}2q^n t,t\right)e^{iq^n x} - f\left(x+\frac{\hbar}{2m}2q^n t,t\right)e^{-iq^n x}\right].\end{aligned}$$

If we choose units as in (4.1) so that $\hbar/2m = 1$ we get (4.33):

$$\begin{aligned}\Psi(x,t) &= \frac{1}{2i}\sum_{n=0}^{\infty} q^{n(s-2)}\left[f(x-2q^n t,t)e^{iq^n x} - f(x+2q^n t,t)e^{-iq^n x}\right]e^{-iq^{2n}t}\\ &= \frac{1}{2i}\sum_{n=0}^{\infty} q^{n(s-2)}\sum_{\varepsilon=\pm 1}\varepsilon f(x-\varepsilon 2q^n t,t)e^{\varepsilon iq^n x - iq^{2n}t}.\end{aligned}$$

If we started from plane waves $e^{iq^n x}$ instead of $\sin(q^n x)$ we would obtain

$$\Psi(x,t) = \sum_{n=0}^{\infty} q^{n(s-2)} f(x - 2q^n t, t) e^{iq^n x - iq^{2n} t}.$$

Appendix 4.B Proof of the Theorem 4.1

"How do you know I'm mad?" said Alice. "You must be," said the Cat, "or you wouldn't have come here".

Lewis Carroll, *"Alice's adventures in Wonderland"*

Theorem 4.1 *Let $P(x,t)$ denote the probability density of a Weierstrass-like wave function (4.8):*

$$\Psi(x,t) = N \sum_{n=0}^{\infty} q^{n(s-2)} \sin(q^n x) e^{-iq^{2n} t}.$$

Then

1. *at the initial time $t = 0$ the probability density, $P_0(x) = P(x,0)$, forms a fractal graph in the space variable (i.e. a* space fractal*) of dimension $D_x = \max\{s, 1\}$;*
2. *the dimension D_x of graph of $P_t(x)$ does not change in time;*
3. *for almost every x inside the well the probability density, $P_x(t) = P(x = \mathrm{const}, t)$, forms a fractal graph in the time variable (i.e. a* time fractal*) of dimension $D_t(x) = D_t := 1 + s/2$;*
4. *for a discrete, dense set of points x_d, $P_{x_d}(t) = P(x_d, t)$ is smooth and thus $D_t(x_p) = 1$;*
5. *for even q the average velocity $\frac{d\langle x\rangle}{dt}(t)$ is fractal with the dimension of its graph equal to $D_v = \max\{(1+s)/2, 1\}$;*
6. *the surface $P(x,t)$ has dimension $D_{xy} = 2 + s/2$.*

Proof:

1., 2. *For every t $\dim_B \mathrm{graph} P_t(x) = s$.*

We will show that for every fixed t the graph of the probability density (4.A.1) has the box-counting dimension s.

(a) Fix t. Let

$$P_n(x) := \sum_{k=0}^{n} q^{k(s-2)} \sum_{l=0}^{k} \sin q^l x \sin q^{k-l} x \cos(q^{2l} - q^{2(k-l)}) t,$$

($q = 2, 3, \ldots$ for us, but in fact any $q > 1$ will do). It is a smooth function whose derivative at every point satisfies

$$\begin{aligned}
|P_n'(x)| &\leq 2\sum_{k=0}^{n} q^{k(s-2)} \sum_{l=0}^{k} q^l |\cos q^l x \sin q^{k-l} x| \\
&\leq 2\sum_{k=0}^{n} q^{k(s-2)} (1 + q + \ldots + q^k) \\
&= 2\sum_{k=0}^{n} q^{k(s-2)} \frac{q^{k+1} - 1}{q - 1} \\
&\leq 2\sum_{k=0}^{n} q^{k(s-2)} \frac{q^{k+1}}{q - 1} \\
&= \frac{2q}{q-1} \sum_{k=0}^{n} q^{k(s-1)} \\
&= \frac{2q}{q-1} \frac{q^{(n+1)(s-1)} - 1}{q^{s-1} - 1} \\
&\leq \frac{2q^s}{(q-1)(q^{s-1} - 1)} q^{n(s-1)} \\
&= d_1(s,q) q^{n(s-1)},
\end{aligned}$$

where

$$d_1(s,q) = \frac{2q^s}{(q-1)(q^{s-1} - 1)}.$$

Let $\delta = q^{-n}$. Then

$$\begin{aligned}
\operatorname{osc}_\delta(x) P_n &\leq 2\delta \sup_{x \in [0,\pi]} |P_n'(x)| \\
&\leq 2\delta\, d_1(s,q) q^{n(s-1)} \\
&= 2 d_1(s,q) \delta^{2-s}.
\end{aligned}$$

On the other hand, for

$$\begin{aligned}
R_n(x) &:= P(x) - P_n(x) \\
&= \sum_{k=n+1}^{\infty} q^{k(s-2)} \sum_{l=0}^{k} \sin q^l x \sin q^{k-l} x \cos(q^{2l} - q^{2(k-l)}) t
\end{aligned}$$

we have[3]

$$\begin{aligned}
\operatorname{osc}_\delta(x) R_n &\leq 2 \sum_{k=n+1}^{\infty} q^{k(s-2)} (k+1) \\
&= \frac{2q^{(n+1)(s-2)} [n + 2 - (n+1) q^{s-2}]}{(1 - q^{s-2})^2} \\
&\leq \frac{4q^{(n+1)(s-2)} n}{(1 - q^{s-2})^2},
\end{aligned}$$

[3]Note that $u := q^{s-2} < 1$, because $s \in]1, 2[$.

where we used the simple identity

$$\sum_{k=n}^{\infty} q^{kx} k = \frac{d}{dx} \sum_{k=n}^{\infty} q^{kx} \frac{1}{\ln q} = \frac{1}{\ln q} \frac{d}{dx} \frac{q^{nx}}{1-q^x}.$$

But the polynomial growth is slower than the exponential one, therefore for arbitrarily small ε there is some M such that

$$\forall n > M: \quad n < (q^{\varepsilon})^n.$$

This leads to the following estimate of the oscillation of R_n:

$$\begin{aligned} \operatorname{osc}_\delta(x) R_n &\leq \frac{4q^{s-2}}{(1-q^{s-2})^2} q^{n(s-2+\varepsilon)} \\ &= d_2(s,q)\delta^{2-s-\varepsilon}, \end{aligned}$$

where

$$d_2(s,q) = \frac{4q^{s-2}}{(1-q^{s-2})^2}.$$

Of course, ε can be arbitrarily small, but n grows and δ decreases with decreasing ε. Nevertheless, for all x, ε and $\delta < q^{-n}$ we have

$$\begin{aligned} \operatorname{osc}_\delta(x) P &\leq \operatorname{osc}_\delta(x) P_n + \operatorname{osc}_\delta(x) R_n \\ &\leq (2d_1 + d_2)\delta^{2-s-\varepsilon}. \end{aligned}$$

From theorem 1.5 it follows that

$$\dim_B \operatorname{graph} P_t(x) \leq 2 - (2 - s - \varepsilon) = s + \varepsilon \xrightarrow[\varepsilon \to 0]{} s.$$

(b) Fix t. Let $f(x) = P(x,t)$. We want to show that

$$W := \int_a^b |f(x+\delta) - f(x-\delta)| dx \geq c\delta^{2-s}.$$

Since $\operatorname{osc}_\delta(x)(f) \geq |f(x+\delta) - f(x-\delta)|$ this gives us lower bound on the variation $\operatorname{Var}_\delta(f) \geq W$. Take $a = 0$, $b = \pi$ for convenience. This choice lets us get rid of the oscillating terms we encountered in the proof of fractality of the Weierstrass function in subsection 1.3.4. We could take arbitrary a, b it would merely make the formulae more cumbersome. Notice that (we skip the normalization constant)

$$\begin{aligned} W &= \int_0^\pi |f(x+\delta) - f(x-\delta)| dx \qquad (4.B.1) \\ &= \int_0^\pi \left| \sum_{k=0}^{\infty} q^{k(s-2)} \sum_{l=0}^{k} \{\sin q^l (x+\delta) \sin q^{k-l}(x+\delta) + \right. \\ &\quad \left. - \sin q^l (x-\delta) \sin q^{k-l}(x-\delta)\} \, a_{kl} \right| dx \\ &= \int_0^\pi \left| \sum_{k=0}^{\infty} q^{k(s-2)} \sum_{l=0}^{k} \{\cos q^l x \sin q^{k-l} x \sin q^l \delta \cos q^{k-l} \delta\} \, a_{kl} \right| dx \end{aligned}$$

where

$$a_{kl} = \cos(q^{2k} - q^{2l})t.$$

Observe, that

$$\begin{aligned}
\int_a^b \left|\sum_i f_i(x)\right| dx &\geq \int_a^b |h(x)| \left|\sum_i f_i(x)\right| dx \\
&\geq \left|\int_a^b \sum_i h(x) f_i(x) dx\right| \qquad (4.B.2)\\
&\geq \left|\int_a^b h(x) f_k(x) dx\right| - \sum_{i\neq k} \left|\int_a^b h(x) f_i(x) dx\right|,
\end{aligned}$$

where $|h(x)| \leq 1$. One can interchange the order of summation and integration because $f(x)$ is absolutely convergent. Let us take $\delta = q^{-N}$, $h(x) = \sin q^m x \cos q^n x$. After substitution in (4.B.1) using (4.B.2) we obtain

$$\begin{aligned}
W &\geq \left|\sum_{k=0}^{\infty} q^{k(s-2)} \sum_{l=0}^{k} \sin q^{l-N} \sin q^{k-l-N} \cdot\right.\\
&\quad \left.\cdot \int_0^\pi dx \, \sin q^l x \cos q^{k-l} x \cos q^m x \cos q^n x \, a_{kl}\right| \\
&= \frac{\pi}{4} q^{(m+n)(s-2)} \left|\cos q^{m-N} \sin q^{n-N} \cos(q^{2(m+n)} - q^{2m})t\right| \\
&=: \frac{\pi}{4} \widetilde{W}
\end{aligned}$$

In what follows we will show three consecutive proofs that

$$\exists c: \quad \widetilde{W} = q^{(m+n)(s-2)} \left|\cos q^{m-N} \sin q^{n-N} \cos(q^{2(m+n)} - q^{2m})t\right| \geq c q^{N(s-2)},$$

for $t = \frac{k\pi}{q^l}$, $t \in \mathbb{Q}$, and a general proof for arbitrary real t. We will take advantage of the fact that q is natural: $q = 2, 3, \ldots$

Let $N = m + n$. Then

$$\widetilde{W} = q^{N(s-2)} \left|\cos q^{m-N} \sin q^{-m} \cos(q^{2N} - q^{2m})t\right|.$$

It is enough to consider $t \in [0, \pi[$, because if we alter t by a multiple of π we can at most change the sign of the cosine.

i. Let $t = \frac{k\pi}{q^l}$. Take m such that $2m \geq l$, for instance $m = l$. Then

$$(q^{2N} - q^{2m}) \frac{k\pi}{q^l} = (q^{2N-l} - q^l) k\pi,$$

therefore

$$\left|\cos\left[(q^{2N} - q^{2l}) \frac{k\pi}{q^l}\right]\right| = 1.$$

We also have $\sin q^{-l} = \text{const}$ and

$$\cos 1 = \cos q^0 \leq \cos q^{l-N} \leq \cos q^{-\infty} = \cos 0.$$

This means that for $t = \frac{k\pi}{q^l}$

$$\widetilde{W} \geq q^{N(s-2)} \cos 1 \cdot \sin q^{-l} \cdot \cos 0 = \text{const } q^{N(s-2)}.$$

ii. For the next two proofs let us write t/π in q basis

$$\frac{t}{\pi} = \frac{a_1}{q} + \frac{a_2}{q^2} + \frac{a_3}{q^3} + \ldots = \sum_{k=1}^{\infty} \frac{a_k}{q^k}, \tag{4.B.3}$$

where $a_k \in \{0, 1, \ldots, q-1\}$. Therefore

$$\begin{aligned}
&\cos[(q^{2N} - q^{2m})t] \\
&\quad = \cos[\pi(q^{2N-1}a_1 + q^{2N-2}a_2 + \ldots + a_{2N} + q^{-1}a_{2N+1} + \ldots + \\
&\qquad + q^{2m-1}a_1 + q^{2m-2}a_2 + \ldots + a_{2m} + q^{-1}a_{2m+1} + \ldots)] \\
&\quad = \cos\left[\pi\left(\frac{a_{2N+1} - a_{2m+1}}{q} + \frac{a_{2N+2} - a_{2m+2}}{q^2} + \ldots\right)\right].
\end{aligned} \tag{4.B.4}$$

If we could only choose m so that the first two terms in this series cancel out, we would have a lower estimate on the cosine, because in this case

$$\left|\frac{a_{2N+3} - a_{2m+3}}{q^3} + \ldots\right| \leq (q-1)\left(\frac{1}{q^3} + \frac{1}{q^4} + \ldots\right) = \frac{1}{q^2}.$$

Thus

$$\cos[(q^{2N} - q^{2m})t] \geq \cos(\pi/q^2) \geq \cos\pi/4.$$

Take a rational t. In any basis q the expansion (4.B.3) of t/π is finite or periodic. Finite expansions have been treated in the previous point, thus we assume here the expansion of t/π is periodic with period T. Thus for sufficiently large n we have

$$a_{n+T} = a_n$$

so that t/π can be written as

$$t/\pi = 0.a_1 a_2 \ldots a_K (a_{K+1} \ldots a_{K+T}),$$

where $(a_{K+1} \ldots a_{K+T})$ means "repeat $a_{K+1} \ldots a_{K+T}$ periodically ad infinitum". We shall now estimate $\widetilde{W}$ for this t. Every $N > K$ can be written as $N = K + pT + r$, where p is natural or 0 and $r \in \{1, 2, \ldots, T\}$. If we now take $m = K + r$ then not only the first two but all the terms in (4.B.4) cancel out, therefore

$$\cos[(q^{2N} - q^{2m})t] = 1.$$

Obviously,

$$\begin{aligned}
\sin q^{-m} &\geq \sin q^{-(K+T)}, \\
\cos q^{m-N} &= \cos q^{-pT} \geq \cos 1,
\end{aligned}$$

Therefore

$$\widetilde{W} \geq q^{N(s-2)} \sin q^{-(K+T)} \cos 1 = \text{const } q^{N(s-2)}.$$

iii. Take arbitrary $t \in [0, \pi]$. Its expansion in q basis is given by (4.B.3). Let A be the set of all the two element sequences with elements from the set $\{0, 1, \ldots, q-1\}$. Thus

$$A = \{\{0,0\}, \{0,1\}, \ldots, \{0, q-1\}, \{1,0\}, \ldots, \{q-1, q-1\}\},$$

we write $A_{k,l} := \{k,l\}$, $k,l \in \{0,1,\dots,q-1\}$. Consider all the pairs of consecutive q-digits of x of the form

$$\{a_{2m+1}, a_{2m+2}\}, \tag{4.B.5}$$

i.e. $\{a_1,a_2\},\{a_3,a_4\}$, etc. Every such pair is equal to some $A_{k,l}$. Let $N_{k,l}$ be the first such m for which

$$A_{k,l} = \{a_{2m+1}, a_{2m+2}\}.$$

If $A_{k,l}$ for given k,l doesn't appear in the sequence of all the pairs (4.B.5) we set $N_{k,l}=0$. Let

$$M = \sup_{k,l} N_{k,l}.$$

Thus if $n > M$ the sequence $\{a_{2n+1}, a_{2n+2}\}$ has appeared at least once among the pairs $\{a_1,a_2\},\{a_3,a_4\},\dots,\{a_{2M+1},a_{2M+2}\}$. Therefore, for every $N > M$ we can find such an $m \in 1,2,\dots,M$ that

$$\left|\cos\left[(q^{2N}-q^{2m})\frac{t}{\pi}\pi\right]\right| \geq \cos\frac{\pi}{q^2} \geq \cos\frac{\pi}{4} = \frac{\sqrt{2}}{2}.$$

Also

$$\begin{aligned} \sin q^{-m} &\geq \sin q^{-M}, \\ \cos q^{m-N} &\geq \cos q^{M-N} \geq \cos 1, \end{aligned}$$

which leads to

$$\widetilde{W} \geq q^{N(s-2)}\frac{\sqrt{2}}{2}\sin q^{-M}\cos 1 = \text{const}\ q^{N(s-2)}.$$

We have thus shown that for every t, for natural q and for $\delta = q^{-N}$

$$\mathrm{Var}_\delta(f) \geq W \geq \text{const}\ \delta^{2-s},$$

therefore

$$\dim_B \operatorname{graph} P_t(x) \geq 2-(2-s) = s.$$

3. *For almost every x, $D_t(x) = \dim_B \operatorname{graph} P_x(t) = D_t := 1 + s/2$.*

We will use the form (4.A.2) of the probability density. It is enough to analyze the dimension of

$$\widetilde{P}(t) := \sum_{c=1}^{\infty} q^{2c(s-2)}\sin q^c x \sum_{d=1}^{c} q^{-d(s-2)}\sin q^{c-d}x\cos[(q^{2c}-q^{2(c-d)})t].$$

(a) Let

$$P_n(t) := \sum_{c=1}^{n} q^{2c(s-2)}\sin q^c x \sum_{d=1}^{c} q^{-d(s-2)}\sin q^{c-d}x\cos[(q^{2c}-q^{2(c-d)})t].$$

Then

$$\begin{aligned}
|P'_n(t)| &= \left|\sum_{c=1}^{n} q^{2c(s-2)} \sin q^c x \sum_{d=1}^{c} q^{-d(s-2)} \sin q^{c-d} x \cdot \right. \\
&\quad \left. \cdot (q^{2c} - q^{2(c-d)}) \sin[(q^{2c} - q^{2(c-d)})t] \right| \\
&\leq \sum_{c=1}^{n} q^{2c(s-2)} \sum_{d=1}^{c} q^{-d(s-2)} (q^{2c} - q^{2(c-d)}) \\
&= \sum_{c=1}^{n} q^{2c(s-2+1)} \sum_{d=1}^{c} q^{-d(s-2)} (1 - q^{-2d}) \\
&= \sum_{c=1}^{n} q^{2c(s-1)} \left\{ q^{2-s} \frac{q^{(2-s)c} - 1}{q^{2-s} - 1} - q^{-s} \frac{q^{-sc} - 1}{q^{-s} - 1} \right\} \\
&= \frac{q^{2-s}}{q^{2-s} - 1} \left[\sum_{c=1}^{n} q^{cs} - \sum_{c=1}^{n} q^{2c(s-1)} \right] + \\
&\quad - \frac{q^{-s}}{q^{-s} - 1} \left[\sum_{c=1}^{n} q^{c(s-2)} - \sum_{c=1}^{n} q^{2c(s-1)} \right] \\
&= \frac{q^{2-s}}{q^{2-s} - 1} \left[q^s \frac{q^{ns} - 1}{q^s - 1} - q^{2(s-1)} \frac{q^{2n(s-1)} - 1}{q^{2(s-1)} - 1} \right] + \\
&\quad - \frac{q^{-s}}{q^{-s} - 1} \left[q^{s-2} \frac{q^{n(s-2)} - 1}{q^{s-2} - 1} - q^{2(s-1)} \frac{q^{2n(s-1)} - 1}{q^{2(s-1)} - 1} \right].
\end{aligned}$$

Therefore, for n large enough

$$|P'_n(t)| \leq c_1 q^{n \max\{s, 2(s-1), s-2\}} = c q^{ns}.$$

Let $\delta = q^{-\alpha n}$. Then $q^n = \delta^{-1/\alpha}$ and

$$\mathrm{osc}_\delta(t) P_n \leq c_1 2\delta q^{ns} = 2c_1 \delta^{1-s/\alpha}.$$

Let

$$R_n(t) := \widetilde{P}(t) - P_n(t).$$

Then

$$\begin{aligned}
\mathrm{osc}_\delta(t) R_n &\leq 2 \sum_{c=n+1}^{\infty} q^{2c(s-2)} \sum_{d=1}^{c} q^{-d(s-2)} \\
&= 2 \sum_{c=n+1}^{\infty} q^{2c(s-2)} q^{2-s} \frac{q^{c(2-s)} - 1}{q^{2-s} - 1} \\
&\leq \frac{2q^{2-s}}{q^{2-s} - 1} \sum_{c=n+1}^{\infty} q^{2c(s-2)+c(2-s)} \\
&= \frac{2q^{2-s}}{q^{2-s} - 1} \frac{q^{(s-2)(n+1)}}{q^{s-2} - 1} \\
&= c_2 q^{n(s-2)} \\
&= c_2 \delta^{(s-2)/\alpha}.
\end{aligned}$$

To obtain consistent estimate we must set

$$1 - \frac{s}{\alpha} = \frac{2}{\alpha} - \frac{s}{\alpha},$$

which gives $\alpha = 2$. Thus

$$\mathrm{osc}_\delta(t)\widetilde{P} \leq (2c_1 + c_2)\delta^{1-s/2}.$$

(b) Now we want to show that

$$W = \int_a^b dt\, |\widetilde{P}(t+\delta) - \widetilde{P}(t-\delta)| \geq c\delta^{1-s/2}.$$

Set $a = 0, b = 2\pi$ for convenience. Then

$$\begin{aligned} W &= \int_0^{2\pi} dt \left| \sum_{c=1}^{\infty} q^{2c(s-2)} \sin q^c x \sum_{d=1}^{c} q^{-d(s-2)} \sin q^{c-d} x \,\cdot \right. \\ &\quad \left. \cdot \left\{ \cos[(q^{2c} - q^{2(c-d)})(t+\delta)] - \cos[(q^{2c} - q^{2(c-d)})(t-\delta)] \right\} \right| \\ &= \int_0^{2\pi} dt \left| \sum_{c=1}^{\infty} q^{2c(s-2)} \sin q^c x \sum_{d=1}^{c} q^{-d(s-2)} \sin q^{c-d} x \,\cdot \right. \\ &\quad \left. \cdot \left\{ -2\sin[(q^{2c} - q^{2(c-d)})t] \sin[(q^{2c} - q^{2(c-d)})\delta] \right\} \right|. \end{aligned}$$

Using our standard arguments we multiply the integrand by a suitable function smaller or equal to 1:

$$\begin{aligned} W &\geq \int_0^{2\pi} dt\, |h(t)||\widetilde{P}(t+\delta) - \widetilde{P}(t-\delta)| \\ &\geq \left| \int_0^{2\pi} dt\, h(t)[\widetilde{P}(t+\delta) - \widetilde{P}(t-\delta)] \right|. \end{aligned}$$

We choose $h(t) = \sin[(q^{2c} - q^{2(c-d)})t]$ and set $\delta = q^{-2N}$. It follows that

$$W \geq 2\pi q^{(2c-d)(s-2)} \left| \sin(q^c x)\sin(q^{c-d}x)\sin[(q^{2c} - q^{2(c-d)})q^{-2N}] \right|.$$

We now want to show that for almost all x

$$W \geq c_3 \delta^{1-s/2} = c_3 q^{N(s-2).}$$

Set $2c - d = N$. Then

$$W \geq 2\pi q^{N(s-2)} \left| \sin(q^c x)\sin(q^{N-c}x)\sin[q^{2(c-N)} - q^{-2c}] \right|.$$

Thus it is enough to bound

$$\left| \sin(q^c x)\sin(q^{N-c}x)\sin[q^{2(c-N)} - q^{-2c}] \right| \tag{4.B.6}$$

from below.

Choose rational x/π. All the rational numbers in a given basis q have one of the two possible forms: finite or periodic. In the first case ($x/\pi = k/q^l$) we cannot find the lower bound on (4.B.6). This is obvious, because at these points the function $P_x(t)$ is smooth (cf. the next point).
The other case means that x/π can be written as

$$x/\pi = 0.a_1 a_2 \dots a_K (a_{K+1} \dots a_{K+T}),$$

where again $(a_{K+1} \dots a_{K+T})$ denotes the periodic part. Therefore, for every $N > K$, $q^n x \bmod \pi$ can take only one of T values: $q^{K+1} x \bmod \pi, \dots, q^{K+T} x \bmod \pi$. Let us take $c = 1$, $N > K$. Then $|\sin(q^c x)| = |\sin(qx)| > 0$ and is a constant. $|\sin(q^{N-1}x)|$ takes one of T values, none of which is 0, therefore it is always bounded from below by

$$\inf_{l=1,2,\dots,T} |\sin(q^{K+l}x)| > 0.$$

Also the last term can be bounded:

$$|\sin(q^{-2(N-c)} - q^{-2c})| \geq \sin(q^{-2} - q^{-2(N-1)}) \geq \sin q^{-3}$$

for $N \geq 3$. We have thus shown that for all rational x incommensurate with π

$$W \geq c_3 q^{N(s-2)},$$

where $c_3 = 2\pi |\sin(qx)\sin(q^{-3}x)| \inf_{l=1,2,\dots,T} |\sin(q^{K+l}x)|$.
Now we know everything about the case of rational numbers. The case of irrational numbers is much more difficult. We conjecture that the set of irrational numbers giving the expected lower bound on (4.B.6) is of full measure.

4. *For a discrete, dense set of points x_d, $D_t(x_d) = \dim_B \mathrm{graph} P_{x_d}(t) = 1$.*

   Let $x_{k,m} = \frac{m\pi}{q^k}$, where $k \in \mathbb{N}$, $m = 0, 1, \dots, q^k - 1$. The set $\{x_{k,m}\}$ is dense in $[0,1]$. At these points $\Psi(x_{k,m}, t)$ is a sum of a finite number of terms:

$$\Psi\left(\frac{m\pi}{q^k}, t\right) = \sqrt{\frac{2}{\pi}\left(1 - \frac{1}{q^{2(2-s)}}\right)} \sum_{n=0}^{k-1} q^{(s-2)n} \sin(q^{n-k} m\pi)\, e^{-iq^{2n}t}.$$

   Therefore,

$$\dim_B \mathrm{graph} \left|\Psi\left(\frac{m\pi}{q^k}, t\right)\right|^2 = 1.$$

5. *For even q the average velocity $\frac{d\langle x\rangle}{dt}(t)$ is fractal with the dimension of its graph equal to $D_v = \max\{(1+s)/2, 1\}$.*

   Heuristically, this is rather obvious because

$$\begin{aligned} \frac{d\langle x\rangle}{dt}(t) &\approx \sum_{k=1}^{\infty} \frac{q^{k(s-1)}}{q^{2k}} \sin q^{2k} t \\ &= \sum_{k=1}^{\infty} q^{2k(s-3)/2} \sin q^{2k} t. \end{aligned}$$

Thus the average velocity is essentially a Weierstrass-like function and the dimension of its graph should be

$$2 - \frac{3-s}{2} = \frac{1+s}{2}.$$

We will show it using the Tricot's theorem 1.3. It is enough to consider

$$W(t) := \sum_{k=1}^{\infty} \frac{q^{k(s-1)}}{q^{2k}-1} \sin(q^{2k}-1)t.$$

(a) Let

$$W_n(t) := \sum_{k=1}^{n} \frac{q^{k(s-1)}}{q^{2k}-1} \sin(q^{2k}-1)t.$$

Set $\delta = q^{-\alpha n}$. Then

$$\begin{aligned} |W_n'(t)| &= \left| \sum_{k=1}^{n} q^{k(s-1)} \cos(q^{2k}-1)t \right| \\ &\leq \sum_{k=1}^{n} q^{k(s-1)} \\ &= \frac{q^{(n+1)(s-1)} - q^{s-1}}{q^{s-1}-1} \\ &\leq c_1 q^{n(s-1)} \\ &= c_1 \delta^{\frac{1-s}{\alpha}}, \end{aligned}$$

where

$$c_1 = \frac{q^{s-1}}{q^{s-1}-1}.$$

Therefore

$$\operatorname{osc}_\delta(t) W_n \leq 2c_1 \delta^{\frac{1-s}{\alpha}} \delta = 2c_1 \delta^{1+\frac{1-s}{\alpha}}.$$

Now, for

$$P_n(t) := W(t) - W_n(t)$$

we have

$$\begin{aligned} |P_n(t)| &= \left| \sum_{k=n+1}^{\infty} \frac{q^{k(s-1)}}{q^{2k}-1} \sin(q^{2k}-1)t \right| \\ &\leq \sum_{k=n+1}^{\infty} \frac{q^{k(s-1)}}{q^{2k}-1} \\ &\leq 2 \sum_{k=n+1}^{\infty} \frac{q^{k(s-1)}}{q^{2k}} \\ &= 2 \sum_{k=n+1}^{\infty} q^{k(s-3)} \\ &= \frac{2 \cdot q^{(n+1)(s-3)}}{1-q^{s-3}} \\ &= c_2 \delta^{-\frac{s-3}{\alpha}}, \end{aligned}$$

where

$$c_2 = \frac{2q^{s-3}}{1-q^{s-3}}.$$

Thus

$$\mathrm{osc}_\delta(t)P_n \le 2c_2\delta^{\frac{3-s}{\alpha}}.$$

To obtain consistent estimate for both P_n and W_n we must set

$$1+\frac{1-s}{\alpha} = \frac{3-s}{\alpha},$$

thus $\alpha = 2$ and $\delta = q^{-2N}$. Therefore

$$\begin{aligned} \mathrm{osc}_\delta(t)W &\le \mathrm{osc}_\delta(t)W_n + \mathrm{osc}_\delta(t)P_n \\ &\le 2(c_1+c_2)\delta^{2-\frac{s+1}{2}}. \end{aligned}$$

(b) Consider

$$\begin{aligned} &\int_a^b |W(t+\delta)-W(t-\delta)|dt \\ &= \int_a^b dt \left| \sum_{k=1}^{\infty} \frac{q^{k(s-1)}}{q^{2k}-1}\cos(q^{2k}-1)t \, \sin(q^{2k}-1)\delta \right| \\ &\ge \left| \int_a^b dt\, h(t) f_N(t) \right| - \sum_{k\ne N} \left| \int_a^b dt\, h(t) f_k(t) \right|, \end{aligned}$$

where

$$f_k(t) = \frac{q^{k(s-1)}}{q^{2k}-1}\cos(q^{2k}-1)t \, \sin(q^{2k}-1)\delta.$$

Let $h(t) = \cos(q^{2N}-1)t$, $\delta = q^{-2N}$. Then

$$\begin{aligned} &\left| \int_a^b h(t) f_N(t) dt \right| \\ &= \frac{q^{N(s-1)}}{q^{2N}-1}\sin(1-q^{-2N}) \int_a^b \cos^2(q^{2N}-1)t\, dt \\ &\ge \frac{q^{N(s-1)}}{q^{2N}} \sin\frac{\pi}{6} \int_a^b \cos^2(q^{2N}-1)t\, dt \\ &\ge \frac{1}{2} q^{N(s-3)} \left[\frac{b-a}{2} + \frac{\sin(2b(q^{2N}-1)) - \sin(2a(q^{2N}-1))}{4(q^{2N}-1)} \right] \\ &\ge \frac{1}{2}\delta^{\frac{3-s}{2}} \left[\frac{b-a}{2} - \frac{2\cdot 2}{4\cdot q^{2N}} \right] \\ &= \frac{1}{2}\delta^{\frac{3-s}{2}} \left[\frac{b-a}{2} - \delta \right] \\ &\ge \frac{1}{8}\delta^{\frac{3-s}{2}}(b-a). \end{aligned}$$

On the other hand

$$\begin{aligned}
&\left|\int_a^b h(t) f_k(t) dt\right| \\
= &\ \frac{q^{k(s-1)}}{q^{2k}-1} \sin\left[(q^{2k}-1)q^{-2N}\right] \int_a^b \cos(q^{2k}-1)t \cos(q^{2N}-1)t\, dt \\
\leq &\ \frac{q^{k(s-1)}}{q^{2k}-1} \left| \frac{\sin(b(q^{2N}-q^{2k})) - \sin(a(q^{2N}-q^{2k}))}{2(q^{2N}-q^{2k})} + \right. \\
&\ \left. \frac{\sin(b(q^{2N}+q^{2k})) - \sin(a(q^{2N}+q^{2k}))}{2(q^{2N}+q^{2k})} \right| \\
\leq &\ 2q^{k(s-3)} \left[\frac{1}{|q^{2N}-q^{2k}|} + \frac{1}{q^{2N}+q^{2k}} \right] \\
\leq &\ 2q^{k(s-3)} \left[\frac{1}{q^{2N}-q^{2(N-1)}} + \frac{1}{q^{2N}} \right] \\
\leq &\ 5 \cdot q^{k(s-3)} \delta.
\end{aligned}$$

Therefore

$$\begin{aligned}
W &\geq \frac{1}{8}\delta^{\frac{3-s}{2}}(b-a) - \sum_k 5q^{k(s-3)}\delta \\
&\geq \frac{1}{8}\delta^{\frac{3-s}{2}}(b-a) - 5\frac{q^{s-3}}{q^{s-3}-1}\delta.
\end{aligned}$$

But $\frac{3-s}{2} < 1$, thus for large enough N (small enough δ) the first term dominates the other, therefore

$$W \geq c\delta^{2-\frac{1+s}{2}},$$

one can put $c = \frac{b-a}{16}$, for example.

From theorem 1.3 it follows that

$$D_v = \frac{1+s}{2}.$$

6. *The surface $P(x,t)$ has dimension $D_{xy} = 2 + s/2$.*

From theorem 1.6 we have

$$D_{xt} = 1 + \max\{D_x, D_t\} = 2 + \frac{s}{2}. \tag{4.B.7}$$

□

Chapter 5

Concluding remarks

5.1 Main results

Rabbit never minded saying things again, so he asked where he should begin from; and when Pooh had said from the moment when the fluff got in his ear, and Rabbit had asked when that was, Pooh said he didn't know because he hadn't heard properly.
A. A. Milne, *"Winnie-the-Pooh"*

Our aim in this work has been to show that the fractal geometry is as fruitful theory today as it was twenty years ago. In order to do it we proposed a method to distinguish interacting from non-interacting systems on the basis of given time series, which is a practical outcome of this work. On the other hand, as an example of surprises there are still hidden in the physical world we constructed a fractal wave function, a non-chaotic quantum object of strange properties. The most important results of this work have been presented in the last two chapters.

In chapter 3 we introduced a method to distinguish interacting from non-interacting subsystems of a given system when two time series of measurements are available, one from each of the subsystems. The idea is to form another time series by taking a function of the two experimental sets. This new time series contains information of the dynamics of the whole system. If we now reconstruct the phase spaces of the subsystems and the system using delay variables (chapter 2) we can calculate the Rényi dimensions of the attractors underlying the dynamics. Next, from the three obtained numbers we form the *dimension of interaction* which is approximately the dimension of the attractor of the subsystem formed by the variables common to both of the subsystems of interest.

We show that if the two subsystems do not interact, the dimension of interaction is zero. When they do interact, it is greater than zero. We prove these statements in several cases, one of which holds only for the information dimension, but this is not an obstacle to our method due to the Holmes principle[1].

[1] *It is an old maxim of mine that when you have excluded the impossible, whatever remains, however improbable, must be the truth*, Arthur Conan Doyle, *"The Adventures of Sherlock Holmes"*; line 11710 of Gutenberg text `advsh11.txt`.

After showing correctness of our method in principle, that is for infinite, clean time series, we check it in practice for several interacting and non-interacting systems. They are logistic maps and Hénon systems in various configurations. In all the analyzed cases our method is shown to give correct results.

We also discuss and classify the possible results that can be obtained with our method and propose a simple way of checking which case holds for given sets of data.

In chapter 4 we have constructed a family of fractal solutions of the Schrödinger equation for a wide family of potentials. The solutions are parametrized by $0 \leq s \leq 2$. It is shown that the box-counting dimension of the graph of the probability density at a constant time t (the "space dimension" D_x) is usually equal to $\max\{1, s\}$ (for almost all t). The evolution of the probability density at a fixed point in space is a fractal function for almost every x and its dimension is $1+s/2$ (the "time dimension" D_t). Given this information we are able to calculate the dimension of the graph of the probability density in both variables: it is $2 + s/2$. This result is based on a simple fact which we derived in chapter 1 but it seems so basic that we think it must have been obtained earlier by mathematicians. We have not been able to find any references, however.

The strongest results have been obtained for the case of the infinite potential well, whose dimensional properties we understand quite well. Here we have been able to prove in full rigor the following facts:

1. the graph of the probability density at the fixed time t is fractal in the space variable, and dimension of its graph is $D_x = \max\{s, 1\}$;

2. the evolution of the probability density at a certain discrete, dense set of points x is smooth thus the dimension of its graph is 1.

3. the average velocity $\frac{d\langle x\rangle}{dt}(t)$ is fractal and the dimension of its graph is equal to $D_v = \max\{(1+s)/2, 1\}$;

4. the surface $P(x,t)$ has dimension $D_{xy} = 2 + s/2$.

We have also conjectured that for almost every x inside the well the probability density, $P_x(t) = P(x = \text{const}, t)$, forms a fractal graph in the time variable of dimension $D_t(x) = D_t := 1 + s/2$. Here we have been able to obtain rigorously the upper bound (to show that $D_t(x) \leq 1 + s/2$ holds always) and the lower bound for all the rational numbers for which the graph is not smooth (x incommensurate with π).

The reader might wonder why the result for the average velocity does not carry over to the general case. The answer is that while the fractality of the probability density is its local property, average velocity depends on the *global* properties of the wave function, and the WKB analysis we use cannot give us correct solution in this case. For example, in the case of harmonic oscillator, the average velocity can be easily shown to be smooth, in fact

$$\langle x\rangle = A\cos(\omega t + \varphi),$$

where ω is the oscillator frequency. This result holds for arbitrary states of the oscillator.

Nevertheless, we believe that the example of harmonic oscillator is not generic and that any small perturbation of the potential in this case would lead to fractal average velocity with the dimension of its graph $D_v = (1 + s)/2$. This conjecture needs to be proved.

In conclusion, we have achieved our aim. We have proved both practical and cognitive values of the fractal geometry.

5.2 Future directions

'Would you tell me, please, which way I ought to go from here?' 'That depends a good deal on where you want to get to,' said the Cat. 'I don't much care where–' said Alice. 'Then it doesn't matter which way you go,' said the Cat. '–so long as I get SOMEWHERE,' Alice added as an explanation. 'Oh, you're sure to do that,' said the Cat, 'if you only walk long enough' .

Lewis Carroll, *"Alice's adventures in Wonderland"*

Both of the problems considered in this work, apart from promoting the value of the fractal geometry, are interesting in itself and pose more questions than they answer.

Our method of distinguishing interacting from non-interacting systems would be most valuable if it could be used in analysis of spatiotemporal systems, like fluids or neuronal tissue. In these cases, however, the difficulty is that the dimensions which have to be estimated are usually rather large, the signals are noisy and often non-stationary. Thus an important question in this respect is what the best way to distinguish interacting from non-interacting systems is? Several methods may be considered apart from ours. The linear correlations method is most often used due to its simplicity even though there is no theoretical justification in the case of nonlinear systems. The method based on mutual nonlinear prediction used by Schiff et al. [203] may be of value. Several other more or less justified methods have been proposed, for instance in [237] or [46]. The ranges of validity and precision of these methods have never been compared as far as we know. This is why we have attempted a case study.

The aim of an experiment which is now being carried on with the experimental group at the Institute of Physics, Polish Academy of Sciences (Y. Hluschchuk, N. Savitsky, S. Bauch, L. Sirko) is firstly to test our method on the real life data, and secondly to compare the validity and precision of all the available methods. The preliminary results in the first case are promising, namely whenever we are able to estimate dimensions our method gives correct answers. Sometimes, however, no scaling region is present in the data. This only happens in the case of strong coupling between the examined systems (which are two electronic circuits similar to the Chua system). This is probably due to non-stationarity of the system in this case — it may be switching between several different attractors. We hope to eliminate these problems soon and announce the results. The next step will be a comparison of the above-mentioned methods in the case of our systems.

The true challenge, the spatiotemporal systems, will first be tackled in the case of coupled map lattices (e.g. [122]) and only when we find the best procedure of dealing with these systems and gain some confidence in the methods we shall attempt analysis of the real systems.

The second part of our work provokes other kinds of questions. We have shown that the structure of the quantum theory admits fractal solutions, but how typical are they? Are they a rule or an exception? The recent results of Brian Hunt from the University of Maryland on the prevalence of fractal functions of maximal available dimensions in the set of continuous functions [262] seem to suggest the former, but the true question is, of course, how many physically interesting states will exhibit scaling over enough scales to make it sufficiently interesting. We expect that fractal states are prevalent among the continuous states in the Hilbert space. None of them, however, will belong to the domain of the Hamiltonian. Here again we must emphasize the distinction between mathematical and physical fractals. The question "How many physical fractals are there among the physical states" is difficult because it's hard to make precise the notion of a physical fractal, but anyway the answer seems to be "The higher the average energy, the better scaling is to be expected". This needs further investigation.

The constructions of the Weierstrass-like states in the case of power-law potentials in one dimension can be extended to the N-dimensional case, however the analysis becomes more elaborate. We hope to report on this in the close future.

In the examples we have constructed the real and imaginary parts of the wave functions, their squares and the sums of their squares (that is the probability densities) are fractal and have the same dimensions. Can one construct a wave function with smooth probability density and a fractal phase?

Using the wavelet methods one could try to calculate the multifractal spectrum of graphs of our wave functions [118, 119]. This is probably of little interest, but the probability density of our wave function is certainly fractal. What is the multifractal spectrum (we would be happy with just the information dimension) of the measure induced by the probability density? It is certainly of more physical interest than the box-counting dimension we just calculated.

Can one invent simple methods to calculate dimensions of such probability measures? One thing that comes to mind is finding a hyperbolic dynamical system for which this measure would be the natural invariant measure and using the thermodynamic formalism. Such problems are considered in the literature under the name of inverse Frobenius-Perron problem [59, 58, 181, 32]. Perhaps constructing Iterated Function Systems whose invariant measures would approximate our probability density might turn out to be effective. Can these ideas lead to effective numerical methods?

To prove the theorem 4.1 we used some number theoretical ideas. One would like to find other proofs based on the ergodic theorems. They would probably give weaker answers (the results would be obtained for almost all points instead of all) but they should more easily carry over to general cases. The theorem 4.2 still remains to be proved in full generality.

We criticize Berry's proof of fractality of his states. What remains is to calculate oscillations of a typical state of Berry's function and prove that he was right (for we believe he *was* right).

An often used means of calculating dimension is by checking the power-law behavior of the power spectrum of the function. But the power spectrum contains no information on the phases which are important for the dimension, as we have claimed in the previous chapter (see also interesting paper by Higuchi [115]). Scaling of the power spectrum seems to give the upper bound to the dimension of the graph of function. What extra conditions must be satisfied to give the lower bound?

We have attempted to construct fractal states in the free particle problem. Even though we failed we gained some insight. There is a chance that another envelope will lead to fractal free particle states, for instance $1/(1 + x^2)$ instead of the Gaussian. The calculations in this case lead to much more complicated wave functions. We hope to investigate this possibility in some detail in the future.

We have shown that fractals in quantum mechanics are equally legitimate as in the classical theory. In practice, the obvious physical limitations will not allow one to find in nature a Platonic structure of mathematical fractals, for which the property of scaling holds at all scales. On the other hand, one may well try to construct experimentally quantum states, for which scaling may be observed for at least a few decades. It will be a challenging task, to find a physical mechanism responsible for generation of such fractal states in problems described by quantum mechanics. Perhaps observations of Ketzmerick [131] and Casati [41] might lead to an answer. One could also look for such states in quantum optics or in microwave cavities. In the last case the connection between the dimensions of space and time fractals would be different, but the idea would remain the same.

All the questions raised above will be subjects of further study.

> *"Yes," said Winnie-the-Pooh. "I see now," said Winnie-the-Pooh. "I have been Foolish and Deluded," said he, "and I am a Bear of no Brain at All."* .
>
> A. A. Milne, *"Winnie-the-Pooh"*

Bibliography

[1] H. D. I. Abarbanel. *Analysis of Observed Chaotic Data.* Springer-Verlag, New York Berlin Heidelberg, 1996.

[2] H. D. I. Abarbanel, R. Brown, J. L. Sidorowich, and L. S. Tsimring. The analysis of observed chaotic data in physical systems. *Rev. Mod. Phys.*, 65:1331–1392, 1993.

[3] L. F. Abbott and M. B. Wise. Dimension of a quantum-mechanical path. *Am. J. Phys.*, 49(1):37, 1981.

[4] A. Aharony and J. Feder, editors. *Fractals in physics*, *Physica D*, volume 38, Amsterdam, 1989. North-Holland.

[5] I. S. Averbukh and N. F. Perelman. Fractional revivals: universality in the long-term evolution of quantum wave packets beyond the correspondence principle dynamics. *Phys. Lett. A*, 139:449–453, 1989.

[6] R. Badii and A. Politi. Statistical description of chaotic attractors: the dimension function. *J. Stat. Phys.*, 40:725–750, 1985.

[7] R. Badii and A. Politi. Rényi dimensions from local expansion rates. *Phys. Rev. A*, 35:1288–1293, 1987.

[8] R. Badii and A. Politi. *Complexity : Hierarchical structures and scaling in physics*, volume 6 of *Cambridge Nonlinear Science Series.* Cambridge University Press, Cambridge, 1997.

[9] P. Bak and K. Chen. Self-organized criticality. *Sci. Amer.*, 264:46–53, 1991.

[10] P. Bak, C. Tang, and K. Wiesenfeld. Self-organized criticality. *Phys. Rev. A*, 38:364–374, 1988.

[11] J. Balatoni and A. Rényi. On the notion of entropy. *Publ. Math. Inst. Hung. Akad. Sci.*, 1:9–40, 1956.

[12] Y. Bar-Yam. *Dynamics of Complex Systems.* Studies in Nonlinearity. Addison-Wesley, Reading, Massachusetts, 1997.

[13] M. Barnsley. *Fractals everywhere.* Academic Press, New York, 1988.

[14] M. F. Barnsley and S. Demko. Iterated function systems and the global construction of fractals. *Proc. Roy. Soc. London*, 399:243–275, 1985.

[15] C. Beck. Upper and lower bounds on the Rényi dimensions and the uniformity of multifractals. *Physica D*, 41:67, 1990.

[16] C. Beck and F. Schlögl. *Thermodynamics of Chaotic Systems.* Cambridge University Press, Cambridge, UK, 1997.

[17] E. Ben-Jacob, R. Godbey, J. Goldenfeld, N. D. an Koplik, H. Levine, T. Muller, and L. M. Sander. Experimental demonstration of the role of anisotropy in interfacial pattern formation. *Phys. Rev. Lett.*, 55:1315–1318, 1985.

[18] A. Ben-Mizrachi, I. Procaccia, N. Schmidt, R. A., and H. G. Schuster. Real and apparent divergences in low-frequency spectra of nonlinear dynamical systems. *Phys. Rev. A*, 31:1830–1840, 1985.

[19] C. M. Bender, K. Olaussen, and P. S. Wang. Numerological analysis of the WKB approximation in large order. *Phys. Rev. B*, 16(6):1740, 1977.

[20] G. Benettin, L. Galgani, and J. M. Strelcyn. Kolmogorov entropy and numerical experiments. *Phys. Rev. A*, 14:2338–2345, 1976.

[21] A. Berera and L.-Z. Fang. Stochastic fluctuations and structure formation in the universe. *Phys. Rev. Lett.*, 72:458–461, 1994.

[22] M. V. Berry. Quantum fractals in boxes. *J. Phys. A: Math. Gen.*, 29:6617–6629, 1996.

[23] M. V. Berry and S. Klein. Integer, fractional and fractal Talbot effects. *J. Mod. Opt.*, 43(10):2139–2164, 1996.

[24] M. V. Berry and Z. V. Lewis. On the Weierstrass-Mandelbrot function. *Proc. R. Soc. Lond. A*, 370:459–484, 1980.

[25] A. Białas and R. Peschanski. Moments of rapidity distributions as a measure of short-range fluctuations in high-energy collisions. *Nucl. Phys. B*, 273:703–718, 1986.

[26] A. Białas and R. Peschanski. Intermittency in multiparticle production at high-energy. *Nucl. Phys. B*, 308:857–867, 1988.

[27] I. Białynicki-Birula, M. Cieplak, and J. Kamiński. *Teoria kwantów.* Polish Scientific Publishers PWN, Warszawa, 1991. in Polish (English edition exists).

[28] S. Bingham and M. Kot. Multidimensional trees, range searching, and a correlation dimension algorithm of reduced complexity. *Phys. Lett. A*, 140:327–330, 1989.

[29] S. Bleher, C. Grebogi, and E. Ott. Bifurcation to chaotic scattering. *Physica D*, 46:87–121, 1990.

[30] S. Bleher, E. Ott, and C. Grebogi. Routes to chaotic scattering. *Phys. Rev. Lett.*, 63:919–922, 1989.

[31] T. Bohr, M. H. Jensen, G. Paladin, and A. Vulpiani. *Dynamical systems approach to turbulence*, volume 8 of *Cambridge nonlinear science series*. Cambridge University Press, Cambridge, 1998.

[32] E. M. Bollt. On the inverse Frobenius-Perron problem: global stabilization of arbitrary invariant measures. preprint, short version published in *J. Bif. Chaos*, 1998.

[33] S. Borgani. Scaling in the universe. *Phys. Rep.*, 251(1&2):1–152, 1995.

[34] J.-P. Bouchaud and A. Georges. Anomalous diffusion in disordered media: statistical mechanisms, models and physical applications. *Phys. Rep.*, 195(4/5):127–293, 1990.

[35] R. Bowen. *Equilibrium states and the ergodic theory of Anosov diffeomorphisms*, volume 470 of *Lecture Notes in Mathematics*. Springer-Verlag, Berlin, 1975.

[36] R. M. Brady and R. C. Ball. Fractal growth of copper electrodeposits. *Nature*, 309:225–229, 1984.

[37] D. S. Broomhead and G. P. King. Extracting qualitative dynamics from experimental data. *Physica D*, 20:217–236, 1986.

[38] A. Buka, J. Kertész, and T. Vicsek. Transitions of viscous fingering patterns in nematic liquid crystals. *Nature*, 323:424–425, 1986.

[39] T. Buzug and G. Pfister. Comparison of algorithms calculating optimal parameters for delay time coordinates. *Physica D*, 58:127, 1992.

[40] J. M. Carlson and J. Doyle. Highly optimized tolerance: A mechanism for power laws in designed systems. *Phys. Rev. E*, 60(2):1412, 1999.

[41] G. Casati, I. Guarneri, and G. Maspero. Fractal survival probability. *Phys. Rev. Lett.*, 84(1):63, 2000.

[42] M. Casdagli. Nonlinear prediction of chaotic time series. *Physica D*, 35:335–356, 1989.

[43] M. Casdagli and S. Eubank. Nonlinear modeling and forecasting. *Proceedings of the NATO/ Santa Fe Institute conference on nonlinear forecasting and modeling, September 1990*, volume XII, Reading Mass., 1992. Addison-Wesley.

[44] M. Casdagli, S. Eubank, J. D. Farmer, and J. Gibson. State space reconstruction in the presence of noise. *Physica D*, 51:52–98, 1991.

[45] R. Cawley and G. H. Hsu. Local-geometric projection method for noise reduction in chaotic maps and flows. *Phys. Rev. A*, 46:3057–3082, 1992.

[46] A. Cenys, G. Lasiene, and K. Pyragas. Estimation of interrelations between chaotic observables. *Physica D*, 52:332–337, 1991.

[47] J. D. Chen and D. Wilkinson. Pore-scale viscous fingering in porous media. *Phys. Rev. Lett.*, 55:1892–1895, 1985.

[48] A. Cohen and I. Procaccia. Computing the Kolmogorov entropy from time signals of dissipative and conservative dynamical systems. *Phys. Rev. A*, 31:1872–1882, 1985.

[49] P. H. Coleman and L. Pietronero. The fractal structure of the universe. *Phys. Rep.*, 213(6):311–389, 1992.

[50] M. C. Cross and P. C. Hohenberg. Pattern formation outside of equilibrium. *Rev. Mod. Phys.*, 65:851–1112, 1993.

[51] J. P. Crutchfield and B. S. McNamara. Equations of motion from a data series. *Complex Systems*, 1:417–452, 1987.

[52] C. D. Cutler. Some results on the behavior and estimation of the fractal dimensions of distributions on attractors. *J. Stat. Phys.*, 62:651–708, 1991.

[53] M. Davies. Noise reduction schemes for chaotic time series. *Physica D*, 79:174–192, 1994.

[54] F. Davis. Is the universe homogeneous on large scales? In N. Turok, editor, *Critical dialogues in cosmology*, Singapore, 1997. World Scientific.

[55] S. de Arcangelis, Redner and A. Coniglio. Anomalous voltage distribution of random resistor networks and a new model for the backbone of the percolation threshold. *Phys. Rev. B*, 31:4725, 1985.

[56] P. G. de Gennes. *Scaling concepts in polymer physics.* Cornell University Press, Ithaca, New York, 1979.

[57] E. de Wolf, I. Dremin, and W. Kittel. Scaling laws for density correlations and fluctuations in multiparticle dynamics. *Phys. Rep.*, 270(1–2):1–141, 1996.

[58] F. K. Diakonos, D. Pingel, and Schmelcher. A stochastic approach to the construction of one-dimensional chaotic maps with prescribed statistical properties. *Phys. Lett. A*, 264:162–170, 1999.

[59] F. K. Diakonos and P. Schmelcher. On the construction of one-dimensional iterative maps from the invariant density: the dynamical route to the beta distribution. *Phys. Lett. A*, 211(4):199–203, 1996.

[60] M. Ding, C. Grebogi, E. Ott, T. Sauer, and J. A. Yorke. Estimating correlation dimension from a chaotic time series: When does plateau onset occur? *Physica D*, 69:404–424, 1993.

[61] B. Dubuc, J. F. Quiniou, C. Roques-Carmes, C. Tricot, and S. W. Zucker. Evaluating the fractal dimension of profiles. *Phys. Rev. A*, 39:1500–1512, 1989.

[62] B. Dubuc, S. W. Zucker, , C. Tricot, J. F. Quiniou, and D. Wehbi. Evaluating the fractal dimension of surfaces. *Proc. R. Soc. Lond. A*, 425:113–127, 1989.

[63] B. Eckhardt. Irregular scattering. *Physica D*, 33:89, 1988.

[64] J.-P. Eckmann. Roads to turbulence in dissipative dynamical systems. *Rev. Mod. Phys.*, 53:643–654, 1981.

[65] J.-P. Eckmann, E. Järvenpää, and M. Järvenpää. Porosities and dimensions of measures. *Nonlinearity*, 13:1–18, 2000.

[66] J.-P. Eckmann and D. Ruelle. Ergodic theory of chaos and strange attractors. *Rev. Mod. Phys.*, 57:617–656, 1985.

[67] G. A. Edgar. *Measure, topology, and fractal geometry.* Springer-Verlag, New York, 1990.

[68] G. A. Edgar, editor. *Classics on fractals.* Addison-Wesley, Reading, Massachusetts, 1993.

[69] G. A. Edgar. *Integral, probability, and fractal measures.* Springer, New York, 1998.

[70] W. T. Elam, S. A. Wolf, J. Sprague, D. U. Gubser, D. Van Vechten, G. L. Barz Jr., and P. Meakin. Fractal aggregates in sputter-deposited $NbGe_2$ films. *Phys. Rev. Lett.*, 54:701–703, 1987.

[71] R. Engelking. *Dimension theory.* North Holland, Amsterdam, 1978.

[72] R. Engelking. *Teoria wymiaru*, volume 51 of *Mathematical Library.* Polskie Wydawnictwo Naukowe PWN, Warszawa, II edition, 1981. in Polish.

[73] A. Erzan, L. Pietronero, and A. Vespignani. The fixed scale transformation approach to fractal growth. *Rev. Mod. Phys.*, 67(3):545, 1995.

[74] C. J. G. Evertsz and B. B. Mandelbrot. *Multifractal Measures*, Appendix B, pages 921–953. Springer, Berlin, New York, 1992.

[75] K. J. Falconer. *The geometry of fractal sets.* University Press, Cambridge, 1985.

[76] K. J. Falconer. *Fractal geometry.* Wiley, Chichester, New York, 1990.

[77] K. J. Falconer. *Techniques in Fractal Geometry.* John Wiley and Sons, New York, 1997.

[78] D. Farmer and J. Sidorowich. Exploiting chaos to predict the future and reduce noise. *Physica D*, 47:373, 1988.

[79] J. D. Farmer. Information dimension and the probabilistic structure of chaos. *Z. Naturforsch. A*, 37:1304–1325, 1982.

[80] J. D. Farmer, E. Ott, and J. A. Yorke. The dimension of chaotic attractors. *Physica D*, 7:153–180, 1983.

[81] J. D. Farmer and J. J. Sidorowich. Predicting chaotic time series. *Phys. Rev. Lett.*, 59:845–848, 1987.

[82] J. D. Farmer and J. J. Sidorowich. Optimal shadowing and noise reduction. *Physica D*, 47:373–392, 1991.

[83] J. Feder. *Fractals.* Plenum, New York, 1988.

[84] M. Frank, H.-R. Blank, J. Heindl, M. Kaltenhäuser, H. Köchner, N. Müller, S. P. R. Sporer, and T. Wagner. Improvement of K2-entropy calculations by means of dimension scaled distances. *Physica D*, 65:359, 1993.

[85] A. M. Fraser and H. L. Swinney. Independent coordinates for strange attractors from mutual information. *Phys. Rev. A*, 33(2):1134–1140, 1986.

[86] U. Frisch and G. Parisi. On the singularity structure of fully developed turbulence. In M. Ghil, R. Benzi, and G. Parisi, editors, *Turbulence and predictability in geophysical fluid dynamics and climate dynamics*, pages 84–88. North-Holland, New York, 1985.

[87] H. Froehling, J. P. Crutchfield, J. D. F. N. H. Packard, and R. S. Shaw. On determining the dimension of chaotic flows. *Physica D*, 3:605–617, 1981.

[88] P. Gaspard and S. A. Rice. Scattering from a classical chaotic repeller. *J. Chem. Phys.*, 90:2225, 1989.

[89] P. Gaspard and X.-J. Wang. Noise, chaos and (ϵ, τ)-entropy per unit time. *Physics Reports*, 235:291–343, 1993.

[90] K. Geist, U. Parlitz, and W. Lauterborn. Comparison of different methods for computing Lyapunov exponents. *Prog. Theor. Phys.*, 83:875–893, 1991.

[91] N. Gershenfeld. An experimentalist's introduction to the observation of dynamical systems. In B.-L. Hao, editor, *Directions in Chaos*, volume 2, pages 310–384. World Scientific, Singapore, 1988.

[92] J. Gerver. The differentiability of the Riemann function at certain rational multiples of π. *Am. J. Math.*, 92:33–55, 1970.

[93] P. Grassberger. Generalized dimensions of strange attractors. *Phys. Lett. A*, 97:227–230, 1983.

[94] P. Grassberger. Finite sample corrections to entropy and dimension estimates. *Phys. Lett. A*, 128:369–373, 1988.

[95] P. Grassberger. An optimized box-assisted algorithm for fractal dimensions. *Phys. Lett. A.*, 148(1/2):63–68, 1990.

[96] P. Grassberger, R. Badii, and A. Politi. Scaling laws for invariant measures on hyperbolic and non-hyperbolic attractors. *J. Stat. Phys.*, 51:135–178, 1988.

[97] P. Grassberger, R. Hegger, H. Kantz, C. Schaffrath, and T. Schreiber. On noise reduction methods for chaotic data. *Chaos*, 3:127–140, 1993.

[98] P. Grassberger and I. Procaccia. Measuring the strangeness of strange attractors. *Physica D*, 9:189–208, 1983.

[99] P. Grassberger and I. Procaccia. On the characterization of strange attractors. *Phys. Rev. Lett.*, 50:346–349, 1983.

[100] P. Grassberger and I. Procaccia. Dimensions and entropies of strange attractors from a fluctuating dynamics approach. *Physica D*, 13:34–54, 1984.

[101] C. Grebogi, E. Ott, S. Pelikan, and J. A. Yorke. Strange attractors that are not chaotic. *Physica D*, 13:261–268, 1984.

[102] C. Grebogi, E. Ott, and J. A. Yorke. Chaos, strange attractors, and fractal basin boundaries in nonlinear dynamics. *Science*, 238:632–638, 1987.

[103] H. S. Greenside, A. Wolf, J. Swift, and T. Pignataro. Impracticality of a box-counting algorithm for calculating the dimensionality of strange attractors. *Phys. Rev. A*, 25:3453–3456, 1982.

[104] J. Guckenheimer and G. Buzyna. Dimension measurement for geostrophic turbulence. *Phys. Rev. Lett.*, 51:1438–1441, 1983.

[105] E. G. Gwinn and R. M. Westervelt. Fractal basin boundaries and intermittency in the driven damped pendulum. *Phys. Rev. A*, 33:4143, 1986.

[106] M. J. W. Hall, M. S. Reineker, and W. P. Schleich. Unraveling quantum carpets: a travelling-wave approach. *J. Phys. A*, 32:8275–8291, 1999.

[107] T. C. Halsey, M. H. Jensen, L. P. K. I. Procaccia, and B. I. Shraiman. Fractal measures and their singularities: The characterization of strange sets. *Phys. Rev. A*, 33:1141–1151, 1986.

[108] G. H. Hardy. Weierstrass's non-differentiable function. *Trans of AMS*, 17:301–325, 1916.

[109] G. H. Hardy, J. E. Littlewood, and G. Pólya. *Inequalities*. Cambridge University Press, Cambridge, 1952.

[110] F. Hausdorff. Dimension und äußeres maß. *Math. Annalen*, 79:157, 1919.

[111] S. Havlin and D. Ben-Avraham. Diffusion in disordered media. *Adv. Phys.*, 36(6):695–798, 1987.

[112] R. Hegger, H. Kantz, and T. Schreiber. Practical implementation of nonlinear time series methods: The TISEAN package. *Chaos*, 9(2):413–435, 1999.

[113] M. Hénon. A two-dimensional mapping with a strange attractor. *Commun. Math. Phys.*, 50:69–77, 1976.

[114] H. G. E. Hentschel and I. Procaccia. The infinite number of generalized dimensions of fractals and strange attractors. *Physica D*, 8:435–444, 1983.

[115] T. Higuchi. Relationship between the fractal dimension and the power law index for a time series: a numerical investigation. *Physica D*, 46:254–264, 1990.

[116] B. R. Hunt. The Hausdorff dimension of graphs of Weierstrass functions. *Proc. AMS*, 126(3):791, 1998.

[117] W. Hurewicz and H. Wallman. *Dimension Theory*. Princeton University Press, Princeton, 1941.

[118] S. Jaffard. Multifractal formalism for functions part I: results valid for all functions. *SIAM J. Math. Anal.*, 28(4):944–970, 1997.

[119] S. Jaffard. Multifractal formalism for functions part II: self-similar functions. *SIAM J. Math. Anal.*, 28(4):971–998, 1997.

[120] E. Jakeman. Scattering by fractals. In L. Pietronero and E. Tosatti, editors, *Fractals in physics*, pages 55–60, Amsterdam, 1986. Elsevier Science.

[121] L. P. Kadanoff. Scaling and universality in statistical physics. *Physica A*, 163:1–14, 1990.

[122] K. Kaneko. Spatiotemporal chaos in one- and two-dimensional coupled map lattices. *Physica D.*, 37(1-3):60–82, 1989.

[123] H. Kantz and P. Grassberger. Repellers, semi-attractors, and long-lived chaotic transients. *Physica D*, 17:75–86, 1985.

[124] H. Kantz and T. Schreiber. Dimension estimates and physiological data. Chaos, 1995.

[125] H. Kantz and T. Schreiber. *Nonlinear Time Series Analysis*. Cambridge Univ. Press, Cambridge, UK, 1997.

[126] H. Kantz, T. Schreiber, I. Hoffmann, T. Buzug, G. Pfister, L. G. Flepp, J. Simonet, R. Badii, and E. Brun. Nonlinear noise reduction: A case study on experimental data. *Phys. Rev. E*, 48:1529–1538, 1993.

[127] D. T. Kaplan and L. Glass. Direct test for determinism in a time series. *Phys. Rev. Lett.*, 68:427–430, 1992.

[128] J. L. Kaplan and J. A. Yorke. Chaotic behavior of multidimensional difference equations. In H. O. Walter and H.-O. Peitgen, editors, *Functional Differential Equations and Approximation of Fixed Points*, volume 730 of *Lecture Notes in Mathematics*, pages 204–227. Springer-Verlag, Berlin, 1979.

[129] D. Katzen and I. Procaccia. Phase transitions in thermodynamic formalism of multifractals. *Phys. Rev. Lett.*, 58:1169, 1987.

[130] M. B. Kennel, R. Brown, and H. D. I. Abarbanel. Determining embedding dimension for phase-space reconstruction using a geometrical construction. *Phys. Rev. A*, 45:3403–3411, 1992.

[131] R. Ketzmerick. Fractal conductance fluctuations in generic chaotic cavities. *Phys. Rev. B*, 54(15):10841, 1996.

[132] J. Klafter, M. F. Shlesinger, and G. Zumofen. Beyond Brownian motion. *Phys. Today*, 49(2):33, February 1996.

[133] E. J. Kostelich and T. Schreiber. Noise reduction in chaotic time-series data: A survey of common methods. *Phys. Rev. E*, 48:1752–1762, 1993.

[134] E. J. Kostelich and J. A. Yorke. Noise reduction in dynamical systems. *Phys. Rev. A*, 38:1649–1652, 1988.

[135] H. Kröger. Fractal geometry in quantum mechanics, field theory and spin systems. *Phys. Rep.*, 323(2):818–181, 2000.

[136] L. Lam, editor. *Introduction to nonlinear physics*. Springer, New York, Berlin, Heidelberg, 1997.

[137] L. Landau and E. Lifszic. *Mechanika kwantowa*. Polish Scientific Publishers PWN, Warszawa, 1958.

[138] A. Lasota and M. C. Mackey. *Probabilistic properties of deterministic systems.* University Press, Cambridge, 1985.

[139] A. Lasota and M. C. Mackey. *Chaos, Fractals, and Noise (Applied Mathematical Sciences)*, volume 97. Springer-Verlag, Berlin, 1994.

[140] C. Leichtle, I. S. Averbukh, and W. P. Schleich. Generic structure of multilevel quantum beats. preprint univ Ulm, 1996.

[141] W. Liebert and H. G. Schuster. Proper choice of the time delay for the analysis of chaotic time series. *Phys. Lett. A*, 142(2-3):107–111, 1989.

[142] X. Luo and D. N. Schramm. Fractals and cosmological large-scale structure. *Science*, 256:513–515, 1992.

[143] K. J. Maløy, J. Feder, and T. Jøssang. Viscous fingering fractals in porous media. *Phys. Rev. Lett.*, 55:2688–2691, 1985.

[144] B. Mandelbrot. *Les objets fractals: Forme, hasard et dimension.* Flammarion, Paris, 1975.

[145] B. Mandelbrot. *Fractals - form, chance, and dimension.* Freeman, San Francisco, 1977.

[146] B. Mandelbrot. *The fractal geometry of nature.* Freeman, San Francisco, 1982.

[147] T. Matsumoto. Chaos in electronic circuits. *Proc. IEEE*, 75:1033–1057, 1987.

[148] M. Matsushita, M. Sano, Y. Hayakawa, H. Honjo, and Y. Sawada. Fractal structures of zinc metal leaves grown by electrodeposition. *Phys. Rev. Lett.*, 53:286–289, 1984.

[149] P. Mattila. *Geometry of sets and measures in Euclidean spaces.* Cambridge Univ. Press, Cambridge, 1995.

[150] G. Mayer-Kress. Dimension and entropies in chaotic systems; quantification of complex behavior. In G. Mayer-Kress, editor, *Springer Ser. in Synerg.*, volume 32. 1986.

[151] G. Mayer-Kress. Application of dimension algorithms to experimental chaos. In B.-L. Hao, editor, *Directions in chaos*, volume 1, pages 122–147. World Scientific, Singapore, 1987.

[152] G. Mayer-Kress and T. Kurz. Dimension density of coupled map lattices. *J. Complex Syst.*, 1:821–829, 1987.

[153] J. L. McCauley. Introduction to multifractals in dynamical systems theory and fully developed fluid turbulence. *Phys. Rep.*, 189(5):225–266, 1990.

[154] J. L. McCauley. *Chaos, Dynamics and fractals. An algorithmic approach to deterministic chaos.* University Press, Cambridge, 1993.

[155] P. Meakin. Fractal aggregates and their fractal measures. In C. Domb and J. L. Lebowitz, editors, *Phase transitions and critical phenomena*, volume 12. Academic, New York, 1988.

[156] P. Meakin. The growth of rough surfaces and interfaces. *Phys. Rep.*, 235(4-5):189–289, 1993.

[157] P. Meakin. *Fractals, scaling and growth far from equilibrium*, volume 5 of *Cambridge Nonlinear Science Series.* Cambridge University Press, Cambridge, 1998.

[158] E. W. Montroll and M. F. Schlesinger. On the wonderful world of random walks. In J. L. Lebowitz and E. W. Montroll, editors, *Nonequilibrium phenomena II*, volume XI of *Studies in statistical mechanics*, pages 1–121. North-Holland, Amsterdam, 1984.

[159] E. W. Montroll and B. J. West. On an enriched collection of stochastic processes. In E. W. Montroll and J. L. Lebowitz, editors, *Fluctuation phenomena*, volume VII of *Studies in statistical mechanics*, pages 61–176. North-Holland, Amsterdam, 1979.

[160] K. Murali and M. Lakshmanan. Chaotic dynamics of the driven Chua's circuit. *IEEE Trans. Circ. Syst. I*, 40(1):836, 1993.

[161] J. Nittmann, G. Daccord, and H. E. Stanley. Fractal growth of viscous fingers: Quantitative characterization of a fluid instability phenomenon. *Nature*, 314:141–144, 1985.

[162] J. Nittmann and H. E. Stanley. Tip splitting without interfacial tension and dendritic growth patterns arising from molecular anisotropy. *Nature*, 321:663–668, 1986.

[163] A. Nowak and R. R. Vallacher. *Dynamical social psychology.* Guilford, New York, 1998.

[164] L. Olsen. A multifractal formalism. *Advances in Mathematics*, 116:82–195, 1995.

[165] L. Olsen. Multifractal dimensions of product measures. *Math. Proc. Camb. Phil. Soc.*, 120:709–734, 1996.

[166] A. R. Osborne and A. Provenzale. Finite correlation dimension for stochastic systems with power-law spectra. *Physica D*, 35:357–381, 1989.

[167] E. Ott. Strange attractors and chaotic motions of dynamical systems. *Rev. Mod. Phys.*, 53(4):655–671, 1981.

[168] E. Ott. *Chaos in Dynamical Systems.* University Press, Cambridge, 1993.

[169] E. Ott. *Chaos w układach dynamicznych.* Wydawnictwa Naukowo-Techniczne, Warszawa, 1997.

[170] E. Ott, T. Sauer, and J. A. Yorke. Lyapunov partition functions for the dimensions of chaotic sets. *Phys. Rev. A*, 39:4212, 1989.

[171] E. Ott, W. D. Withers, and J. A. Yorke. Is the dimension of chaotic attractors invariant under coordinate change? *J. Stat. Phys.*, 36:687–697, 1984.

[172] N. H. Packard, J. P. Crutchfield, J. D. Farmer, and R. S. Shaw. Geometry from a time series. *Phys. Rev. Lett.*, 45:712–716, 1980.

[173] G. Paladin and A. Vulpiani. Anomalous scaling laws in multifractal objects. *Phys. Rep.*, 156:147–225, 1987.

[174] G. Parisi, L. Pietronero, and M. Virasoro, editors. *Complex systems: fractals, spin glasses and neural networks*, *Physica A*, volume 185, Amsterdam, 1992. North-Holland.

[175] L. M. Pecora and T. L. Carroll. Synchronization in chaotic systems. *Phys. Rev. Lett.*, 64:821–824, 1990.

[176] L. M. Pecora, T. L. Carroll, and J. F. Heagy. Statistics for mathematical properties of maps between time series embeddings. *Phys. Rev. E*, 52(4):3420–3439, 1995.

[177] L. M. Pecora, T. L. Carroll, and J. F. Heagy. Statistics for continuity and differentiability: An application to attractor reconstruction from time series. In C. D. Cutler and D. T. Kaplan, editors, *Nonlinear Dynamics and Time Series*, volume 11 of *Fields Inst. Communications*, pages 49–62. American Math. Soc., Providence, Rhode Island, 1997.

[178] Y. B. Pesin. *Dimension Theory in Dynamical systems: Contemporary Views and Applications.* Chicago Lectures in Mathematics. Chicago University Press, Chicago and London, 1997.

[179] L. Pietronero, M. Montuori, and F. Sylos Labini. On the fractal structure of the visible universe. In N. Turok, editor, *Critical dialogues in cosmology*, Singapore, 1997. World Scientific.

[180] A. S. Pikovsky and P. Grassberger. Symmetry breaking bifurcation for coupled chaotic attractors. *J. Physics A*, 24:4587, 1991.

[181] D. Pingel, P. Schmelcher, and F. K. Diakonos. Theory and examples of the inverse Frobenius-Perron problem for complete chaotic maps. *Chaos*, 9(2):357, 1999.

[182] Y. Pomeau. Mesure de la dinsité d'information en turbulence. *C. R. Acad. Sc. Paris*, 300, series II:239, 1985.

[183] R. F. Port and T. Van Gelder. *Mind as motion.* MIT Press, London, 1995.

[184] D. Prichard and J. Theiler. Generating surrogate data for time series with several simultaneously measured variables. *Phys. Rev. Lett.*, 73:951–954, 1994.

[185] M. B. Priestley. *Non-linear and Non-stationary Time Series Analysis.* Academic Press, 1988.

[186] I. Procaccia. Fractal structures in turbulence. *J. Stat. Phys.*, 36:649, 1984.

[187] A. Provenzale, L. A. Smith, R. Vio, and G. Murante. Distinguishing between low-dimensional dynamics and randomness in measured time series. *Physica D*, 58:31–49, 1992.

[188] K. Ramasubramanian and M. S. Sriram. A comparative study of computation of Lyapunov spectra with different algorithms. *Physica D*, 139:72–86, 2000.

[189] A. Rényi. On the dimension and entropy of probability distributions. *Acta Math. Acad. Sci. Hung.*, 10:193–215, 1959.

[190] A. Rényi. *Probability theory.* North-Holland, Amsterdam, 1971.

[191] M. Robnik and V. G. Romanovski. Some properties of WKB series. `nlin.CD`/0003069; accepted by J. Phys. A, 2000.

[192] C. A. Rogers. *Hausdorff measures.* Cambridge Univ. Press, Cambridge, 1970.

[193] J.-C. Roux, R. H. Simoyi, and H. L. Swinney. Observation of a strange attractor. *Physica D*, 8:257–255, 1983.

[194] D. Ruelle. *Thermodynamic formalism.* Addison-Wesley, Reading Mass., 1978.

[195] D. Ruelle. Strange attractors. *Math. Intelligencer*, 2:126–137, 1980.

[196] D. Ruelle and F. Takens. On the nature of turbulence. *Comm. Math. Phys.*, 20:167–192, 1971.

[197] N. F. Rulkov, M. M. Sushchik, L. S. Tsimring, and H. D. I. Abarbanel. Generalized synchronization of chaos in directionally coupled chaotic systems. *Phys. Rev. E*, 51(2):980–994, 1995.

[198] D. A. Russel, J. D. Hanson, and E. Ott. Dimension of strange attractors. *Phys. Rev. Lett.*, 45:1175–1178, 1980.

[199] A. Sáiz and V. J. Martínez. Multifractal analysis of the atomic spectral line series. *Phys. Rev. E*, 54(3):2431–2437, September 1996.

[200] T. Sauer. A noise reduction method for signals from nonlinear systems. *Physica D*, 58:193–201, 1992.

[201] T. Sauer, J. A. Yorke, and M. Casdagli. Embedology. *J. Stat. Phys.*, 65:579–616, 1991.

[202] L. I. Schiff. *Quantum mechanics.* McGraw-Hill, New York, 1968.

[203] S. J. Schiff, P. So, T. Chang, R. E. Burke, and T. Sauer. Detecting dynamical interdependence and generalized synchrony through mutual prediction in a neural ensemble. *Phys. Rev. E*, 54(6):6708–6724, December 1996.

[204] T. Schreiber. Interdisciplinary application of nonlinear time series methods. *Phys. Rep.*, 308(1):2–64, 1999.

[205] L. S. Schulman and P. E. Seiden. Percolation and galaxies. *Science*, 233:425–431, 1986.

[206] H. G. Schuster. *Deterministic chaos: An introduction.* VCH, Weinheim, 1988.

[207] H. G. Schuster. *Chaos deterministyczny. Wprowadzenie.* Polish Scientific Publishers PWN, Warszawa, 1993.

[208] H. G. Schuster, editor. *Handbook of Chaos Control.* Wiley-VCh, Weinheim, New York, 1998.

[209] P. E. Seiden and L. S. Schulmann. Percolation model of galactic structure. *Adv. Phys.*, 39:1–54, 1993.

[210] Y. G. Sinai. Gibbssian measures in ergodic theory. *Russ. Math. Surv.*, 27:21–69, 1972.

[211] S. K. Sinha. Scattering from fractal surfaces. *Physica D*, 38:283–303, 1989.

[212] A. Smith. The differentiability of Riemann's function. *Proc. of Am. Math. Soc.*, 34:463–468, 1972.

[213] L. A. Smith. Identification and prediction of low dimensional dynamics. *Physica D*, 58:50–76, 1992.

[214] P. So, E. Barretto, and B. R. Hunt. Box-counting dimension without boxes: Computing d_0 from average expansion rates. *Phys. Rev. E*, 59(6):1–8, 1999.

[215] J. Spanier and K. B. Oldham. *An atlas of Functions.* Hemisphere Publishing, Washington, 1987.

[216] H. E. Stanley. *Introduction to phase transitions and critical phenomena.* Oxford Univ. Press, Oxford, 1971.

[217] H. E. Stanley and P. Meakin. Multifractal phenomena in physics and chemistry. *Science*, 335:405, 29 Sept. 1988.

[218] K. Suave. Gamma-band synchronous oscillations: recent evidence regarding their functional significance. *Consciousness and cognition*, 8:213–224, 1999.

[219] G. Sugihara and R. May. Nonlinear forecasting as a way of distinguishing chaos from measurement errors in time series. *Nature*, 344:734–741, 1990.

[220] D. Sweet, E. Ott, and J. A. Yorke. Topology in chaotic scattering. *Nature*, 399:315, 1999.

[221] F. Sylos Labini, M. Montuori, and L. Pietronero. Scale-invariance of galaxy clustering. *Phys. Rep.*, 293(2–4):61–226, 1998.

[222] P. Szépfalusy, T. Tél, A. Csordas, and Z. Korva's. Phase transitions associated with dynamical properties of chaotic systems. *Phys. Rev. A*, 36:3525–3528, 1987.

[223] F. Takens. Detecting strange attractors in turbulence. In D. A. Rand and L.-S. Young, editors, *Dynamical Systems and Turbulence (Warwick 1980)*, volume 898 of *Lecture Notes in Mathematics*, pages 366–381. Springer-Verlag, Berlin, 1980.

[224] F. Takens. On the numerical determination of the dimension of an attractor. In B. L. J. Braaksma, H. W. Broer, and F. Takens, editors, *Dynamical systems and bifurcations, Groningen 1984*, volume 1125 of *Lecture Notes in Mathematics*, pages 99–106. Springer-Verlag, Berlin, 1985.

[225] S. Tasaki, T. Gilbert, and J. R. Dorfman. An analytical construction of the SRB measures for baker-type maps. *Chaos*, 8(2):424–443, 1998.

[226] S. Taylor. The measure theory of random fractals. *Math. Proc. Cambridge Phil. Soc.*, 100:383–406, 1986.

[227] T. Tél. Fractals and multifractals. *Z. Naturforsch. A*, 43:1154, 1988.

[228] J. Theiler. Spurious dimensions from correlation algorithms applied to limited time-series data. *Phys. Rev. A*, 34:2427–2432, 1986.

[229] J. Theiler. Efficient algorithm for estimating the correlation dimension from a set of discrete points. *Phys. Rev. A*, 36:4456–4473, 1987.

[230] J. Theiler. Lacunarity in a best estimator of fractal dimension. *Phys. Lett. A*, 133:195–200, 1988.

[231] J. Theiler. Estimating fractal dimensions. *J. Opt. Soc. Am. A*, 7:1055–1073, 1990.

[232] J. Theiler. Some comments on the correlation dimension of 1/f-alpha noise. *Phys. Lett. A*, 155:480–493, 1991.

[233] J. Theiler, S. Eubank, A. Longtin, B. Galdrikian, and J. D. Farmer. Testing for nonlinearity in time series: the method of surrogate data. *Physica D*, 58:77–94, 1992.

[234] J. Theiler and D. Prichard. Constrained-realization Monte-Carlo method for hypothesis testing. *Physica D*, 94:221, 1996.

[235] E. Thelen and L. B. Smith. *A dynamical systems approach to the development of cognition and action.* MIT press, London, 1994.

[236] H. Tong. *Nonlinear time series analysis: A dynamical system approach.* University Press, Oxford, 1990.

[237] G. Tononi and M. Edelman. Consciousness and complexity. *Science*, 282:1846, 1998.

[238] C. Tricot. *Curves and fractal dimension.* Springer-Verlag, New York, Berlin, 1995.

[239] C. Tricot, J. F. Quiniou, D. Wehbi, C. Roques-Carmes, and B. Dubuc. Evaluation de la dimension fractale d'un graphe. *Revue Phys. Appl.*, 23:111–124, 1988.

[240] S. M. Ulam and J. von Neumann. On combinations of stochastic and deterministic processes. *Bull. Am. Math. Soc.*, 53:1120, 1947.

[241] R. R. Vallacher and A. Nowak, editors. *Dynamical systems in social psychology.* Academic Press, San Diego, 1994.

[242] W. van de Water and P. Schram. Generalized dimensions from near-neighbour information. *Phys. Rev. A*, 37:3118, 1988.

[243] T. Vicsek. *Fractal growth phenomena.* World Scientific, Singapore, 1992.

[244] T. Vicsek and A. S. Szalay. Fractal distribution of galaxies modeled by a cellular-automaton-type stochastic process. *Phys. Rev. Lett.*, 58:2818–2821, 1987.

[245] A. Voros. Exact anharmonic quantization condition (in one dimension). In J. Rauch and B. Simon, editors, *Quasiclassical methods*, volume 95 of *IMA series*, pages 189–224, New York, 1995. Springer.

[246] A. Voros. Airy function — exact WKB results for potentials of odd degree. *J. Phys. A*, 32:1301–1311, 1999.

[247] F. Weierstrass. Über kontinuierliche funktionen eines reellen arguments, die für keinen wert des letzteren einen bestimmten differential quotienten besitzen. In *Mathematische Werke II*, pages 71–74. Mayer & Muller, Berlin, 1895.

[248] A. S. Weigend and N. A. Gershenfeld. *Time series prediction: Forecasting the future and understanding the past*, volume XV of *Santa Fe Institute Studies in the Science of Complexity, Proc.* Addison -Wesley, Reading, 1993.

[249] M. Weissman. 1/f noise and other slow, non-exponential kinetics in condensed matter. *Rev. Mod. Phys.*, 60:537–571, 1988.

[250] D. A. Weitz and M. Oliveria. Fractal structures formed by kinetic aggregation of aqueous gold colloids. *Phys. Rev. Lett,*, 52:1433–1436, 1984.

[251] B. J. West and W. Deering. Fractal physiology for physicists: Lévy statistics. *Phys. Rep.*, 246(1&2):1–100, 1994.

[252] K. G. Wilson. Problems in physics with many scales of length. *Sci. Am.*, 241(2):140–158, 1979.

[253] T. A. Witten and L. M. Sander. Diffusion-limited aggregation, a kinetic critical phenomena. *Phys. Rev. Let.*, 47:1400, 1981.

[254] T. A. Witten and L. M. Sander. Diffusion-limited aggregation. *Phys. Rev. B*, 27:5686, 1983.

[255] D. Wójcik, I. Białynicki-Birula, and K. Życzkowski. Fractal carpets in a quantum well. in preparation, 2000.

[256] D. Wójcik, I. Białynicki-Birula, and K. Życzkowski. Time evolution of quantum fractals. `quant-ph/0005060`, submitted to Phys. Rev. Lett., 2000.

[257] D. Wójcik, Y. Hlushchuk, N. Savitsky, S. Bauch, M. Kuś, and L. Sirko. Distinguishing interacting from non-interacting systems on the example of Chua systems. in preparation, 2000.

[258] D. Wójcik, A. Nowak, and M. Kuś. Dimension of interaction dynamics. `nlin.CD/0002026`, submitted to Phys. Rev. E, 2000.

[259] A. Wolf, J. B. Swift, H. L. Swinney, and J. A. Vastano. Determining Lyapunov exponents from a time series. *Physica D*, 16:285–317, 1985.

[260] J. Żebrowski and A. Sukiennicki. Chaotic dynamics in spatially extended system with solitons. In H. Wisniewski, editor, *Chaos/Nonlinear Dynamics: Methods and Commercialization*, volume 2037 of *Proc. SPIE*, pages 290–299. SPIE, 1994.

[261] M. Zochowski and L. S. Liebovitch. Synchronization of the trajectory as a way to control the dynamics of a coupled system. *Phys. Rev E*, 56(3):3701–3704, 1997.

[262] K. Życzkowski. private communication, 1999.